



The Water Colour Simulator WASI

User manual for version 4

Peter Gege



The actual version of WASI and of this manual can be downloaded from the web site of the International Ocean-Colour Coordinating Group (IOCCG):

<http://www.ioccg.org/data/software.html>

Copyright

The software was developed by Dr. Peter Gege, German Aerospace Center (DLR), Institut für Methodik der Fernerkundung, 82234 Oberpfaffenhofen, Germany. He owns all copyrights.

- WASI version 4 is a public domain software and can be used free of charge.
- There is no warranty in case of errors.
- There is no user support.
- Commercial distribution is not allowed.
- Commercial use is not allowed unless an agreement with the author is made.
- Publication of results obtained from using the software requires to
 - quote the use of WASI in the text,
 - cite a recent publication about WASI,
 - inform Peter Gege via email,
 - send Peter Gege a copy of the paper (as file or paper hardcopy).

WASI version: 4
Date: 17 January 2014
Author: Peter Gege
Contact: peter.gege@dlr.de



**Deutsches Zentrum
für Luft- und Raumfahrt**
German Aerospace Center

Table of contents

1. Introduction	5
2. Models	7
2.1 Absorption	7
2.1.1 Water constituents	7
2.1.2 Natural water	9
2.2 Backscattering.....	10
2.2.1 Pure water.....	10
2.2.2 Suspended particles of Type I	10
2.2.3 Suspended particles of Type II.....	11
2.3 Attenuation	12
2.3.1 Diffuse attenuation for downwelling irradiance.....	12
2.3.2 Diffuse attenuation for upwelling irradiance.....	12
2.3.3 Attenuation for upwelling radiance.....	13
2.4 Specular reflectance.....	14
2.5 Irradiance reflectance.....	15
2.5.1 Deep water.....	15
2.5.2 Shallow water	15
2.6 Remote sensing reflectance	16
2.6.1 Deep water.....	16
2.6.2 Shallow water	16
2.6.3 Above the surface	17
2.7 Bottom reflectance.....	19
2.7.1 For irradiance sensors.....	19
2.7.2 For radiance sensors	19
2.8 Downwelling irradiance.....	21
2.8.1 Above water surface.....	21
2.8.2 Below water surface	23
2.8.3 At depth z	23
2.9 Sky radiance.....	25
2.10 Upwelling radiance	26
2.10.1 Below the water surface	26
2.10.2 Above the water surface	26
2.11 Fluorescence	27
2.11.1 Phytoplankton.....	27
2.12 Miscellaneous	30
2.12.1 Depth of light penetration.....	30
3. Forward mode	31
3.1 Graphical user interface	31
3.2 Calculation of a single spectrum.....	32
3.2.1 Mode selection	32
3.2.2 Spectrum type selection.....	32
3.2.3 Parameter selection.....	33
3.2.4 Calculation options.....	33
3.2.5 Start calculation	34
3.2.6 Example.....	34
3.3 Calculation of a series of spectra	37
3.3.1 General	37
3.3.2 Specification of the iteration	37
3.3.3 Data storage	38

3.3.4 Example.....	39
4. Inverse mode	41
4.1 Graphical user interface	41
4.2 Inversion of a single spectrum.....	43
4.2.1 Spectrum selection	43
4.2.2 Definition of initial values.....	44
4.2.3 Fit strategy.....	45
4.2.4 Definition of fit region and number of iterations	46
4.3 Inversion of a series of spectra	47
4.3.1 Selection of spectra	47
4.3.2 Definition of initial values.....	48
4.4 Optimisation of inversion	50
4.4.1 Irradiance reflectance of deep water	50
4.4.2 Irradiance reflectance of shallow water.....	54
4.4.3 Remote sensing reflectance of deep water	57
4.4.4 Remote sensing reflectance of shallow water	58
4.4.5 Downwelling irradiance	59
5. Reconstruction mode.....	60
5.1 Definition of parameter values	60
5.2 Definition of output information	61
6. 2D mode	64
7. Model options.....	65
7.1 Downwelling irradiance.....	65
7.2 Irradiance reflectance.....	67
7.3 Absorption	71
7.4 Bottom reflectance.....	73
8. Implicite spectra	75
9. Program options	77
9.1 Data format	77
9.2 Directories.....	79
9.3 Display options	80
9.4 General options.....	81
10. References	82
Appendix 1: Installation	87
Appendix 2: WASI4.INI	88
Appendix 3: Parameters	94
Appendix 4: Constants	95
Appendix 5: Input spectra	96
Appendix 6: Calculated spectra.....	97

1. Introduction

The Water Colour Simulator WASI is a software tool for analyzing and simulating the most common types of spectra that are measured by ship-borne optical instruments. The deep-water version is described in Gege (2004), the shallow-water version in Gege and Albert (2006).

The spectrum types and major calculation options are listed in Table 1.1. A more comprehensive summary including the fit parameters is given in Appendix 7. WASI can be used to generate the spectra of Table 1.1 ("Forward mode"), or to analyze such spectra ("Inverse mode"). Both modes can be combined to perform sensitivity studies ("Reconstruction mode"). The three modes of operation are described in chapter 3 (forward mode), chapter 4 (inverse mode) and chapter 5 (reconstruction mode). Model options are depicted in chapter 6, program options in chapter 8. The installation of WASI is described in Appendix 1.

Basis of all calculations are analytical models with experimentally easily accessible parameters, which are well established among "ocean colour" modelers and experimentally and theoretically validated. These models are described in detail in chapter 2, the corresponding references are cited in chapter 9.

Spectrum type	Model options
Absorption	Of water constituents Of natural water bodies
Attenuation	For downwelling irradiance
Specular reflectance	Wavelength dependent Constant
Irradiance reflectance	For deep water For shallow water
Remote sensing reflectance	Below surface for deep water Below surface for shallow water Above surface for deep water Above surface for shallow water
Bottom reflectance	For irradiance sensors For radiance sensors
Downwelling irradiance	Above surface Below surface
Upwelling radiance	Below surface Above surface

Table 1.1: Spectrum types and major model options.

The program consists of an executable file, WASI.EXE, an initialisation file, WASI.INI, and 29 input spectra. WASI.INI is an ASCII file that comprises all paths and file names of the data files, parameter values, constants and user settings. An example listing is given in Appendix 2. Much effort was spent to make the user interface as clear as possible. Since most settings in the different pop-up windows are self-explanatory, not every detail is described in this manual.

Alternatively to the usual interactive mode of operation, WASI can also be started from another program through the command `WASI INI_File`. In this case the file `INI_File` is read instead of `WASI.INI`, then calculation is started automatically without opening the graphical user interface, and finally WASI is terminated after the calculations are finished. This mode of operation is useful for combining WASI with another program. For example, WASI has been combined with a radiative transfer simulation program for the atmosphere (6S) to estimate the influence of errors in atmospheric correction on the retrieval of phytoplankton, Gelbstoff and suspended matter from MERIS and MODIS data (Pyhälähti and Gege, 2001).

Changes compared to version 3

The major differences between version 4 and the previous version 3 (Gege 2005) are:

- *Image processing.* Version 3 was able to import and process an unlimited number of spectra from file, version 4 supports additionally multi- and hyperspectral images (Gege 2014).
- *Sensor response.* The spectral response of each sensor band can be taken into account.
- *Simulation of noise.* Constant sensor noise could be simulated in version 3; version 4 supports also wavelength dependent noise.
- *Simulation of offset.* It is now possible to include in the simulations measurement and preprocessing errors which lead to a spectral offset.
- *Sensor depth.* In version 3, models for reflectance, radiance and irradiance were implemented for sensors located directly above or below the water surface; version 4 supports submersed sensors in any depth.
- *Model of downwelling irradiance.* In version 3 an empirical model of Gege (1994, 1995) was included; it was replaced in version 4 by an extended version of the model of Gregg and Carder (1990). See Gege (2012) for details.
- *Fluorescence.* Fluorescence was neglected in version 3, phytoplankton fluorescence has been included in version 4.
- *Implicite spectra.* The number of implicite spectra which can be visualised was increased, the relevant menu was re-structured, and a description was added (chapter 7).
- *File format.* Several options concerning the format of input files were added to facilitate data analysis: support of multi-column ASCII tables, import of the sun zenith angle and day of year from the file header.
- *Layout.* The parameter list was simplified: in version 3 each spectrum type had its own parameter list, now all 36 model parameters are always visible, but actually irrelevant parameters are deactivated.
- *Netbook compatibility.* The GUI of version 3 was too large for netbooks with a screen height of 600 pixels; it is now automatically adjusted to small screens.
- *Break processing.* Data processing can be stopped using the 'Pause' button.

2. Models

2.1 Absorption

2.1.1 Water constituents

Absorption of a mixture of water constituents is the sum of the components' absorption coefficients:

$$a_{WC}(\lambda) = \sum_{i=0}^5 C_i \cdot a_i^*(\lambda) + Y \cdot a_Y^*(\lambda) + D \cdot a_d^*(\lambda). \quad (2.1)$$

λ denotes wavelength. Three groups of absorbing water constituents are considered: phytoplankton, Gelbstoff, and detritus.

Phytoplankton. The high number of species that occur in natural waters causes some variability in phytoplankton absorption properties. This is accounted for by the inclusion of 6 specific absorption spectra $a_i^*(\lambda)$. If no phytoplankton classification is performed, the spectrum $a_0^*(\lambda)$ is selected to represent the specific absorption of phytoplankton. C_i indicates pigment concentration, where "pigment" is the sum of chlorophyll-a and phaeophytin-a.

The default spectra provided with WASI are shown in Fig. 2.1. They are based on measurements at Lake Constance. The five spectra $a_1^*(\lambda) \dots a_5^*(\lambda)$ represent relevant optical classes "cryptophyta type L", "cryptophyta type H", "diatoms", "dinoflagellates", and "green algae" (Gege 1994, 1995, 1998b). The spectrum $a_0^*(\lambda)$, labeled "phytoplankton" in Fig. 2.1, is a weighted sum of these five spectra and represents a mixture which can be considered as typical for Lake Constance. It was calculated by Heege (2000) using phytoplankton absorption spectra¹ and pigment data² from 32 days in 1990 and 1991, and he validated it using 139 irradiance reflectance and 278 attenuation measurements³ from 1990 to 1996.

Gelbstoff (dissolved organic matter). Gelbstoff absorption is the product of concentration Y and specific absorption $a_Y^*(\lambda)$. The spectrum $a_Y^*(\lambda)$ can either be read from file or calculated using the usual exponential approximation (Nyquist 1979; Bricaud et al. 1981):

$$a_Y^*(\lambda) = \exp[-S \cdot (\lambda - \lambda_0)], \quad (2.2)$$

where S denotes the spectral slope, and λ_0 is a reference wavelength with a_Y^* normalized to 1. Default values are $\lambda_0 = 440$ nm and $S = 0.014$ nm⁻¹, which can be considered representative of a great variety of water types (Bricaud et al. 1981; Carder et al. 1989).

Gelbstoff absorption is calculated in WASI by default using the exponential approximation of eq. (2.2). However, Gege (2000) showed that this approximation provides model errors below 10 % only for the wavelength interval of $[\lambda_0 - 60$ nm, $\lambda_0 + 60$ nm], and a better approximation is a sum of 3 Gaussian distributions (the x-axis must be transformed from the wavelength scale (nm) to the energy scale (cm⁻¹)). The Gaussian model is physically more reasonable

¹ Derived from above-water reflectance spectra by inverse modelling (Gege 1994, 1995).

² Measured at the University of Constance by Beese, Richter, and Kenter.

³ Measured by Tilzer, Hartig, and Heege (Tilzer et al. 1995, Heege 2000).

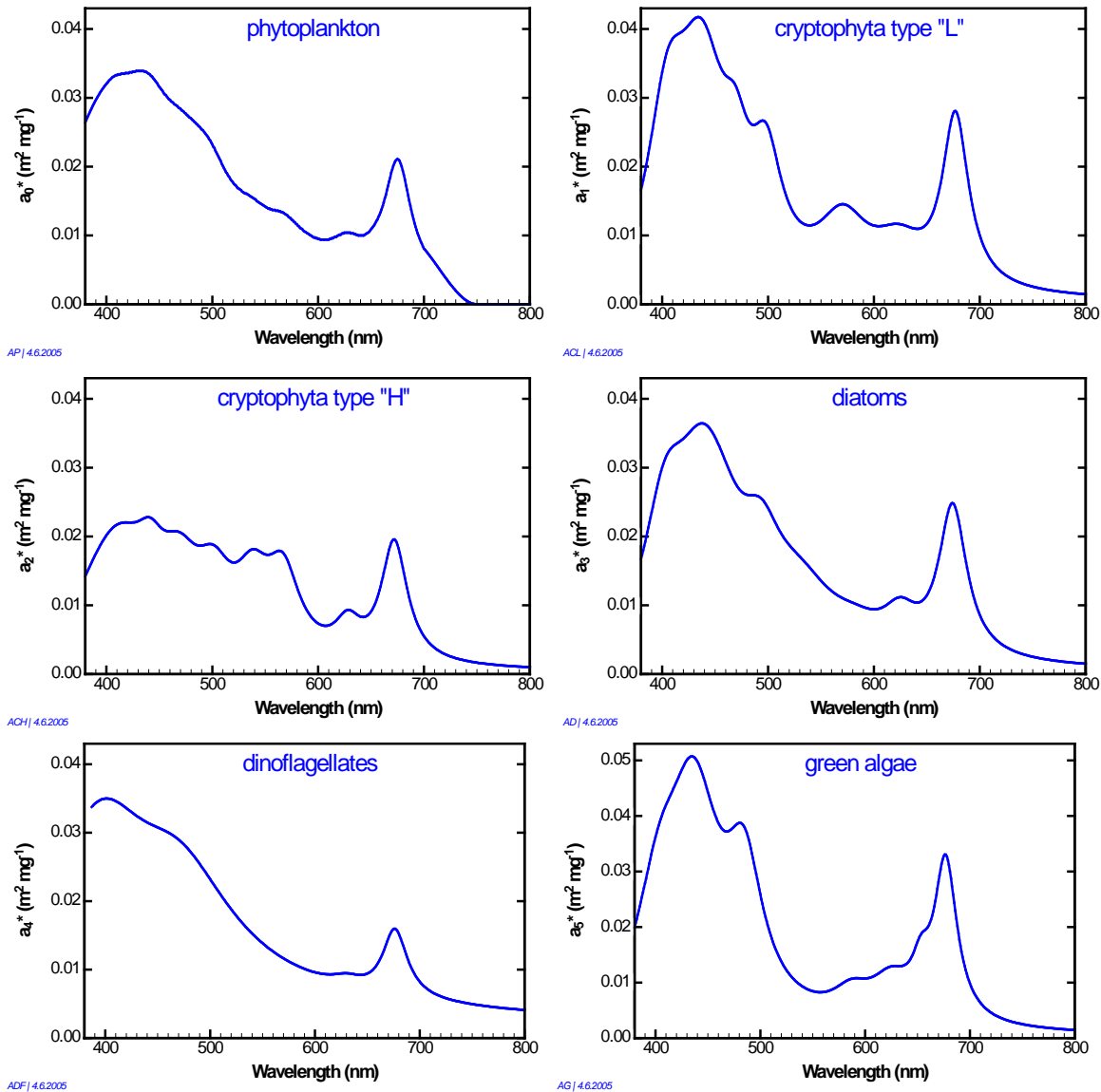


Fig. 2.1: Specific absorption spectra of 6 phytoplankton classes.

than the exponential model and offers a deeper understanding of the chemical interactions affecting CDOM molecular structure (Schwarz et al. 2002). Thus, a spectrum ($Y.A$) is provided with WASI which was calculated using the Gaussian model (eq. (3) in Gege 2000) and the average model parameters determined for Lake Constance (Table 1 in Gege 2000). It is shown in Fig. 2.2.

Detritus. Detritus is the collective name for all absorbing non-algal particles in the water. It is also known as tripton (Gitelson et al. 2008) or bleached particles (Doerffer and Schiller 2007). Its absorption spectrum is parameterised as $a_d(\lambda) = D a_d^*(\lambda)$, with $a_d^*(\lambda)$ denoting specific absorption, normalized at the same wavelength λ_0 as Gelbstoff, and $D = a_d(\lambda_0)$ describing the absorption coefficient at λ_0 . The spectrum $a_d^*(\lambda)$ is imported from file. The default spectrum provided with WASI is shown in Fig. 2.2. It was calculated as $\exp[-S_d(\lambda-\lambda_0)]$ using $\lambda_0 = 440$ nm and $S_d = 0.008$ nm⁻¹ (Doerffer and Schiller 2007).

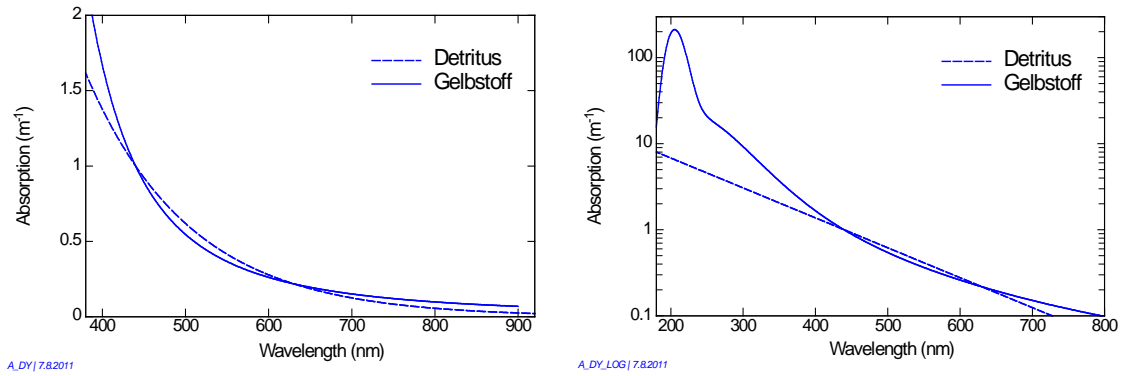


Fig. 2.2: Normalised absorption spectra of Gelbstoff, $a_Y^*(\lambda)$, and detritus, $a_D^*(\lambda)$. Left: y-axis linear, right: y-axis logarithmic.

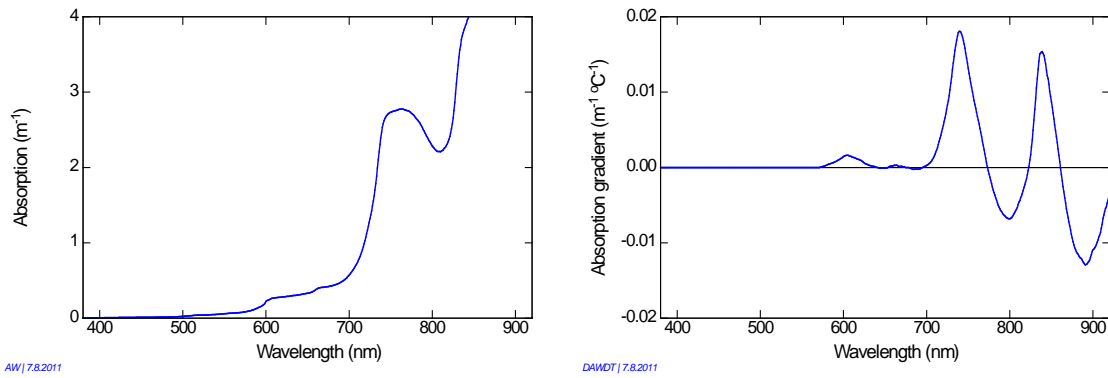


Fig. 2.3: Pure water absorption, $a_W(\lambda)$, and temperature gradient of water absorption, $da_W(\lambda)/dT$.

2.1.2 Natural water

The bulk absorption of a natural water body is the sum of absorption of pure water and of the water constituents:

$$a(\lambda) = a_W(\lambda) + (T - T_0) \cdot \frac{da_W(\lambda)}{dT} + a_{WC}(\lambda). \quad (2.3)$$

Absorption of pure water is split up into a temperature-independent term a_W , which is valid at a reference temperature T_0 , and a temperature gradient da_W/dT with T being the actual water temperature. The spectra $a_W(\lambda)$ and $da_W(\lambda)/dT$ are shown in Fig. 2.3.

The spectrum $a_W(\lambda)$ provided with WASI is a combination from different sources for a temperature of $T_0 = 20$ °C. 196-227 nm: Quickenden & Irvin (1980); 228-390 nm: Interpolation between Quickenden & Irvin (1980) and Buiteveld et al. (1994); 391-787 nm: Buiteveld et al. (1994); 788-874 nm: own unpublished measurements on UV-treated pure water of 20°C; 875-2000 nm: Palmer & Williams (1974), 27°C. For $da_W(\lambda)/dT$ a spectrum is provided which was measured by Gege (unpublished data).

2.2 Backscattering

Backscattering b_b of a water body is the sum of backscattering by pure water (index "W") and suspended matter. For the latter, a mixture of two spectrally different types is implemented:

$$b_b(\lambda) = b_{b,W}(\lambda) + X \cdot b_{b,X^*} \cdot b_X(\lambda) + C_{Mic} \cdot b_{b,Mic^*} \cdot (\lambda/\lambda_S)^n. \quad (2.4)$$

The first type is defined by a scattering coefficient with arbitrary wavelength dependency, $b_X(\lambda)$, the second type by a scattering coefficient following the Angström law $(\lambda/\lambda_S)^n$.⁴

2.2.1 Pure water

For pure water, the empirical relation of Morel (1974) is used: $b_{b,W}(\lambda) = b_1 \cdot (\lambda/\lambda_1)^{-4.32}$. The specific backscattering coefficient, b_1 , depends on salinity. It is $b_1 = 0.00111 \text{ m}^{-1}$ for fresh water and $b_1 = 0.00144 \text{ m}^{-1}$ for oceanic water with a salinity of 35–38 ‰, when $\lambda_1 = 500 \text{ nm}$ is chosen as reference wavelength.

2.2.2 Suspended particles of Type I

Suspended particles of Type I are defined by a scattering coefficient with arbitrary wavelength dependency, $b_X(\lambda)$, which is imported from file. X is the concentration and b_{b,X^*} the specific backscattering coefficient. The user has several options for calculation:

- X can be treated either as an independent parameter, or $X = C_0$ can be set, where C_0 is the concentration of phytoplankton class no. 0 (see eq. 1). The latter is useful for Case 1 water types where the concentrations of particles and phytoplankton are highly correlated.
- b_{b,X^*} can be treated either as constant with a default value of $0.0086 \text{ m}^2 \text{ g}^{-1}$ (Heege 2000), or as $b_{b,X^*} = A \cdot X^B$. Such a non-linear dependency of scattering on concentration was observed for phytoplankton (Morel 1980). It may be used for Case 1 water types, while $b_{b,X^*} = \text{constant}$ is appropriate for Case 2 waters with significant sources of non-phytoplankton suspended matter. Typical values of the empirical constants are $A = 0.0006 \text{ m}^2 \text{ g}^{-1}$ and $B = -0.37$ (Sathyendranath et al. 1989), which are set as defaults in WASI.
- $b_X(\lambda)$ can either be read from file, or it can be calculated as $b_X(\lambda) = a_0^*(\lambda_L) / a_0^*(\lambda)$, where $a_0^*(\lambda)$ is the specific absorption spectrum of phytoplankton class no. 0 (see eq. 1), and λ_L denotes a reference wavelength ($\lambda_L = 550 \text{ nm}$ by default). This method assumes that particle backscattering originates mainly from phytoplankton cells, and couples absorption and scattering according to the Case 1 waters model of Sathyendranath et al. (1989). However, such coupling may be used in exceptional cases only, since living algae have a negligible influence on the backscattering process by oceanic waters (Ahn et al. 1992), and in Case 2 waters particle scattering is weakly related to phytoplankton absorption in general. In WASI, $b_X(\lambda) = 1$ is set as default.

⁴ In previous versions of WASI, the first type was termed "large particles" and the second type "small particles".

2.2.3 Suspended particles of Type II

Suspended particles of Type II are defined by the normalized scattering coefficient $(\lambda/\lambda_S)^n$, where the Angström exponent n is related to the particle size distribution. C_{Mie} is the concentration and $b_{b,Mie}^*$ the specific backscattering coefficient. The parameters are set by default to $b_{b,Mie}^* = 0.0042 \text{ m}^2 \text{ g}^{-1}$, $\lambda_S = 500 \text{ nm}$, $n = -1$, which are representative for Lake Constance (Heege 2000).

In the open ocean, the exponent n typically ranges from -1 for low to 0 for high (above $2 \mu\text{g/l}$) chlorophyll-a concentrations (Morel 1988, Morel and Maritorena 2001). In coastal waters, the backscattering coefficients are spectrally rather flat, corresponding to n values around zero (Babin et al. 2003, Chami et al. 2005). Mass-specific scattering coefficients are typically in the order of 0.5 to $1.0 \text{ m}^2 \text{ g}^{-1}$ at 555 nm (Babin et al. 2003), and the ratio of backscattering to total scattering ranges from about 0.2% to 3% (Chami et al. 2005, Antoine et al. 2011), hence $b_{b,Mie}^*$ is in the range from about 0.001 to $0.03 \text{ m}^2 \text{ g}^{-1}$ for λ_S around 555 nm .

2.3 Attenuation

The diffuse attenuation coefficient of irradiance E is defined as $K = -(1/E) dE/dz$, where z is the depth. Similarly, the attenuation coefficient of radiance L is defined as $k = -(1/L) dL/dz$. Attenuation is an apparent optical property (AOP) and depends not only on the properties of the medium, but additionally on the geometric distribution of the illuminating light field.

2.3.1 Diffuse attenuation for downwelling irradiance

The most important attenuation coefficient is K_d , which describes attenuation for downwelling vector irradiance. Gordon (1989) has shown for Case 1 waters that the geometric structure of the light field can be corrected, and the corrected attenuation coefficient, $\bar{\mu}_d K_d$, is, to a high degree of accuracy, an inherent optical property which can be related to absorption $a(\lambda)$ and backscattering $b_b(\lambda)$. The correction factor is the ratio of downwelling vector irradiance to downwelling scalar irradiance: $\bar{\mu}_d = E_d / E_{0d}$. $\bar{\mu}_d$ is also called the average cosine of the downwelling light field, since it were $\bar{\mu}_d = \cos \theta'_{\text{sun}}$ if there were no atmosphere, with θ'_{sun} the sun zenith angle in water. Gordon showed by Monte Carlo simulations that, for sun zenith angles below 60° , the difference between $\bar{\mu}_d$ and $\cos \theta'_{\text{sun}}$ is usually below 3 % near the water surface. Thus, the following parameterization of K_d is adapted from Gordon (1989):

$$K_d(\lambda) = \kappa_0 \cdot \frac{a(\lambda) + b_b(\lambda)}{\cos \theta'_{\text{sun}}}. \quad (2.5)$$

$a(\lambda)$ is calculated according to eq. (2.3), $b_b(\lambda)$ using eq. (2.4). The coefficient κ_0 depends on the scattering phase function. Gordon (1989) determined a value of $\kappa_0 = 1.0395$ from Monte Carlo simulations in Case 1 waters, Albert and Mobley (2003) found a value of $\kappa_0 = 1.0546$ from simulations in Case 2 waters using the radiative transfer program Hydrolight (Mobley et al. 1993). Some authors use eq. (2.5) with $\kappa_0 = 1$ (Sathyendranath and Platt 1988, 1997; Gordon et al. 1975). In WASI, κ_0 is read from the WASI.INI file; the default value is 1.0546.

2.3.2 Diffuse attenuation for upwelling irradiance

For upwelling irradiance two attenuation coefficients are used: K_{uW} for the radiation backscattered in the water, and K_{uB} for the radiation reflected from the bottom. The following parameterization is adopted from Albert and Mobley (2003):

$$K_{uW}(\lambda) = [a(\lambda) + b_b(\lambda)] \cdot [1 + \omega_b(\lambda)]^{1.9991} \cdot \left[1 + \frac{0.2995}{\cos \theta'_{\text{sun}}} \right]. \quad (2.6)$$

$$K_{uB}(\lambda) = [a(\lambda) + b_b(\lambda)] \cdot [1 + \omega_b(\lambda)]^{1.2441} \cdot \left[1 + \frac{0.5182}{\cos \theta'_{\text{sun}}} \right]. \quad (2.7)$$

The function $\omega_b(\lambda)$ depends on absorption $a(\lambda)$ and backscattering $b_b(\lambda)$ of the water body:

$$\omega_b(\lambda) = \frac{b_b(\lambda)}{a(\lambda) + b_b(\lambda)}. \quad (2.8)$$

Eqs. (2.6) and (2.7) are used implicitly in the model of irradiance reflectance in shallow waters, see eq. (2.16).

2.3.3 Attenuation for upwelling radiance

For upwelling radiance two attenuation coefficients are used: k_{uW} for the radiation backscattered in the water, and k_{uB} for the radiation reflected from the bottom. The following parameterization is adopted from Albert and Mobley (2003):

$$k_{uW}(\lambda) = \frac{a(\lambda) + b_b(\lambda)}{\cos \theta'_v} \cdot [1 + \omega_b(\lambda)]^{3.5421} \cdot \left[1 - \frac{0.2786}{\cos \theta'_{sun}} \right]. \quad (2.9)$$

$$k_{uB}(\lambda) = \frac{a(\lambda) + b_b(\lambda)}{\cos \theta'_v} \cdot [1 + \omega_b(\lambda)]^{2.2658} \cdot \left[1 + \frac{0.0577}{\cos \theta'_{sun}} \right]. \quad (2.10)$$

These equations are used implicitly in the model of remote sensing reflectance in shallow waters, see eq. (2.19).

2.4 Specular reflectance

An above-water radiance sensor looking down to the water surface measures the sum of two radiance components: one from the water body, one from the surface. The first comprises the desired information about the water constituents, the second is an unwanted add-on which has to be corrected. However, correction is difficult. For example, the method from the SeaWiFS protocols (Mueller and Austin 1995), which is widely used in optical oceanography, leads to rms errors of the corrected water leaving radiance as large as 90 % under typical field conditions (Toole et al. 2000). Thus, WASI offers different methods.

The radiance reflected from the surface, $L_r(\lambda)$, is a fraction ρ_L of sky radiance $L_s(\lambda)$:

$$L_r(\lambda) = \rho_L \cdot L_s(\lambda). \quad (2.11)$$

$L_s(\lambda)$ is the average radiance of that area of the sky that is specularly reflected into the sensor. It can be imported from file or calculated using eq. (2.26). ρ_L is the Fresnel reflectance and depends on the angle of reflection. The value can either be specified by the user or it can be calculated from the viewing angle θ_v using the Fresnel equation for unpolarized light (Jerlov 1976):

$$\rho_L = \frac{1}{2} \left| \frac{\sin^2(\theta_v - \theta'_v)}{\sin^2(\theta_v + \theta'_v)} + \frac{\tan^2(\theta_v - \theta'_v)}{\tan^2(\theta_v + \theta'_v)} \right|. \quad (2.12)$$

θ'_v is the angle of refraction, which is related to θ_v by Snell's law $n_W \sin\theta'_v = \sin\theta_v$, where $n_W \approx 1.33$ is the refractive index of water. For viewing angles near nadir, $\rho_L \approx 0.02$.

The ratio of the radiance reflected from the water surface to the downwelling irradiance,

$$R_{rs}^{surf}(\lambda) = \frac{L_r(\lambda)}{E_d(\lambda)} = \rho_L \cdot \frac{L_s(\lambda)}{E_d(\lambda)}, \quad (2.13a)$$

is called specular reflectance. $E_d(\lambda)$ and $L_s(\lambda)$ can either be imported from file, or one or both can be calculated using eq. (2.23) or (2.26). If the wavelength-independent model of surface reflection is chosen, it is

$$R_{rs}^{surf} = \frac{\rho_L}{\pi}. \quad (2.13b)$$

Toole et al. (2000) showed that $R_{rs}^{surf}(\lambda)$ is nearly spectrally flat at overcast sky, but clearly not for clear-sky conditions. Thus, eq. (2.13a) should be used in general, and eq. (2.13b) at most for days with overcast sky.

2.5 Irradiance reflectance

The ratio of upwelling irradiance to downwelling irradiance in water, $R(\lambda) = E_u^-(\lambda) / E_d^-(\lambda)$, is called irradiance reflectance (Mobley 1994). It is an apparent optical property (AOP) and depends not only on the properties of the medium, but also on the geometric distribution of the incoming light.

2.5.1 Deep water

A suitable parameterization which separates to a large extent the parameters of water and of the illumination was found by Gordon et al. (1975):

$$R(\lambda) = f \cdot \omega_b(\lambda) + Q \cdot R_{rs,F}^-(\lambda). \quad (2.14)$$

$R_{rs,F}^-(\lambda)$ denotes the contribution caused by fluorescence; it is calculated using eq. (2.31). The function $\omega_b(\lambda)$, which is given by eq. (2.8), depends only on inherent optical properties of the water body, absorption and backscattering. The factor f comprises the illumination dependencies. It can be treated either as an independent parameter with a default value of 0.33 according to Gordon et al. (1975), or the relationship of Albert and Mobley (2003) can be used:

$$f = 0.1034 \cdot \left(1 + 3.3586 \cdot \omega_b - 6.5358 \cdot \omega_b^2 + 4.6638 \cdot \omega_b^3 \right) \cdot \left(1 + \frac{2.4121}{\cos \theta'_{\text{sun}}} \right). \quad (2.15)$$

θ'_{sun} is the sun zenith angle in water. Eq. (2.15) takes into consideration the fact that f depends not only on the geometric structure of the light field, expressed by the parameter θ'_{sun} , but also on the absorption and scattering properties of the water. Some alternate models of f are also included in WASI and can be used if desired, namely those of Kirk (1984), Morel and Gentili (1991), and Sathyendranath and Platt (1997). The equations are given in chapter 6.2.

Independently from Gordon, Prieur (1976) found the relation $R(\lambda) = f' \cdot b_b(\lambda) / a(\lambda)$. It is also included in WASI. However, the Gordon algorithm (2.14) is favoured and set as default, because it restricts the ω_b values to the physically reasonable range from 0 to 1, which is not the case for the Prieur equation.

2.5.2 Shallow water

For shallow water, the parameterization of Albert and Mobley (2003) is used:

$$R^{\text{sh}}(\lambda) = R(\lambda) \cdot \left[1 - A_1 \cdot \exp\left\{-\left(K_d(\lambda) + K_{uW}(\lambda)\right) \cdot z_B\right\}\right] + A_2 \cdot R^b(\lambda) \cdot \exp\left\{-\left(K_d(\lambda) + K_{uB}(\lambda)\right) \cdot z_B\right\} \quad (2.16)$$

The first term on the right-hand side is the reflectance of a water layer of thickness z_B , the second term the contribution of the bottom. Bottom reflectance $R^b(\lambda)$ is calculated using eq. (2.21). The K 's account for attenuation within the water layer and are calculated using eqs. (2.5), (2.6), and (2.7). The empirical constants are set to $A_1 = 1.0546$ and $A_2 = 0.9755$ according to Albert and Mobley (2003) and cannot be changed by the user.

2.6 Remote sensing reflectance

The ratio of upwelling radiance to downwelling irradiance, $R_{rs}(\lambda) = L_u(\lambda) / E_d(\lambda)$, is called remote sensing reflectance (Mobley 1994). It is an apparent optical property (AOP), i.e. it depends on the geometric distribution of the incoming light.

2.6.1 Deep water

The remote sensing reflectance below the water surface is, for deep water, proportional to $R(\lambda)$:

$$R_{rs}^-(\lambda) = \frac{R(\lambda)}{Q}. \quad (2.17a)$$

This follows from the definitions $R_{rs}^- \equiv L_u^- / E_d^-$, $Q \equiv E_u^- / L_u^-$, and $R \equiv E_u^- / E_d^-$. $R(\lambda)$ is either calculated using eq. (2.14), or imported from file. The factor Q , which is a measure of the anisotropy of the light field in water, is treated in WASI as a wavelength-independent parameter with a default value of 5 sr. It depends on the geometric distribution of the upwelling and downwelling light, and thus on the scattering and absorption properties of the water body. Consequently, Q depends on wavelength. However, this is not accounted for in WASI, since no convenient parameterization of Q is known. Yet, an alternative to eq. (2.17a) with a convenient parameterization of the factor f_{rs} was found by Albert and Mobley (2003):

$$R_{rs}^-(\lambda) = f_{rs} \cdot \omega_b(\lambda) + R_{rs,F}(\lambda). \quad (2.17b)$$

$R_{rs,F}$ is the contribution caused by fluorescence and calculated using eq. (2.47). Note that fluorescence is also included in eq. (2.17a) through $R(\lambda)$ according to eq. (2.14). The following parameterization of the factor f_{rs} is valid for both deep and shallow waters (Albert and Mobley 2003):

$$f_{rs} = 0.0512 \cdot \left(1 + 4.6659 \cdot \omega_b - 7.8387 \cdot \omega_b^2 + 5.4571 \cdot \omega_b^3\right) \cdot \left(1 + \frac{0.1098}{\cos \theta'_{sun}}\right) \cdot \left(1 + \frac{0.4021}{\cos \theta'_v}\right). \quad (2.18)$$

Parameters of f_{rs} are ω_b of eq. (2.8), the sun zenith angle in water, θ'_{sun} , and the viewing angle in water, θ'_v . Alternately, f_{rs} can be calculated in WASI as $f_{rs} = f / Q$ using the ill-favoured parameter Q .

2.6.2 Shallow water

For shallow water, the following parameterization is chosen (Albert and Mobley 2003):

$$R_{rs}^{sh-}(\lambda) = R_{rs}^-(\lambda) \cdot \left[1 - A_{rs,1} \cdot \exp\left\{-\left(K_d(\lambda) + k_{uw}(\lambda)\right) \cdot z_B\right\}\right] + A_{rs,2} \cdot R_{rs}^b(\lambda) \cdot \exp\left\{-\left(K_d(\lambda) + k_{ub}(\lambda)\right) \cdot z_B\right\} \quad (2.19)$$

The first term on the right-hand side is the reflectance of a water layer of thickness z_B , the second term the contribution of the bottom. Bottom reflectance $R_{rs}^b(\lambda)$ is calculated using eq. (2.22). K_d , k_{uW} and k_{uB} account for attenuation within the water layer and are calculated using eqs. (2.5), (2.9), and (2.10), respectively. The empirical constants are set to $A_{rs,1} = 1.1576$ and $A_{rs,2} = 1.0389$ according to Albert and Mobley (2003) and cannot be changed by the user.

2.6.3 Above the surface

The remote sensing reflectance above the water surface is related to radiance and irradiance spectra in water as follows:

$$R_{rs}(\lambda) = \frac{L_u(\lambda)}{E_d(\lambda)} = \frac{\frac{1-\sigma_L^-}{n_w^2} \cdot L_u^-(\lambda)}{E_d(\lambda)} + \frac{\rho_L \cdot L_s(\lambda)}{E_d(\lambda)} = \frac{\frac{(1-\sigma_L^-)(1-\sigma)}{n_w^2} \cdot L_u^-(\lambda)}{E_d^-(\lambda) - \rho_u \cdot E_u^-(\lambda)} + \rho_L \cdot \frac{L_s(\lambda)}{E_d(\lambda)}.$$

Eq. (2.29) was used to replace $L_u(\lambda)$, and eq. (2.24) to express $E_d(\lambda)$ in terms of $E_d^-(\lambda)$ and $E_u^-(\lambda)$. The first term on the right-hand side describes reflection in the water, the second at the surface. By using $L_u^-(\lambda) = E_u^-(\lambda) / Q$, multiplying numerator and denominator of the first term with $R(\lambda) / E_u^-(\lambda)$ (where $R(\lambda) = E_u^-(\lambda) / E_d^-(\lambda)$), and expressing the second term as $R_{rs}^{surf}(\lambda)$ according to eq. (2.13a), the following equation is obtained:

$$R_{rs}(\lambda) = \frac{(1-\sigma)(1-\sigma_L^-)}{n_w^2 \cdot Q} \cdot \frac{R(\lambda)}{1-\rho_u \cdot R(\lambda)} + R_{rs}^{surf}(\lambda). \quad (2.20a)$$

Replacing $R(\lambda)$ by $R_{rs}(\lambda)$ according to eq. (2.17a) yields the following relationship:

$$R_{rs}(\lambda) = \frac{(1-\sigma)(1-\sigma_L^-)}{n_w^2} \cdot \frac{R_{rs}^-(\lambda)}{1-\rho_u \cdot Q \cdot R_{rs}^-(\lambda)} + R_{rs}^{surf}(\lambda). \quad (2.20b)$$

This eq. was used, for example, by Lee et al. (1998) for comparing simulated remote sensing reflectance spectra above and below the surface and calculating the conversion factors, for which they found as typical values $(1-\sigma)(1-\sigma_L^-)/n_w^2 = 0.518$ and $\rho_u \cdot Q = 1.562$. The factor Q , which is difficult to assess in practice, can be avoided by replacing in the denominator $Q \cdot R_{rs}^-$ by R :

$$R_{rs}(\lambda) = \frac{(1-\sigma)(1-\sigma_L^-)}{n_w^2} \cdot \frac{R_{rs}^-(\lambda)}{1-\rho_u \cdot R(\lambda)} + R_{rs}^{surf}(\lambda). \quad (2.20c)$$

The three equations (2.20a), (2.20b), and (2.20c) are formally identical. The first term on the right-hand side of each equation describes reflection in the water, the second at the surface. Frequently, the first term alone is called remote sensing reflectance (e.g. Mobley 1994). In WASI, the reflection at the surface is also included in the R_{rs} definition. It is calculated using eq. (2.13a) or (2.13b) and can easily be excluded by setting the reflection factor σ_L equal to zero.

The factors σ , σ_L^- , and ρ_u are the reflection factors for E_d , L_u^- , and E_u^- , respectively. σ depends on the radiance distribution and on surface waves. Typical values are 0.02 to 0.03

for clear sky conditions and solar zenith angles below 45° , and 0.05 to 0.07 for overcast skies (Jerlov 1976; Preisendorfer and Mobley 1985, 1986). It is set to $\sigma = 0.03$ by default. σ_L^- can either be calculated as a function of θ_v using eq. (2.12), or a constant value can be taken. ρ_u is in the range of 0.50 to 0.57 with a value of 0.54 being typical (Jerome et al. 1990; Mobley 1999). The defaults of the other constants are set to $Q = 5$ sr and $n_w = 1.33$.

Which of the equations is used, depends on the application:

- Eq. (20a) is useful when $R_{rs}(\lambda)$ shall be connected to $R(\lambda)$, for example if in-situ measurements of $R(\lambda)$ were performed as "ground truth" for a remote sensing instrument.
- Eq. (20b) links remote sensing reflectance in water to that in air. Since the same spectrum type is used above and below the water surface, it is the most convenient parameterisation. This equation is used by default.
- Eq. (20c) avoids the use of the factor Q , which is difficult to assess. The equation is useful, for example, for optical closure experiments which investigate the consistency of measurements above and below the water surface by measuring simultaneously the spectra $R_{rs}(\lambda)$, $R(\lambda)$, and $R_{rs}^-(\lambda)$.

Eq. (2.20a), (2.20b) or (2.20c) is also used to calculate the corresponding spectrum $R_{rs}^{sh}(\lambda)$ for shallow water. $R(\lambda)$ is replaced by $R^{sh}(\lambda)$, and $R_{rs}^-(\lambda)$ by $R_{rs}^{sh-}(\lambda)$ in the case of shallow water.

2.7 Bottom reflectance

The models of bottom reflectance are used to calculate reflectance and radiance spectra in shallow waters. However, they can be applied as well to land surfaces, if the input spectra are replaced by suitable albedo spectra from terrestrial bottom types.

2.7.1 For irradiance sensors

The irradiance reflectance of a surface is called albedo. When N different surfaces of albedo $a_n(\lambda)$ are viewed simultaneously, the measured albedo is the following sum:

$$R^b(\lambda) = \sum_{n=0}^{N-1} f_n \cdot a_n(\lambda). \quad (2.21)$$

f_n is the areal fraction of surface number n within the sensor's field of view; it is $\sum f_n = 1$. This equation is implemented in WASI for $N = 6$ bottom types. The spectra $a_n(\lambda)$ provided with WASI are shown in Fig. 2.4. They were measured by Pinnel (2005) using a submersible RAMSES spectroradiometer. Three of them represent bare bottom, the other green makrophytes:

0. constant: an artificial spectrum with constant albedo of 10 %;
1. sand: sandy bottom in a coastal shallow area in Bolivar (South Australia);
2. silt: fine-grained sediment in 50 cm water depth close to the shoreline of Starnberger See (Germany);
3. Chara aspera: green makrophyte from Bodensee (Lake Constance, Germany);
4. Potamogeton perfoliatus: green makrophyte from Starnberger See (Germany);
5. Potamogeton pectinatus: green makrophyte from Starnberger See (Germany).

2.7.2 For radiance sensors

When the upwelling radiation is measured by a radiance sensor, the corresponding remote sensing reflectance can be expressed as follows:

$$R_{rs}^b(\lambda) = \sum_{n=0}^{N-1} f_n \cdot B_n \cdot a_n(\lambda). \quad (2.22)$$

B_n is the proportion of radiation which is reflected towards the sensor. In WASI, the B_n 's of all surfaces are assumed to be angle-independent. The default values are set to $B_n = 1/\pi = 0.318 \text{ sr}^{-1}$, which represents isotropic reflection (Lambertian surfaces).

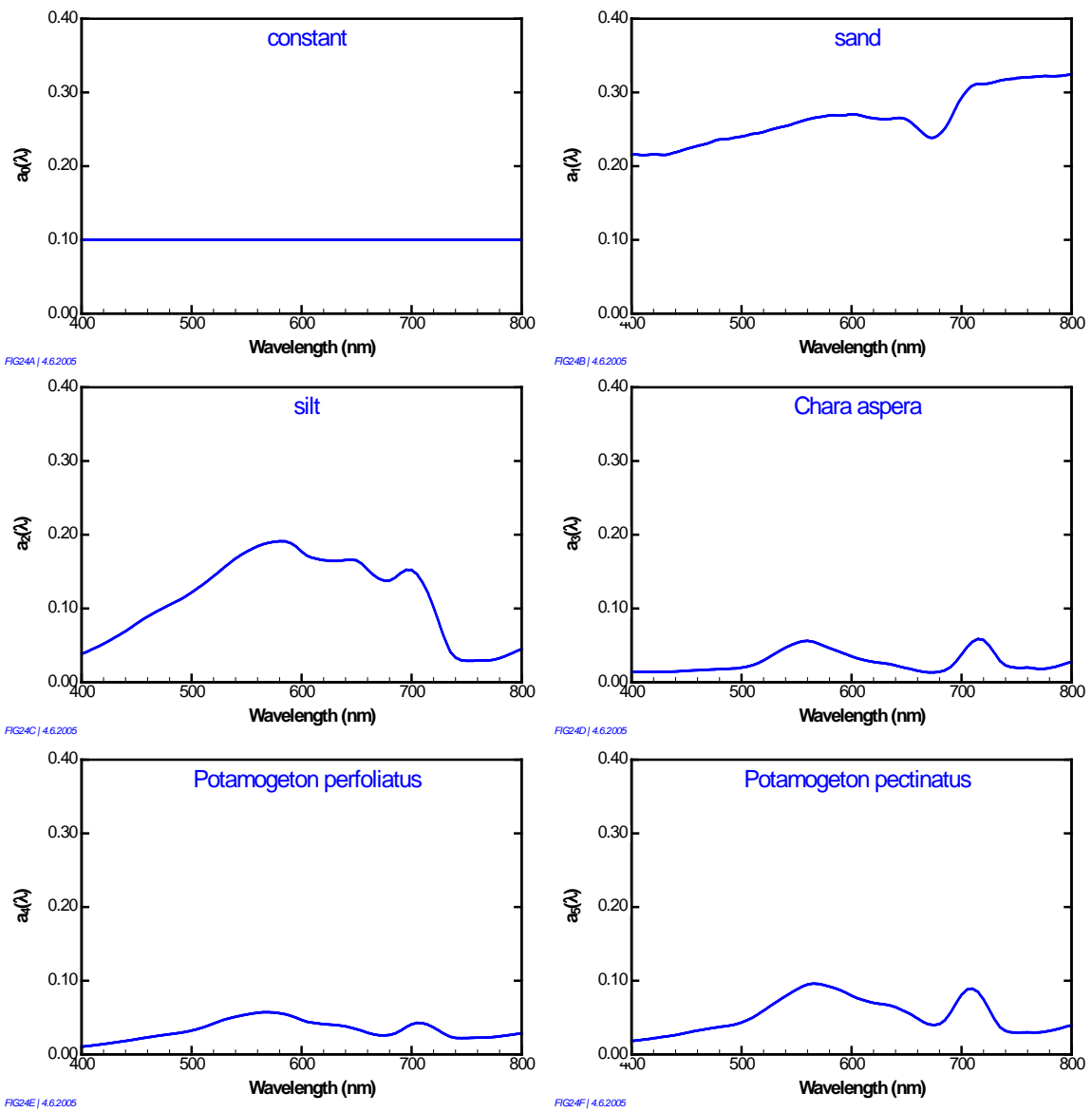


Fig. 2.4: Spectral albedo of 6 bottom types.

2.8 Downwelling irradiance

2.8.1 Above water surface

The downwelling irradiance spectrum, $E_d(\lambda)$, is split into a direct and a diffuse component:

$$E_d(\lambda) = f_{dd} \cdot E_{dd}(\lambda) + f_{ds} \cdot E_{ds}(\lambda). \quad (2.23)$$

$E_{dd}(\lambda)$ is the direct component of the downwelling irradiance, representing the sun disk in the sky as light source. The radiation from the sky, i.e. the diffuse downwelling irradiance, is split into two components: $E_{ds}(\lambda) = E_{dsr}(\lambda) + E_{dsa}(\lambda)$, with $E_{dsr}(\lambda)$ representing Rayleigh scattering, and $E_{dsa}(\lambda)$ aerosol scattering. The parameters f_i are the intensities of the "light sources" E_i relative to conditions with undisturbed illumination geometry. These reference conditions (with $f_i = 1$) are defined by a cloudless atmosphere, unobscured view of the upper hemisphere, and an horizontally oriented sensor with an angular response equal to the cosine of the incidence angle. $0 \leq f_i < 1$ corresponds to measurements when intensity is decreased (due to shadows, sensor tilt or deviations from the cosine response), $f_i > 1$ when intensity is increased.

The calculation of $E_i(\lambda)$ is based on equations and data of Gregg and Carder (1990), which these authors derived from Bird and Riordan (1986). The adopted equations are recalled briefly. Eq. (2.23) extends these models by adding weights f_i which allow simulation and analysis of measurements at non-standard conditions.

The three components of downwelling irradiance are calculated as follows:

$$E_{dd}(\lambda) = E_0(\lambda) \cos\theta_{\text{sun}} T_r(\lambda) T_{aa}(\lambda) T_{as}(\lambda) T_{oz}(\lambda) T_o(\lambda) T_{wv}(\lambda), \quad (2.24)$$

$$E_{dsr}(\lambda) = \frac{1}{2} E_0(\lambda) \cos \theta_{\text{sun}} (1 - T_r(\lambda)^{0.95}) T_{aa}(\lambda) T_{oz}(\lambda) T_o(\lambda) T_{wv}(\lambda), \quad (2.25)$$

$$E_{dsa}(\lambda) = E_0(\lambda) \cos \theta_{\text{sun}} T_r(\lambda)^{1.5} T_{aa}(\lambda) T_{oz}(\lambda) T_o(\lambda) T_{wv}(\lambda) (1 - T_{as}(\lambda)) F_a. \quad (2.26)$$

$E_0(\lambda)$ is the extraterrestrial solar irradiance corrected for earth-sun distance and orbital eccentricity, θ_{sun} the solar zenith angle, F_a aerosol forward scattering probability, and the T_i denote transmittance of the atmosphere after scattering or absorption of component i (T_r : Rayleigh scattering, T_{aa} : aerosol absorption, T_{as} : aerosol scattering, T_{oz} : ozone absorption, T_o : oxygen absorption, T_{wv} water vapour absorption). The T_i are given by:

$$T_r(\lambda) = \exp[-M'/(115.6406\lambda^4 - 1.335\lambda^2)], \quad (2.27)$$

$$T_{aa}(\lambda) = \exp[-(1 - \omega_a)\tau_a(\lambda)M], \quad (2.28)$$

$$T_{as}(\lambda) = \exp[-\omega_a\tau_a(\lambda)M], \quad (2.29)$$

$$T_{oz}(\lambda) = \exp[-a_{oz}(\lambda)H_{oz}M_{oz}], \quad (2.30)$$

$$T_o(\lambda) = \exp\frac{-1.41a_o(\lambda) \cdot M'}{[1 + 118.3a_o(\lambda) \cdot M']^{0.45}}, \quad (2.31)$$

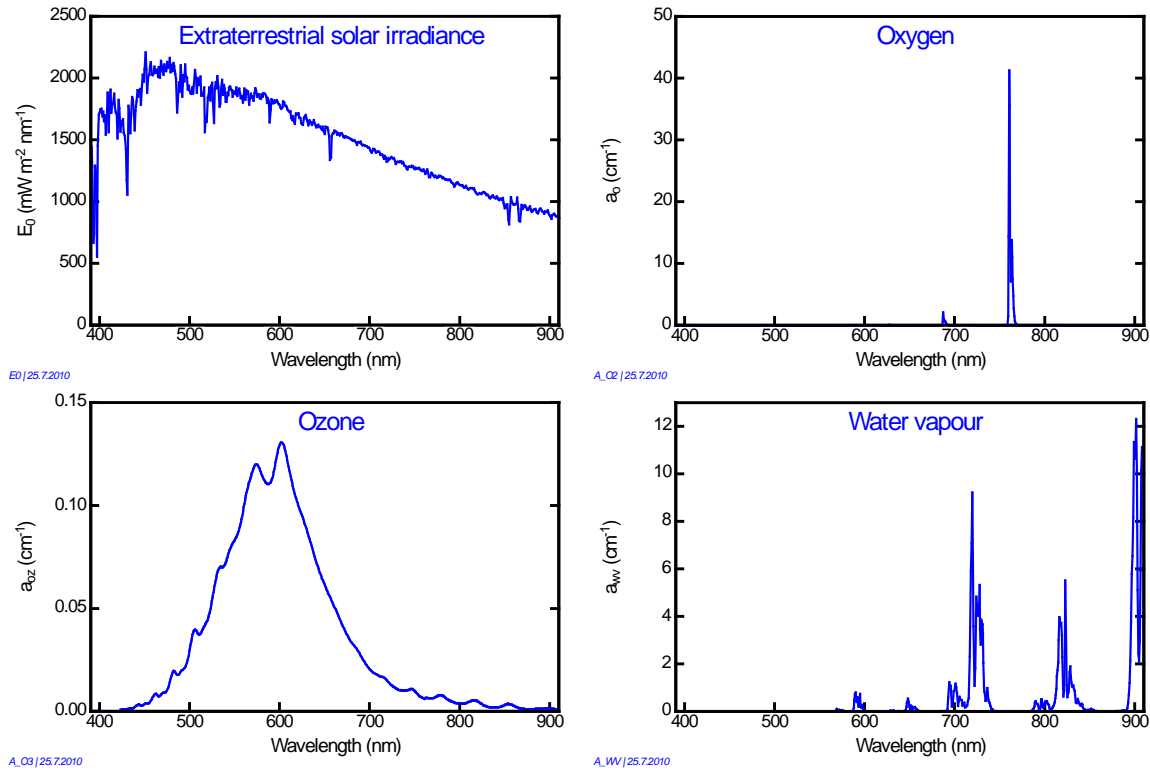


Fig. 2.5: The four input spectra of the irradiance model.

$$T_{wv}(\lambda) = \exp \frac{-0.2385 a_{wv}(\lambda) \cdot WV \cdot M}{[1 + 20.07 a_{wv}(\lambda) \cdot WV \cdot M]^{0.45}} \quad (2.32)$$

The atmospheric path length is $M = 1/[\cos\theta_{\text{sun}} + a(90^\circ + b - \theta_{\text{sun}})^{-c}]$. The numerical values used by Gregg and Carder ($a = 0.15$, $b = 3.885^\circ$, $c = 1.253$) were replaced by updated values $a = 0.50572$, $b = 6.07995^\circ$, $c = 1.6364$ from Kasten and Young (1989). $M' = MP/(1013.25 \text{ mbar})$ is the path length corrected for nonstandard atmospheric pressure P , and $M_{\text{oz}} = 1.0035/(\cos^2\theta_{\text{sun}} + 0.007)^{1/2}$ is the path length for ozone.

Aerosol is parameterised in terms of aerosol optical thickness, $\tau_a = \beta \cdot (\lambda/\lambda_a)^{-\alpha}$, and aerosol single scattering albedo, $\omega_a = (-0.0032AM + 0.972) \cdot \exp(3.06 \cdot 10^{-4}RH)$. The Angström exponent α determines the wavelength dependency, the turbidity coefficient β is a measure of concentration. The reference wavelength λ_a is set in WASI by default to 550 nm.⁵ α typically ranges from 0.2 to 2, β from 0.16 to 0.50. β is related to horizontal visibility V and aerosol scale height H_a : $\beta = \tau_a(550) = 3.91 \cdot H_a/V$. Typical values are 8 to 24 km for V , and 1 km for H_a . The parameters of ω_a are air mass type, AM , which ranges from 1 (typical of open-ocean aerosols) to 10 (typical of continental aerosols), and relative humidity, RH , with typical values from 46 to 91 %. Aerosol forward scattering probability is calculated using the equation $F_a = 1 - 0.5 \exp[(B_1 + B_2 \cos\theta_{\text{sun}}) \cdot \cos\theta_{\text{sun}}]$ with $B_1 = B_3[1.459 + B_3(0.1595 + 0.4129B_3)]$, $B_2 = B_3[0.0783 + B_3(-0.3824 - 0.5874 B_3)]$, $B_3 = \ln(1 - \langle \cos\theta_{\text{sun}} \rangle)$, and $\langle \cos\theta_{\text{sun}} \rangle = -0.1417\alpha + 0.82$. Water vapour concentration, WV , is expressed in units of precipitable water, which typically ranges from 0 to 5 cm.

⁵ Frequently $\lambda_a = 1 \mu\text{m}$ is set, e.g. Gregg and Carder (1990).

The calculations make use of four spectra which are imported from file: $E_0(\lambda)$, $a_o(\lambda)$, $a_{oz}(\lambda)$, and $a_{wv}(\lambda)$. The spectra provided with WASI are shown in Fig. 2.5. They were calculated using the radiative transfer model MODTRAN-3 (Gege 2012).

2.8.2 Below water surface

The downwelling irradiance just below the water surface (indicated by the symbol 0–) is calculated as follows:

$$E_d(\lambda, 0-) = f_{dd} \cdot (1-\rho_{dd}) \cdot E_{dd}(\lambda) + f_{ds} \cdot (1-\rho_{ds}) \cdot E_{ds}(\lambda) + \rho_u \cdot E_u(\lambda, 0-). \quad (2.33)$$

The factors f_{dd} and f_{ds} are much more variable in water than in air, because the wavy water surface induces strong focusing effects (Dera and Stramski 1993, Zanefeld et al. 2001). ρ_{dd} and ρ_{ds} describe the losses of downwelling irradiance at the air–water interface, $E_u(\lambda, 0-)$ is the upwelling spectral irradiance in water, and ρ_u is the reflection factor of the water surface for $E_u(\lambda, 0-)$. The reflection factor for the direct downwelling component is calculated using the Fresnel equation (Jerlov 1976)

$$\rho_{dd} = \frac{1}{2} \left| \frac{\sin^2(\theta_{sun} - \theta'_{sun})}{\sin^2(\theta_{sun} + \theta'_{sun})} + \frac{\tan^2(\theta_{sun} - \theta'_{sun})}{\tan^2(\theta_{sun} + \theta'_{sun})} \right|; \quad (2.34)$$

that of the diffuse downwelling component using the empirical equation (Gege 2012)

$$\rho_{ds} = 0.06087 + 0.03751 \cdot (1-\cos\theta_{sun}) + 0.1143 \cdot (1-\cos\theta_{sun})^2; \quad (2.35)$$

and that of the upwelling component is set to $\rho_u = 0.54$ by default (Jerome et al. 1990, Mobley 1999). Using the irradiance reflectance $R(\lambda) = E_u(\lambda, 0-) / E_d(\lambda, 0-)$ to remove $E_u(\lambda, 0-)$ from eq. (2.33) leads to the following expression:

$$E_d(\lambda, 0-) = f_{dd} \cdot (1-\rho_{dd}) \cdot E_{dd}(\lambda) + f_{ds} \cdot (1-\rho_{ds}) \cdot [1+\rho_u \cdot R(\lambda) \cdot (1+r_d(\lambda, 0-))] \cdot E_{ds}(\lambda). \quad (2.36)$$

$r_d(\lambda, 0-) = f_{dd}/f_{ds} \cdot E_{dd}(\lambda, 0-) / E_{ds}(\lambda, 0-)$ is the ratio of direct to diffuse irradiance just beneath the water surface. It is calculated using the equation (Gege 2012)

$$r_d(\lambda, 0-) = \frac{f_{dd}}{f_{ds}} \cdot \frac{1-\rho_{dd}}{1-\rho_{ds}} \cdot \frac{2 \cdot T_r(\lambda) \cdot T_{as}(\lambda)}{1-T_r(\lambda)^{0.95} + 2 \cdot T_r(\lambda)^{1.5} \cdot [1-T_{as}(\lambda)] \cdot F_a}. \quad (2.37)$$

Equation (2.36) is used in WASI for calculating $E_d(\lambda, 0-)$. $R(\lambda)$ is calculated using eq. (2.14) without fluorescence, i.e. $R_{rs,F}^-(\lambda) = 0$ is set. Downwelling irradiance below the surface in shallow water, $E_d^{sh}(\lambda, 0-)$, is also calculated using eq. (2.36), but with $R^{sh}(\lambda)$ instead of $R(\lambda)$.

2.8.3 At depth z

Since the path lengths are different for the direct and the diffuse component, their depth dependencies are calculated separately. The direct component is attenuated along a path with length $z / \cos\theta'_{sun}$:

$$E_{dd}(\lambda, z) = E_{dd}(\lambda, 0-) \exp\left\{-\frac{[a(\lambda) + b_p(\lambda)] \cdot z \cdot l_{dd}}{\cos \theta'_{sun}}\right\}. \quad (2.38)$$

l_{dd} is the path length of direct radiation relative to sensor depth; it is set equal to one by default. The diffuse component of downwelling irradiance at depth z is related to that below the surface as follows:

$$E_{ds}(\lambda, z) = E_{ds}(\lambda, 0-) \exp\{-[a(\lambda) + b_b(\lambda)] \cdot z \cdot l_{ds}\}. \quad (2.39)$$

The average path length of diffuse radiation relative to sensor depth, l_{ds} , is calculated using the following approximation:

$$l_{ds} = 1.1156 + 0.5504 \cdot (1 - \cos \theta'_{sun}). \quad (2.40)$$

The downwelling irradiance at depth z is the following sum:

$$E_d(\lambda, z) = f_{dd} \cdot E_{dd}(\lambda, z) + f_{ds} \cdot [1 + \rho_u \cdot R(\lambda) \cdot (1 + r_d(\lambda, 0-))] \cdot E_{ds}(\lambda, z). \quad (2.41)$$

Equations (2.36) to (2.39) were validated using Hydrolight simulations (Gege 2012); however, the upwelling radiation reflected at the water surface in downward direction was neglected in that paper (corresponding to $\rho_u = 0$).

2.9 Sky radiance

A parameterization similar to $E_d(\lambda)$ is implemented for the sky radiance, $L_s(\lambda)$:

$$L_s(\lambda) = g_{dd} \cdot E_{dd}(\lambda) + g_{dsr} \cdot E_{dsr}(\lambda) + g_{dsa} \cdot E_{dsa}(\lambda). \quad (2.42)$$

The radiance downwelling from a part of the sky is treated as a weighted sum of three wavelength dependent functions, $E_{dd}(\lambda)$, $E_{dsr}(\lambda)$ and $E_{dsa}(\lambda)$, which are given by eqs. (2.24) to (2.26). In contrast to eq. (2.23), the two diffuse components are treated separately since Rayleigh scattering has a much stronger angle dependency than aerosol scattering. The parameters g_{dd} , g_{dsr} and g_{dsa} are the intensities (in units of sr^{-1}) of $E_{dd}(\lambda)$, $E_{dsr}(\lambda)$ and $E_{dsa}(\lambda)$, respectively. The radiance $\rho_L \cdot g_{dd} \cdot E_{dd}(\lambda)$ that is reflected at the water surface into a radiance sensor is known as sun glint, and the radiance $\rho_L \cdot [g_{dsr} \cdot E_{dsr}(\lambda) + g_{dsa} \cdot E_{dsa}(\lambda)]$ as sky glint.

Note that $L_s(\lambda)$ doesn't represent the radiance of a "piece of sky" at the coordinates (θ_v, ϕ_v) , as the term "sky radiance" may indicate. The functions $E_{dd}(\lambda)$, $E_{dsr}(\lambda)$ and $E_{dsa}(\lambda)$ have been derived to parameterize the downwelling *irradiance*, but not *radiance*. Hence they are only functions of the sun zenith angle, but not of the sun azimuth angle or the viewing angles θ_v, ϕ_v . The purpose of $L_s(\lambda)$ in WASI is modeling of upwelling radiance that originates from the upper hemisphere and is reflected at the water surface [$\rho_L \cdot L_s(\lambda)$ in eq. (2.45)]. Since the water surface is almost never perfectly flat, this radiance originates from different locations of the sky, thus a parameterisation of $L_s(\lambda)$ in terms of (θ_v, ϕ_v) is not considered useful.

g_{dd} , g_{dsr} and g_{dsa} can be used as fit parameters to correct reflections at the water surface. For forward modeling, the user has to specify a value for each parameter. By default, $g_{dd} = 0.05$, $g_{dsr} = 0.5$ and $g_{dsa} = 0.1$ is set.

2.10 Upwelling radiance

The upwelling radiance is that part of the downwelling irradiance which is reflected back from the water into a down-looking radiance sensor. Calculation is based on a model of R_{rs} and a model or a measurement of E_d .

2.10.1 Below the water surface

In water, eq. (2.33) is used for calculating $E_d^-(\lambda)$, and eq. (2.17a), (2.17b) or (2.19) for $R_{rs}^-(\lambda)$. The upwelling radiance is then calculated as follows:

$$L_u^-(\lambda) = R_{rs}^-(\lambda) \cdot E_d^-(\lambda) + L_F(\lambda). \quad (2.43)$$

$L_F(\lambda)$ denotes fluorescence; it is calculated using eq. (2.54). In shallow waters, $R_{rs}^{sh-}(\lambda)$ is used instead of $R_{rs}^-(\lambda)$, and $E_d^{sh-}(\lambda)$ instead of $E_d^-(\lambda)$.

2.10.2 Above the water surface

The upwelling radiance after crossing the water-air boundary is related to the upwelling radiance in water, L_u^- , as follows:

$$L_u(\lambda, \theta_v) = \frac{1 - \sigma_L^-(\theta'_v)}{n_w^2} \cdot L_u^-(\lambda, \theta'_v) + \sigma(\theta_v) \cdot L_d(\lambda, -\theta_v). \quad (2.44)$$

θ_v is the zenith angle of the observer in air, θ'_v in water. These two angles are related to each others according to Snell's law via $n_w \sin \theta'_v = \sin \theta_v$ with n_w = refractive index of water. The first term on the right-hand side of eq. (2.44) is the radiance upwelling in the water, weakened at the interface by Fresnel reflection (factor $1 - \sigma_L^-(\theta'_v)$) and refraction (flux dilution by widening of the solid angle, factor $1/n_w^2$). The second term are specular reflections of downwelling radiance at the surface. Eq. (2.44) is valid for a flat surface, i.e. without waves.

Omitting for simplicity the symbol θ_v and using the more general model (2.11) for the radiance reflected from the surface, the following equation is obtained:

$$L_u(\lambda) = \frac{1 - \sigma_L^-}{n_w^2} \cdot L_u^-(\lambda) + \rho_L \cdot L_s(\lambda). \quad (2.45)$$

This equation is used in WASI for calculating $L_u(\lambda)$. $L_u^-(\lambda)$ is calculated using eq. (2.43). The sky radiance $L_s(\lambda)$ can either be calculated using eq. (2.42), or a measured spectrum can be imported from file. The reflection factor for upwelling radiance is set to $\sigma_L^- = 0.02$ by default. This value, which is valid for a nadir-looking sensor, can be changed in the WASI.INI file. The reflection factor for downwelling radiance, ρ_L , can either be calculated using the Fresnel equation (2.12), or it can be set constant. The default $\rho_L = 0.02$ is valid for a nadir-looking sensor. By setting $\rho_L = 0$ the water leaving radiance can be calculated. Further, $n_w = 1.33$ is set as default.

2.11 Fluorescence

Fluorescence is an inelastic process where a fraction η_F of photons incident at wavelength λ' is emitted at longer wavelengths λ . The ratio $\eta_F(\lambda, \lambda') = N/N'$ is called fluorescence quantum yield, where N and N' denote the number of photons at wavelength intervals $[\lambda, \lambda+d\lambda]$ and $[\lambda', \lambda'+d\lambda']$, respectively (Gordon 1979). The subscript "F" is used to indicate fluorescence, and the prime superscript to denote quantities which are functions of excitation wavelengths.

When fluorescence is expressed in terms of radiation quantities, care must be taken whether radiation is expressed in units of photon numbers or energy. Conversion makes use of the equation $E = hc/\lambda$ for the energy of a single photon: N photons with a wavelength of λ have the energy $E = N hc/\lambda$ and N' photons with λ' have $E' = N' hc/\lambda'$, hence $E/E' = N/N' \cdot \lambda'/\lambda$. Consequently, the ratio of radiation parameters in energy units is equal to that ratio in photon number units times the factor λ'/λ . In particular, if incident and emitted photon fluxes F and F' are expressed in units of $W m^{-3}$, the fluorescence quantum yield is given by

$$\eta_F(\lambda, \lambda') = \frac{N}{N'} = \frac{F}{F'} \cdot \frac{\lambda}{\lambda'}. \quad (2.46)$$

Fluorescence is calculated in WASI in terms of upwelling spectral radiance $L_F(\lambda)$ (in units of $W m^{-2} nm^{-1} sr^{-1}$) as described below. It is the additive term in eq. (2.43) to the radiance caused by reflection. The fluorescence component of remote sensing reflectance is obtained by dividing $L_F(\lambda)$ by $E_d(\lambda)$:

$$R_{rs,F}(\lambda) = \frac{L_F(\lambda)}{E_d(\lambda)}. \quad (2.47)$$

$E_d(\lambda)$ is calculated using eq. (2.41). Eq. (2.47) is used in eq. (2.17b).

2.11.1 Phytoplankton

Phytoplankton shows a characteristic fluorescence peak at 685 nm with a full width at half maximum (FWHM) of 25 nm. It originates almost completely (~95%, Owens 1991) from photosystem II (PS-II). Phytoplankton can use approximately the spectral range from 400 to 700 nm for photosynthesis. This photosynthetic active radiation (PAR) is absorbed within the phytoplankton cells by light harvesting antenna. The excited electrons of the antenna pigments are transferred to PS-II, where water molecules are splitted and oxygen is formed (Abbott and Letelier 1999). The energy wasted here causes the 685 nm fluorescence peak. Consequently, since it is irrelevant which pigment had absorbed the incident photon, chlorophyll-a fluorescence quantum yield $\eta_{chl}(\lambda)$ is largely independent of λ' . A comprehensive overview of the photosynthesis processes is given by Babin et al. (1996).

The flux absorbed by the phytoplankton in depth z is given by:

$$F'(z) = \int_{PAR} \sum_{i=0}^5 C_i \cdot a_i^*(\lambda') \cdot E_0(\lambda', z) d\lambda', \quad (2.48)$$

where C_i denotes concentration of phytoplankton class number i , $a_i^*(\lambda')$ the specific absorption coefficient of that class, and $E_0(\lambda', z)$ the scalar irradiance. Since irradiance at depth z is related to irradiance at the water surface by the Lambert-Beer law,

$$E_0(\lambda', z) = E_0(\lambda', 0) \cdot \exp[-K(\lambda') \cdot z], \quad (2.49)$$

with $K(\lambda')$ the attenuation coefficient of scalar irradiance, $F'(z)$ can be expressed as follows:

$$F'(z) = \int_{PAR} \sum_{i=0}^5 C_i \cdot a_i^*(\lambda') \cdot E_0(\lambda', 0) \cdot \exp[-K(\lambda') \cdot z] d\lambda'. \quad (2.50)$$

The flux (in units of $W m^{-3}$) emitted by a layer at depth z at wavelength λ is:

$$F(\lambda, z) = \eta_{chl}(\lambda) \cdot F'(z) \cdot \frac{\lambda'}{\lambda}, \quad (2.51)$$

see eq. (2.46). $\eta_{chl}(\lambda)$ can be described quite accurately by a Gaussian function:

$$\eta_{chl}(\lambda) = \frac{\eta_{chl}(\lambda_F)}{(2\pi\sigma_F^2)^{1/2}} \exp\left[-\frac{(\lambda - \lambda_F)^2}{2\sigma_F^2}\right]. \quad (2.52)$$

Since fluorescence is in good approximation isotropic, the radiance (in units of $W m^{-2} sr^{-1}$) emitted by a layer of thickness dz is given by:

$$dL_F(\lambda, z) = \frac{1}{4\pi} F(\lambda, z) dz. \quad (2.53)$$

For a downward looking sensor in depth z , the fluorescence radiance is the sum of contributions from layers at depths $z' > z$ down to the bottom (depth z_B), weighted by the transmission of the water column between sensor and each layer. The transmission is obtained from the Lambert-Beer law using the attenuation coefficient for upwelling radiance, k_u . Hence,

$$\begin{aligned} L_F(\lambda, z) &= \int_z^{z_B} dL_F(\lambda, z') \cdot \exp[-k_u(\lambda) \cdot (z' - z)] dz' = \\ &= \frac{1}{4\pi} \int_z^{z_B} \eta_{chl}(\lambda) \cdot \frac{\lambda'}{\lambda} \cdot F'(z') \cdot \exp[-k_u(\lambda) \cdot (z' - z)] dz' = \\ &= \frac{1}{4\pi} \int_z^{z_B} \int_{PAR} \sum_{i=0}^5 C_i \cdot a_i^*(\lambda') \cdot \eta_{chl}(\lambda) \cdot \frac{\lambda'}{\lambda} \cdot E_0(\lambda', 0) \cdot \exp[-(K(\lambda') + k_u(\lambda)) \cdot z'] \cdot \exp[k_u(\lambda) \cdot z] dz' d\lambda'. \end{aligned}$$

Solving the integral over depth leads to:

$$L_F(\lambda, z) = \frac{\eta_{chl}(\lambda_F)}{4\pi\lambda} \cdot \left[e^{-K(\lambda) \cdot z} - e^{-K(\lambda) \cdot z_B} \right] \int_{PAR} \sum_{i=0}^5 C_i \cdot a_i^*(\lambda') \cdot \frac{E_0(\lambda', 0)}{K(\lambda') + k_u(\lambda)} \lambda' d\lambda'. \quad (2.54)$$

Similar equations are used by Maritorena et al. (2000) and Huot et al. (2005) for optically deep water ($z_B = \infty$). Note that the factor λ'/λ is missing in their equations since they use photon number units ($mol m^{-3} s^{-1}$ for fluxes, $mol m^{-2} s^{-1} sr^{-1} nm^{-1}$ for spectral radiances).

$E_0(\lambda', 0)$ is calculated from the downwelling vector irradiance using the approximation

$$E_0(\lambda', 0) = f_{E0} \cdot E_d(\lambda', 0-) \quad (2.55)$$

with $f_{E0} = 1.30$ (Maritorena et al. 2000) and $E_d(\lambda', 0-)$ from eq. (2.33). $K(\lambda')$ is approximated by $K_d(\lambda')$ using eq. (2.5), and $k_u(\lambda)$ is calculated using eq. (2.9).

The chlorophyll-a fluorescence quantum yield, $\eta_{chl}(\lambda_F)$, can be treated as fit parameter in WASI with a default value of 0.01 (Gilerson et al. 2007). The parameters of the Gaussian shaped fluorescence peak are set by default to $\lambda_F = 685$ nm and $\sigma_F = 10.6$ nm, which corresponds to a FWHM of 25 nm. The wavelength range of PAR is set to 400–700 nm.

2.12 Miscellaneous

2.12.1 Depth of light penetration

The light penetration depth z_{Ed} is defined as the depth where the incident irradiance has decreased to a specified percentage p_{Ed} . It is a measure of water clarity. Calculation makes use of the approximation $E_d(z) = E_d(0) \exp\{-K_d z\}$. Solving it for a given fraction $p_{Ed} = E_d(z) / E_d(0)$ leads to:

$$z_{Ed}(\lambda) = -\frac{\ln p_{Ed}}{K_d(\lambda)}. \quad (2.56)$$

$K_d(\lambda)$ is calculated using eq. (2.5). p_{Ed} is set by default to 1 % since the average of $z_{Ed}(\lambda)$ over the photosynthetic active radiation (PAR) range 400 to 700 nm then yields the euphotic zone depth, $z_{1\%}$, which is not only a quality index of an ecosystem but also an important property for primary production and heat transfer in the upper water column (Lee et al. 2007). $z_{Ed}(\lambda)$ and its average over the PAR range can be visualized after $K_d(\lambda)$ has been calculated.⁶

⁶ Select in the menu bar “Display – p_{Ed} depth”. p_{Ed} can be changed in “Options – Models – Irradiance”.

3. Forward mode

The forward mode allows to calculate a single spectrum or a series of spectra according to user-specified parameter settings. The supported spectrum types are listed in Table 1.1.

3.1 Graphical user interface

Fig. 3.1 shows WASI's graphical user interface (GUI) at the example of the spectrum type "Remote sensing reflectance".

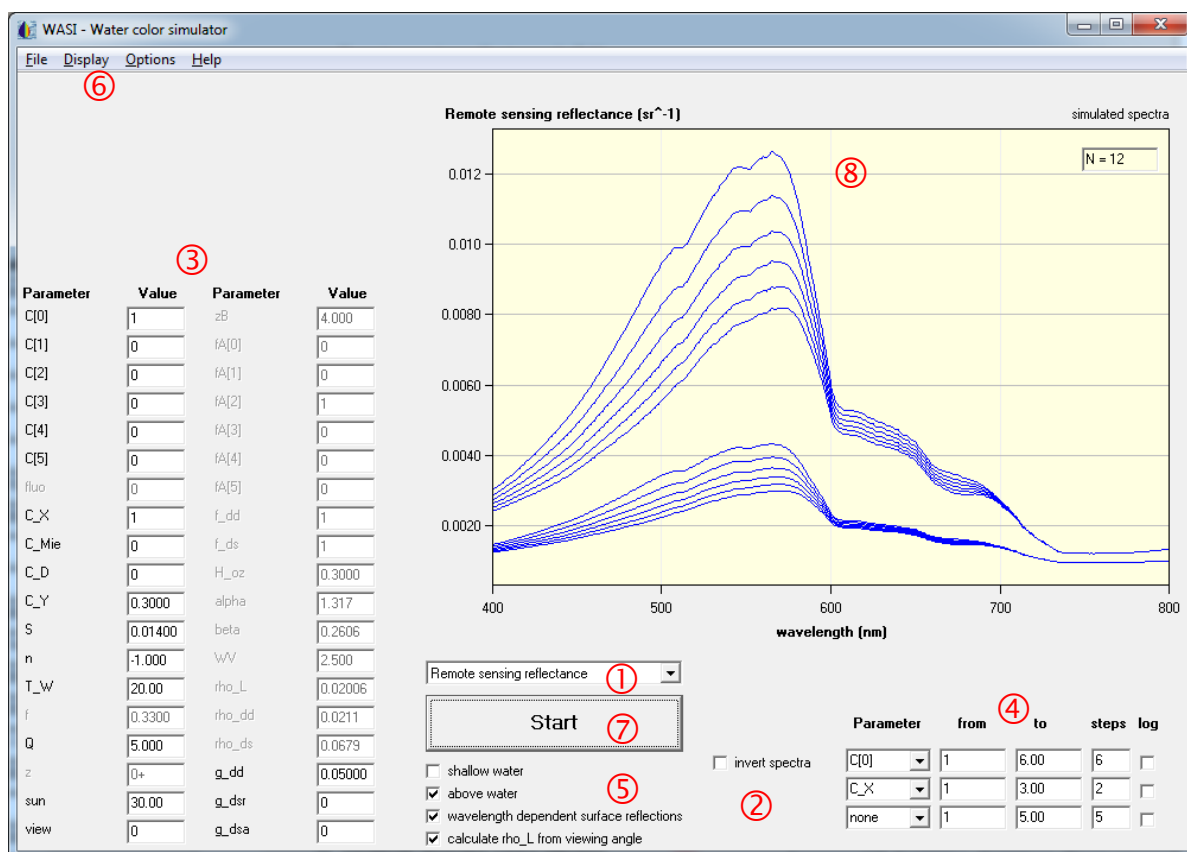


Fig. 3.1: Graphical user interface of the forward mode. 1 = Drop-down list for selecting the spectrum type, 2 = Check box for switching between forward and inverse mode, 3 = Parameter list, 4 = Selection panel for specifying the parameter iterations, 5 = Check boxes for selecting model options (model specific), 6 = Menu bar, 7 = Start button, 8 = Plot window.

The GUI consists of 8 elements:

- (1) Drop-down list for selecting the spectrum type. The user selects one of the spectrum types from Table 1.1. If the spectrum type is changed, the parameter list (3) is updated such that only the relevant parameters are activated. Also the model options (5) are updated.
- (2) Check box for switching between forward and inverse mode. In the forward mode, this box is not checked.

- (3) **Parameter list.** This list tabulates the parameters which are relevant for the selected spectrum type. It displays the parameters' symbols (in WASI notation, see Appendix 3) and their actual values. Default values are read from the WASI.INI file, actual values are set by the user by editing the corresponding "Value" fields. Depending on the model options, not all parameters may be relevant. Irrelevant parameters are disabled, i.e. the corresponding symbol and value is displayed in gray colour, and the value cannot be edited.
- (4) **Selection panel for specifying the iterations.** Up to 3 parameters can be iterated simultaneously during one run, thus the panel has 3 rows, one for each parameter. The iterated parameters are selected in the "Parameter" drop-down lists, their minimum and maximum values in the "from" and "to" fields, and their numbers of values in the "steps" fields. The "log" check boxes specify whether the intervals are equidistant on a linear scale (no hook) or on a logarithmic scale (hook).
- (5) **Check boxes for selecting model options.** Several spectrum types support options which further specify the model, cf. Table 1.1. Each option is either switched on or off.
- (6) **Menu bar.** Further details concerning the model, data storage and visualisation can be specified in various pop-up windows, which are accessed via the menu bar.
- (7) **Start button.** Calculation is started by pressing this button.
- (8) **Plot window.** Each spectrum is plotted in this window after calculation. All curves are plotted together in order to visualize the spectral changes for the chosen iterations. A counter in the upper right corner is updated after each plot.

3.2 Calculation of a single spectrum

3.2.1 Mode selection

For calculating a single spectrum in the forward mode, the following settings must be made:

- Set forward mode: the "invert spectra" box (② in Fig. 3. 1) is unchecked;
- No parameter iteration: select "none" in each "parameter" drop-down list (④ in Fig. 3. 1).

3.2.2 Spectrum type selection

WASI allows to calculate 8 different types of spectra, see Table 1.1. The desired type is selected in the main window from the drop-down list ① of Fig. 3. 1.

Several types of spectra support further options, see Table 1.1. If that is the case for the selected type, the options are displayed at the bottom of the main window (⑤ in Fig. 3. 1). Each option is either switched on or off. The selection is done by marking the corresponding check box with a hook. In the example of Fig. 3.1 three options are available:

- (1) **Above water.** Since the check box is marked, the remote sensing reflectance will be calculated for a sensor above the water surface; when the hook is removed, calculation is performed for below the surface.

- (2) Wavelength dependent surface reflections. Since the check box is unmarked, the surface reflections will be treated as constant ($R_{rs}^{surf}(\lambda) = \sigma_L/\pi$ according to chapter 2.5).
- (3) Calculate sigma_L from viewing angle. Since the check box is unmarked, the reflectance factor for sky radiance, σ_L , is treated as a parameter that can be defined by the user. Otherwise, σ_L would be calculated from the viewing angle using eq. (2.18).

3.2.3 Parameter selection

All model parameters are read during program start from the WASI.INI file. The parameters which are relevant for the actual spectrum type are listed at the left side of the main window (③ in Fig. 3. 1). This list can be edited.

3.2.4 Calculation options

Several calculation settings are made in the pop-up window "Forward calculation settings" which is shown in Fig. 3.2. This pop-up window is accessed from the menu bar via "Options - Forward calculation" (see Fig. 9.1)

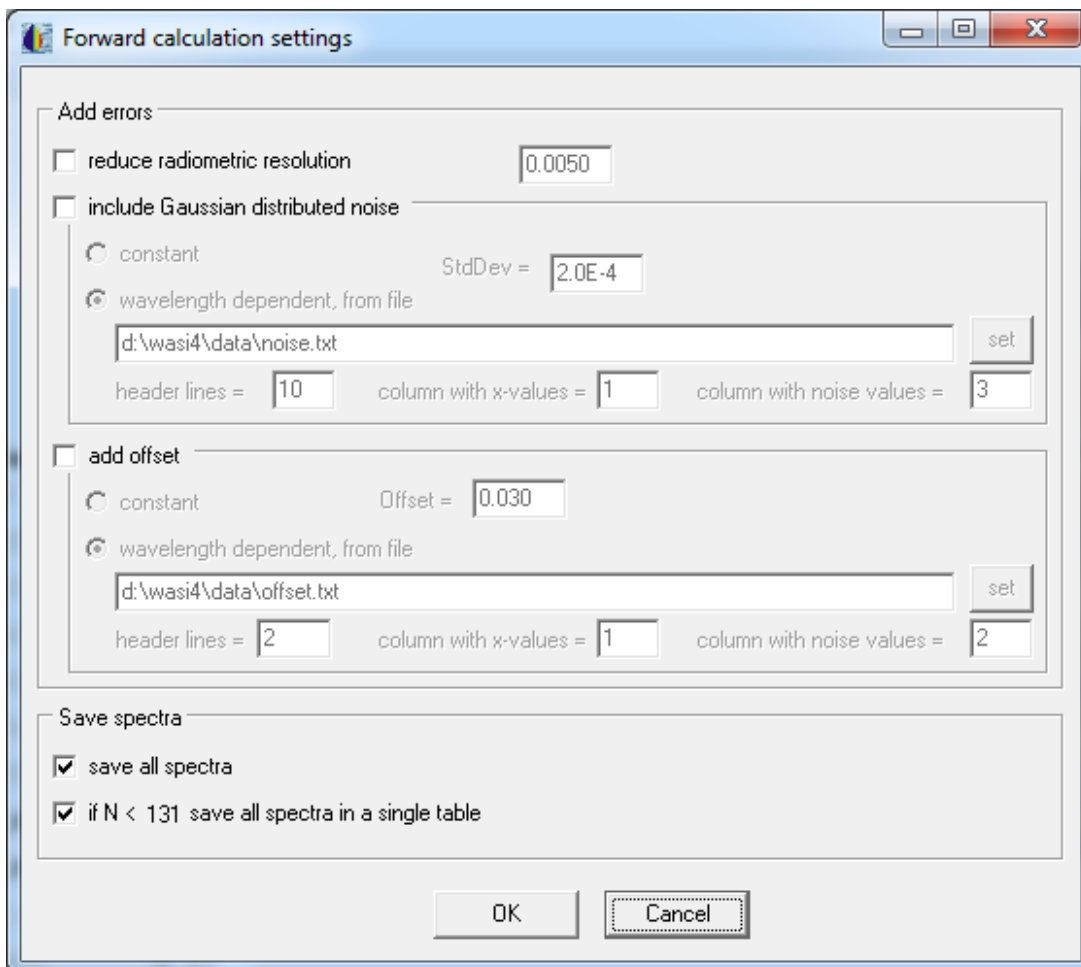


Fig. 3.2: The pop-up window "Forward calculation settings".

Add errors. Three types of measurement errors can be simulated:

- *Low radiometric resolution.* If the check box "reduce radiometric resolution" is marked with a hook, the numerical accuracy is limited to the value shown in the corresponding input field. For example, 0.005 rounds original real numbers such that values of 0.000, 0.005, 0.010, 0.015, etc. result. If "reduce radiometric resolution" is not selected, the corresponding input field is not enabled.
- *Noise.* If the check box "include Gaussian distributed noise" is marked with a hook, Gaussian distributed noise is added to each calculated value. Its standard deviation can be chosen constant or wavelength dependent. A constant value is specified in the input field "StdDev", a spectrally dependent noise pattern is imported from the specified file.
- *Offset.* If the check box "add offset" is marked with a hook, an offset is added to each calculated value. It can be either chosen constant or wavelength dependent. A constant value is specified in the input field "Offset", a spectrally dependent offset is imported from the specified file.

Save spectra. Automatic saving of calculated spectra is activated by a hook in the check box "save all spectra". The directory is selected in the "Directories" window, see section 8.2 (Fig. 8.3). The calculated spectrum is stored in ASCII format as file B1.FWD. Note: If a file with the name B1.FWD already exists, it will be overwritten without warning. Two additional files are created automatically in the same directory as the spectrum. First, a copy of the initialisation file WASI.INI containing the actual parameter settings. It documents the data and parameters used for calculation. Second, a file CHANGES.TXT, which can be ignored; it is relevant only if a series of spectra is calculated.

The check box "if $N < 131$, save all spectra in a single table" is not relevant for calculating a single spectrum.

3.2.5 Start calculation

Calculation is started by pressing the "Start" button (⌚ in Fig. 3. 1).

After calculation, the resulting curve is plotted in the main window (Ⓢ in Fig. 3. 1) and stored automatically, if spectra saving is activated in the pop-up window "Forward calculation settings" (Fig. 3.2).

3.2.6 Example

An example of a spectrum calculated in the forward mode is given in Fig. 3.3. The spectrum type is irradiance reflectance in shallow water. The values of the model parameters are listed in the parameter list at the left-hand side: phytoplankton concentration, $C[0] = 2 \mu\text{g/l}$; phytoplankton fluorescence quantum yield, $\text{fluo} = 0.01$; concentration of suspended particles (type I), $X = 0.6 \text{ mg/l}$; Gelbstoff absorption at 440 nm, $C_Y = 0.3 \text{ m}^{-1}$; Gelbstoff exponent, $S = 0.014 \text{ nm}^{-1}$; n is irrelevant since $C_Mie = 0$; water temperature, $T_W = 20 \text{ }^\circ\text{C}$; anisotropy factor, $Q = 5.0$; sensor depth, $z = 0.5 \text{ m}$; sun zenith angle, $\text{sun} = 30.0^\circ$; bottom depth, $zB = 5 \text{ m}$; areal fraction of bottom surface type no. 2 (fine-grained sediment), $\text{fa}[2] = 1$. The concentra-

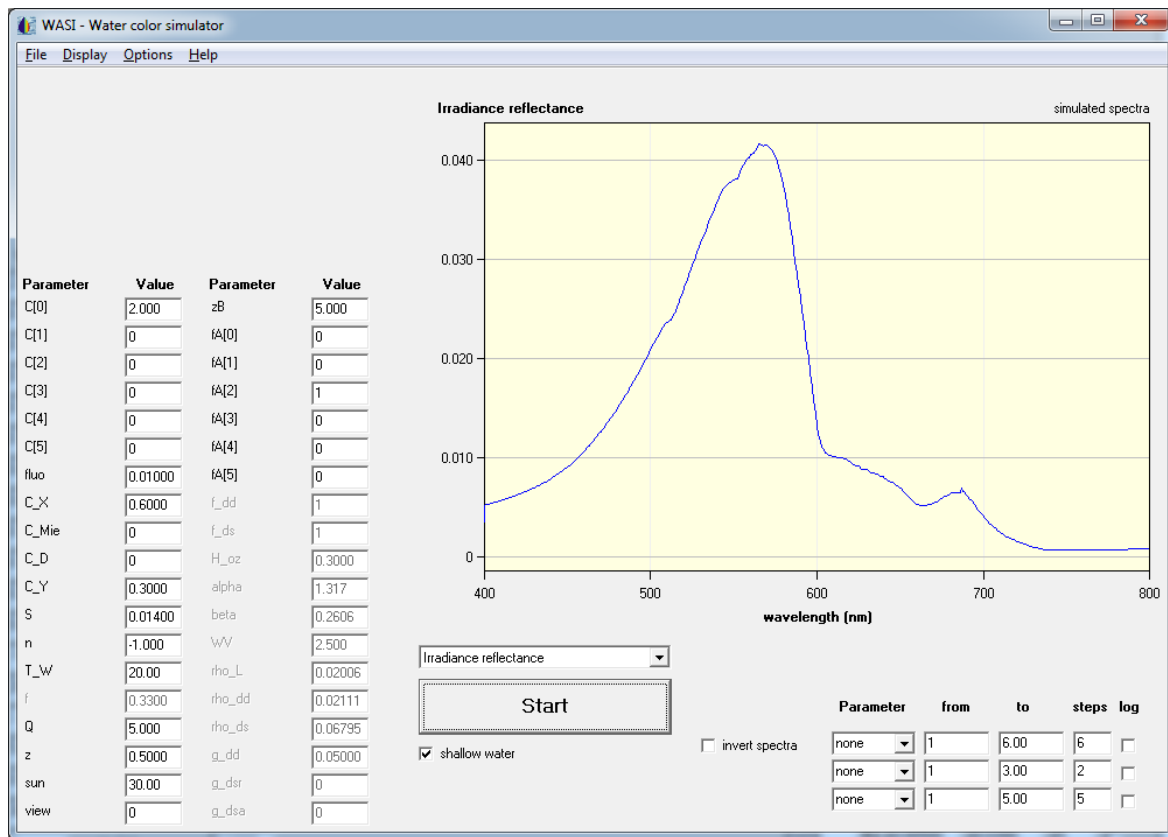


Fig. 3.3: A single irradiance reflectance spectrum calculated in the forward mode.

tions of other water constituents and the areal fractions of other bottom types are set to zero. Irrelevant parameters for the chosen spectrum type are indicated by gray text color. The fact that the displayed spectrum is a model curve (and not a measurement) is indicated by "simulated spectra" at top right.

A listing of the first lines of the file with the calculated spectrum is shown in Fig. 3.4. The header specifies the spectrum type (irradiance reflectance), informs that the spectrum has been created by the program WASI, gives the software version ("latest update"), lists the files which contain additional information (WASI4.INI, CHANGES.TXT), and lists the wavelength range (400 to 700 nm) that was used to calculate the average intensity (Avg). After the header, the calculated spectrum is listed.

Irradiance reflectance

This file was generated by the program WASI
Version 4 - Latest update: 17 January 2014
Parameter values in files: WASI4.INI, CHANGES.TXT
Average from 400 to 700 nm

No. 1
Avg 0.01670

380.00	0.004427
381.00	0.004462
382.00	0.004498
383.00	0.004533
384.00	0.004568
385.00	0.004604
386.00	0.004640
387.00	0.004679
388.00	0.004718
389.00	0.004756
390.00	0.004795

Fig. 3.4: Listening of the first lines of the spectrum from Fig. 3.3.

3.3 Calculation of a series of spectra

3.3.1 General

Calculating a series of spectra in the forward mode is very similar to calculating a single spectrum. The only difference is that the parameter iterations have to be specified. Hence the steps are as follows:

- Define the spectrum type: select the type from the drop-down list (① in Fig. 3.1);
- Set forward mode: uncheck the "invert spectra" box (② in Fig. 3.1);
- Specify the parameter values: set the values of all model parameters in the parameter list (③ in Fig. 3.1).

Up to three model parameters can be iterated simultaneously as described below. For these, the parameter list entries are irrelevant since the values are set during iteration.

3.3.2 Specification of the iteration

3.3.2.1 Iteration over 1 parameter

For studying the dependence of a spectrum on a certain parameter, the values of that parameter can be iterated over a user-defined range. WASI allows to iterate the parameters of Appendix 3. As shown in Fig. 3.5, the parameter to be iterated has to be selected from one of the three "Parameter" drop-down lists of the selection panel (④ of Fig. 3.1 (it is irrelevant, which of the 3 lists)); the selection in the two other drop-down lists must be "none". The range of variation of the iterated parameter is specified by a minimum and a maximum value ("from", "to"), and the number of calculated spectra by the number of steps ("steps"). If the check box "log" is marked with a hook, the parameter intervals are equidistant on a logarithmic scale,

Parameter	from	to	steps	log
C[0]	0.100	10.0	7	<input checked="" type="checkbox"/>
none	0.100	1	4	<input type="checkbox"/>
none	1	5.00	5	<input type="checkbox"/>

Fig. 3.5: Iteration over 1 parameter.

otherwise they are equidistant on a linear scale.

In the example of Fig. 3.5, the phytoplankton concentration C[0] is iterated from 0.100 to 10 $\mu\text{g/l}$ in 7 steps which are equidistant on a logarithmic scale, i.e. 7 spectra with concentrations of 0.100, 0.215, 0.464, 1.0, 2.15, 4.64 and 10 $\mu\text{g/l}$ are calculated.

3.3.2.2 Iteration over 2 parameters

When 2 parameters should be iterated, these parameters, their range of variation and the number of steps must be specified analogously to iterating 1 parameter. This is illustrated in Fig. 3.6.

Parameter	from	to	steps	log
C[0]	0.100	10.0	7	<input checked="" type="checkbox"/>
C_Y	0.100	1	4	<input type="checkbox"/>
none	1	5.00	5	<input type="checkbox"/>

Fig. 3.6: Iteration over 2 parameters.

In the example of Fig. 3.6, the phytoplankton concentration $C[0]$ is iterated as in Fig. 3.5 from 0.100 to 10 $\mu\text{g/l}$ in 7 steps which are equidistant on a logarithmic scale, and Gelbstoff absorption at 440 nm, C_Y , is iterated from 0.100 to 1 m^{-1} in 4 steps which are equidistant on a linear scale, i.e. absorption values of 0.1, 0.4, 0.7 and 1.0 m^{-1} are taken. Spectra are calculated for each combination, hence the number of generated spectra is $7 \cdot 4 = 28$.

3.3.2.3 Iteration over 3 parameters

When 3 parameters should be iterated, these parameters, their range of variation and the number of steps must be specified analogously to iterating 1 or 2 parameters. This is illustrated in Fig. 3.7.

Parameter	from	to	steps	log
C[0]	0.100	10.0	7	<input checked="" type="checkbox"/>
C_Y	0.100	1	4	<input type="checkbox"/>
X	1	5.00	5	<input type="checkbox"/>

Fig. 3.7: Iteration over 3 parameters.

In the example of Fig. 3.7, phytoplankton concentration $C[0]$ and Gelbstoff absorption C_Y are iterated as in Fig. 3.6, but additionally the concentration of suspended particles, X , is iterated from 1 to 5 mg/l in 5 steps which are equidistant on a linear scale, i.e. concentrations of 1, 2, 3, 4 and 5 mg/l are taken. Spectra are calculated for each combination, hence the number of generated spectra is $7 \cdot 4 \cdot 5 = 140$.

3.3.3 Data storage

Calculated spectra are stored automatically if saving is activated in the "Forward calculation settings" pop-up window shown in Fig. 3.2. Each spectrum is stored in a separate file; the file names are Bnr.fwd with nr = file number. The extension fwd indicates that the spectra are the result of forward calculations. The parameters which change from one spectrum to the next are listed in the file changes.txt . A copy of the WASI.INI file is created for documenting completely all parameters and input files. The directory where all the files are stored is selected as described in section 8.2.

If the number of calculated spectra is below 131, the spectra can alternately be stored in a single file, `spec.fwd`. This option is selected by marking the check box "if $N < 131$ save all spectra in a single table" in the "Forward calculation settings" pop-up window (see Fig. 3.2).

3.3.4 Example

An example of a series of spectra calculated in the forward mode is given in Fig. 3.8.

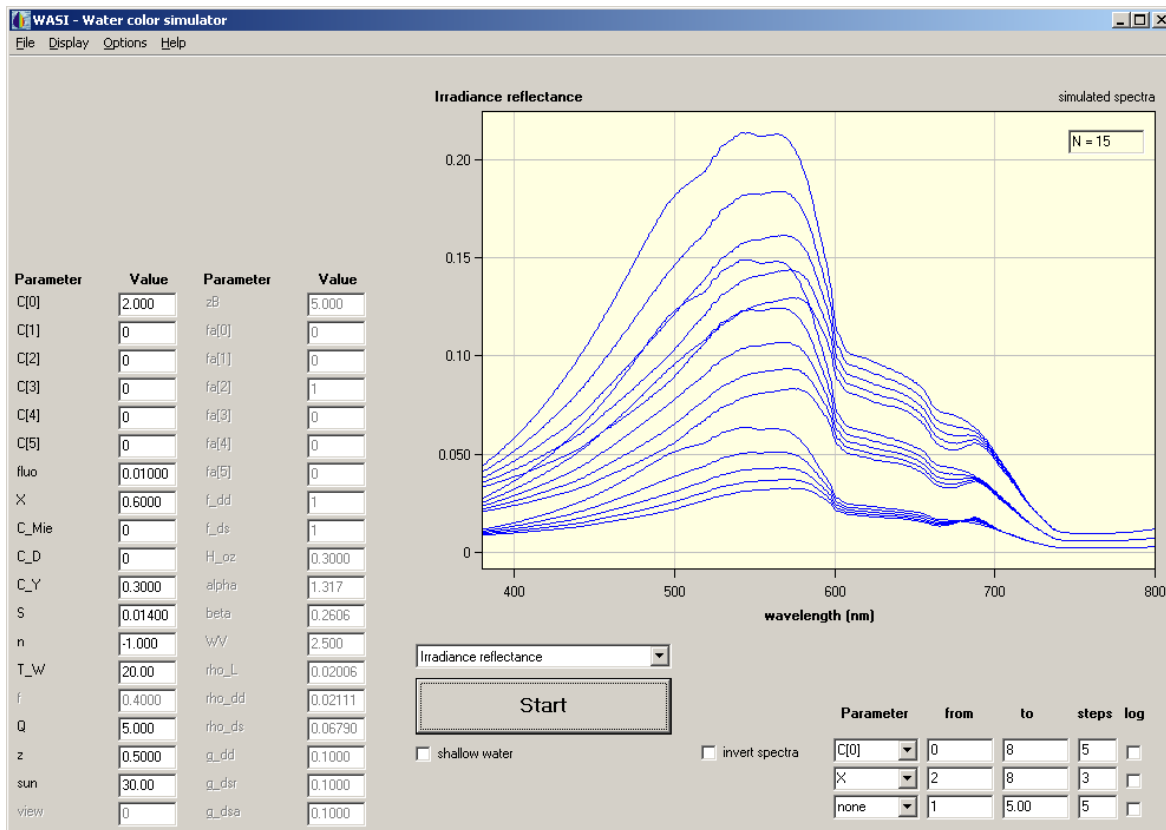


Fig. 3.8: A series of irradiance spectra calculated in the forward mode.

The spectrum type of Fig. 3.8 is irradiance reflectance. $N = 15$ spectra have been calculated by iterating two parameters: phytoplankton concentration, $C[0]$, was changed from 0 to 8 $\mu\text{g/l}$ in 5 steps, i.e. concentrations of 0, 2, 4, 6, 8 $\mu\text{g/l}$ were taken, and the concentration of suspended particles, X , was changed from 2 to 8 mg/l in 3 steps, i.e. concentrations of 2, 5 and 8 mg/l were taken. The values of the other parameters are shown in the parameter list at the left side. The list values of the iterated parameters, $C[0]$ and X , are invalid.

When "save all spectra" is activated in the "Forward calculation settings" popup-window (see Fig. 3.2), all 15 spectra are saved in ASCII format as separate files in the specified directory; an example listening of such a file was given above in Fig. 3.4. The file names are `B01.fwd`, `B02.fwd`, ... `B15.fwd`.

If the number of calculated spectra is less than 131, and if the check box "if $N < 131$ save all spectra in a single table" of the "Batch mode options" menu is marked with a hook, a single table with the file name `SPEC.FWD` is created instead of separate files. An example of that table is shown in Fig. 3.9.

Irradiance reflectance

This file was generated by the program WASI
 Version 4 - Latest update: 16 January 2012
 Parameter values in files: WASI4.INI, CHANGES.TXT
 Average from 400 to 700 nm

No.	1	2	3	4	5
Avg	0.03564	0.08684	0.1311	0.02971	0.07362
380.00	0.01174	0.02756	0.04403	0.01088	0.02551
381.00	0.01189	0.02795	0.04465	0.01100	0.02581
382.00	0.01204	0.02834	0.04529	0.01111	0.02612
383.00	0.01220	0.02874	0.04594	0.01123	0.02643
384.00	0.01235	0.02914	0.04659	0.01135	0.02674
385.00	0.01251	0.02955	0.04725	0.01147	0.02706
386.00	0.01267	0.02996	0.04792	0.01159	0.02738
387.00	0.01283	0.03038	0.04861	0.01171	0.02770
388.00	0.01299	0.03081	0.04930	0.01184	0.02803
389.00	0.01316	0.03125	0.05000	0.01196	0.02836
390.00	0.01333	0.03169	0.05071	0.01209	0.02870

Fig. 3.9: The first lines and the first 5 columns of the file SPEC.FWD of the spectra series of Fig. 3.8.

The parameter values and input files used for calculating the spectra are documented by a copy of the WASI.INI file, which is stored automatically in the directory of the spectra. The values of the iterated parameters are tabulated in the file CHANGES.TXT. An example of that file is given in Fig. 3.10.

This file was generated by the program WASI
 Version 4 - Latest update: 16 January 2012

List of parameter values which differ from one spectrum to the next
 Common parameter set of all spectra in file: WASI4.INI
 All spectra are the results of forward calculations
 Spectra = Irradiance reflectance

Spectrum	C[0]	C_L
B01.fwd	0	2.000
B02.fwd	0	5.000
B03.fwd	0	8.000
B04.fwd	2.000	2.000
B05.fwd	2.000	5.000
B06.fwd	2.000	8.000
B07.fwd	4.000	2.000
B08.fwd	4.000	5.000
B09.fwd	4.000	8.000
B10.fwd	6.000	2.000
B11.fwd	6.000	5.000
B12.fwd	6.000	8.000
B13.fwd	8.000	2.000
B14.fwd	8.000	5.000
B15.fwd	8.000	8.000

Fig. 3.10: The file CHANGES.TXT of the spectra series of Fig. 3.8.

4. Inverse mode

Inverse modeling is the determination of model parameters for a given spectrum. More precisely, those values of the model parameters must be determined for which the correspondence between model curve and given spectrum is maximal.

Three modes of operation are implemented for inverse modeling of spectra:

- **Single spectrum mode.** Inversion is performed for a single spectrum which the user loads from file. After calculation, an overlay of imported spectrum and model curve is automatically shown on screen and resulting fit parameters, number of iterations, and residuum are displayed. This mode allows to inspect the results for individual measurements. It is useful for optimizing the choice of initial values and the fit strategy before starting a batch job.
- **Batch mode.** A series of spectra from file is inverted. After each single run, an overlay of imported spectrum and model curve is automatically shown on screen. This mode is useful for processing large data sets.
- **Reconstruction mode.** Combines forward and inverse modes. Inversion is performed for a series of forward calculated spectra which are not necessarily read from file. The model parameters can be chosen differently for forward and inverse calculations. This mode is useful for performing sensitivity studies.

4.1 Graphical user interface

The graphical user interface (GUI) of WASI in the inverse mode is shown in Fig. 4.1. It consists of 8 elements:

- (1) Drop-down list for selecting the spectrum type. As in the forward mode.
- (2) Check boxes for specifying the operation mode. In the inverse mode, the box "invert spectra" is checked. A hook in the "batch mode" check box indicates that a series of spectra is analyzed. Otherwise, a single spectrum is inverted (single spectrum mode). The check box "read from file" selects whether the spectra are read from files (hook), or if previously forward calculated spectra are used (reconstruction mode, no hook).
- (3) Parameter list. The list tabulates the start values of the fit parameters. Defaults are read from the WASI.INI file, the user can change them by editing the "Value" fields. A hook in a "Fit?" check box makes the corresponding parameter to a fit parameter, otherwise the parameter is kept constant during inversion. In the single spectrum mode, the resulting fit values are displayed after inversion is finished.
- (4) The appearance of this area depends on the mode of operation. In the single spectrum mode, the residuum and the number of iterations are shown here after calculation is finished. In the batch mode, this area is empty. In the reconstruction mode, the panel of the forward mode for specifying the parameter iterations is displayed.
- (5) Check boxes for selecting model options. As in the forward mode.

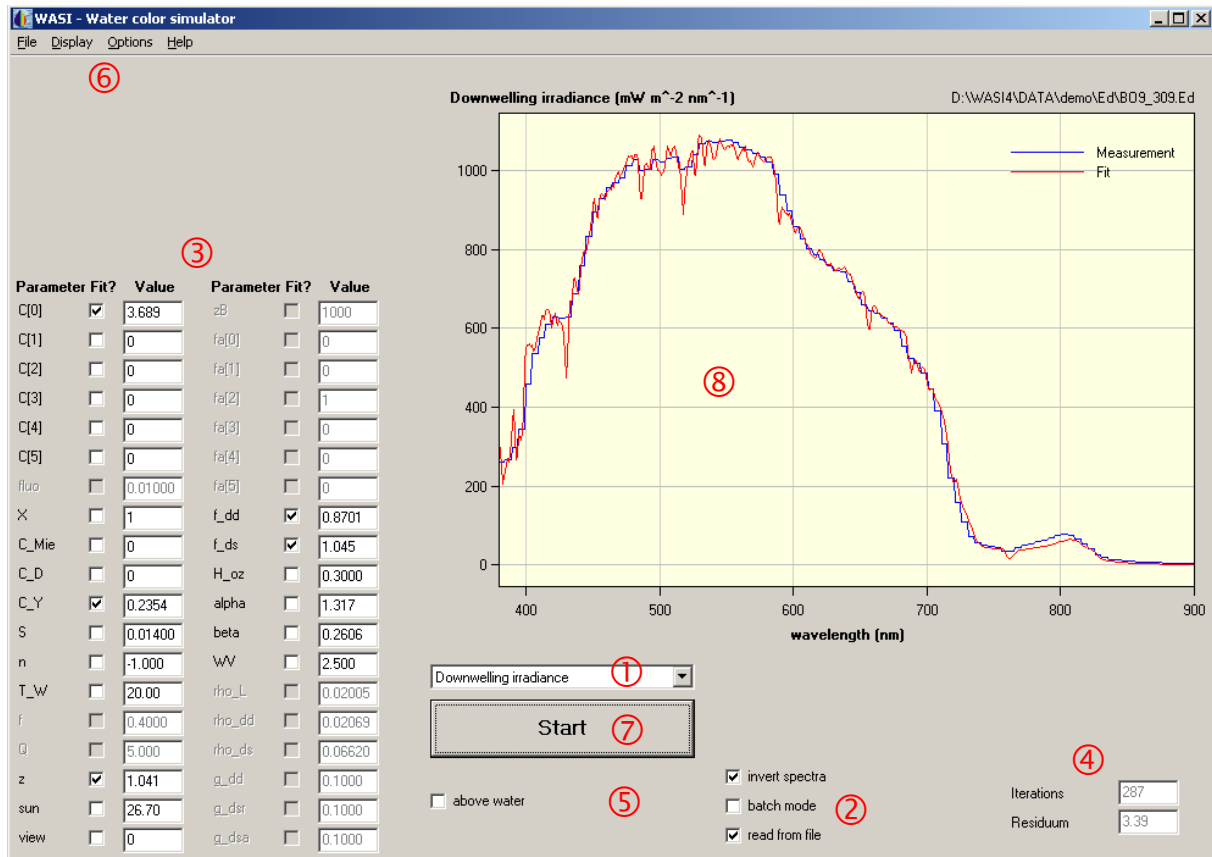


Fig. 4.1: Graphical user interface of the inverse mode. 1 = Drop-down list for selecting the spectrum type, 2 = Check boxes for specifying the operation mode, 3 = Parameter list, 4 = Display elements depending on mode of operation, 5 = Check boxes for selecting model options (model specific), 6 = Menu bar, 7 = Start button, 8 = Plot window.

(6) Menu bar. As in the forward mode.

(7) Start button. Inverse modeling is started by pressing this button.

(8) Plot window. The input spectrum is displayed in blue, the fit curve in red. The window is refreshed before a new pair of spectra is plotted, thus only the last pair remains on screen when a series of spectra is analyzed. The file name of the imported spectrum is shown on top right.

In the example of Fig. 4.1, a downwelling irradiance spectrum with the filename BO9_309.Ed, which had been measured by a submersed irradiance sensor, was inverted in the single spectrum mode. During inversion five parameters were fitted ($C[0]$, C_Y , z , f_dd , f_ds), the other parameters were kept constant. Parameters irrelevant for the spectrum type "downwelling irradiance" are inactive, indicated by gray text and gray check boxes. Fit results are $C[0] = 3.689 \mu\text{g l}^{-1}$, $C_Y = 0.2354 \text{ m}^{-1}$, $z = 1.041 \text{ m}$, $f_dd = 0.8701$ and $f_ds = 1.045$. The fit converged after 287 iterations at a residuum of 3.39 mW m^{-2} .

4.2 Inversion of a single spectrum

4.2.1 Spectrum selection

A single spectrum from file is selected as follows:

- Define the spectrum type: select the type from the drop-down list (① in Fig. 4.1);
- Load the spectrum.

Loading the spectrum is illustrated in Fig. 4.2. The pull-down menu "File" is opened from the menu bar, and "Load" is selected (top). Then a pop-up window for file selection opens, where the desired file is selected (bottom). Note: The layout of the file selection window depends on the operating system and the language; here the version of Windows XP in German is shown.

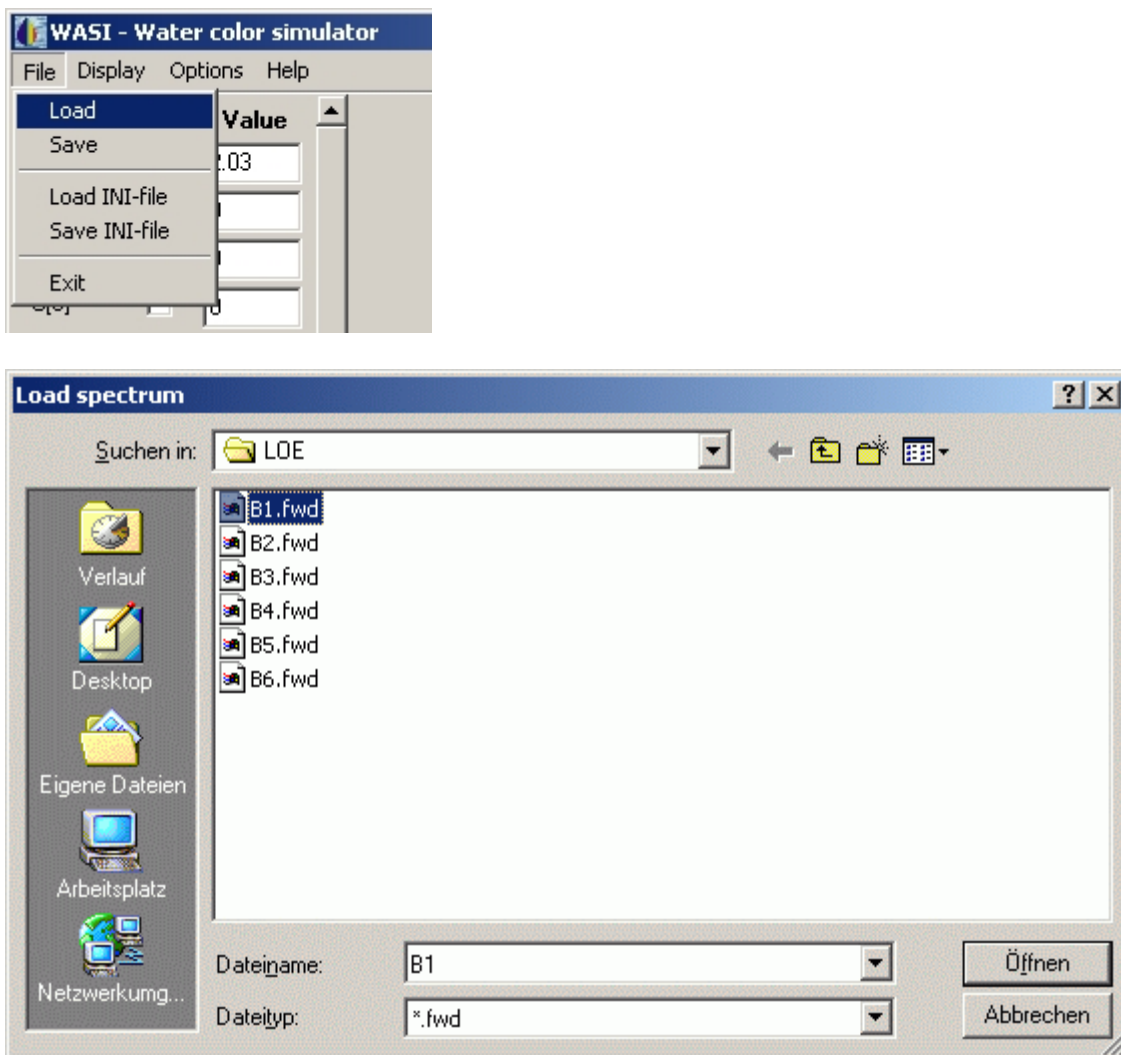


Fig. 4.2: Loading a single spectrum for inversion. Top: Menu bar and pull-down menu "File". Bottom: Pop-up window for selecting the file.

After the spectrum is loaded, it is automatically displayed in the plot window ⑧ of Fig. 4.1, and the program mode is automatically set to "single spectrum mode", i.e. the check boxes ② of Fig. 4.1 are set as shown in Fig. 4.3. No user action is required.

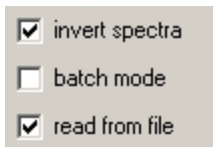


Fig. 4.3: Check box settings of the single spectrum mode.

4.2.2 Definition of initial values

Initial values of each fit parameter are read from the WASI.INI file. The user can change them either in the parameter list ③ of Fig. 4.1, or in the "Fit parameters" pop-up window, which is more detailed, see Fig. 4.4.

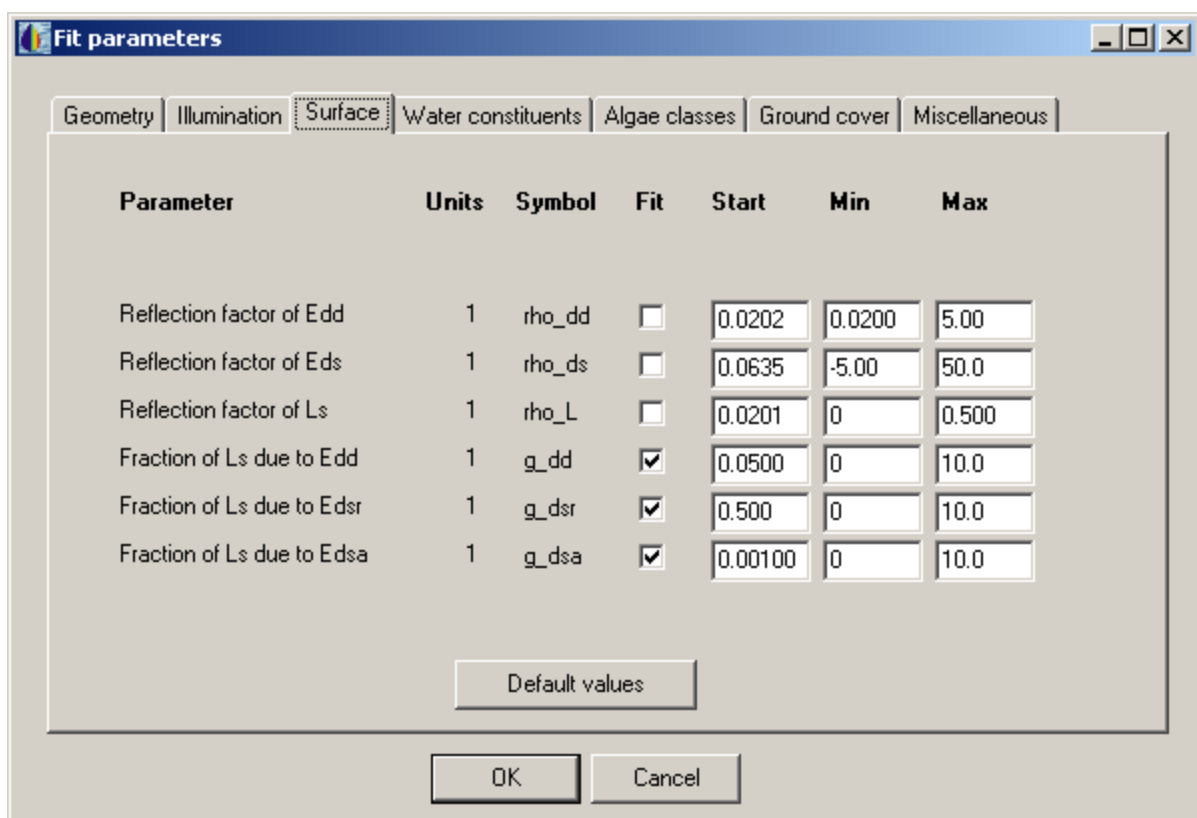


Fig. 4.4: The pop-up window "Fit parameters" with the register card "Surface".

The pop-up window "Fit parameters" is accessed from the menu bar via "Options - Inverse calculation - Fit parameters" (see Fig. 8.1). It has seven register cards which sort the parameters according to the categories Geometry, Illumination, Surface, Water constituents, Algae classes, Ground cover, and Miscellaneous. Fig 4.4 shows as example the register card "Surface". For each parameter, a short description, the physical units, and the symbol are listed. A check box "Fit" determines whether the parameter is fit parameter or kept constant during inverse modeling. The start value, as well as minimum and maximum values that are allowed for the fit routine, can be specified. Pressing the button "Default values" changes the complete set of start values of the displayed register card to the default values from the WASI.INI file. These default values are stored separately from the start values and can be changed only by editing the WASI.INI file.

4.2.3 Fit strategy

Inverse modeling aims to determine the values of unknown model parameters, called fit parameters. These are determined iteratively as follows. In the first iteration, a model spectrum is calculated for user-defined initial values of the fit parameters. This spectrum is compared with the measured one by calculating the residuum as a measure of correspondence. Then, in the further iterations, the fit parameter values are altered using the Downhill Simplex algorithm (Nelder and Mead 1965, Caceci and Cacheris 1984), resulting in altered model curves and altered residuals. The procedure is stopped when the calculated and the measured spectrum agree as good as possible, which corresponds to the minimum residuum, or if the number of iterations is above some threshold. The values of the fit parameter of the step with the smallest residuum are the fit results. WASI supports two options for residuum calculation:

- wavelength dependent weighting,
- 6 different minimisation methods.

The implemented equations to calculate the residuum are summarized in Table 4.1.

no.	method	y-values	residuum
1	least squares	linear	$\sum g_i \cdot m_i - f_i ^2$
2	absolute differences	linear	$\sum g_i \cdot m_i - f_i $
3	relative differences	linear	$\sum g_i \cdot 1 - f_i / m_i $
4	least squares	logarithmic	$\sum g_i \cdot \ln(m_i) - \ln(f_i) ^2$
5	absolute differences	logarithmic	$\sum g_i \cdot \ln(m_i) - \ln(f_i) $
6	relative differences	logarithmic	$\sum g_i \cdot 1 - \ln(f_i) / \ln(m_i) $

Table 4.1: Implemented algorithms to calculate the residuum. g_i = weight of channel i , m_i = measured value of channel i , f_i = modeled value of channel i .

The residuum is calculated by averaging the weighted differences between measured and fit curve over a user-defined wavelength interval. The weights g_i are specified in the "Weights" register card of the pop-up window "Fit tuning", which is shown in Fig. 4.5 and accessed from the menu bar via "Options - Invers calculation - Fit tuning" (see Fig. 8.1). Path and file name of that function are displayed in the "File" field; the file can be exchanged by opening a file selection window by pressing the "..." button. The number of header lines and the columns of the x- and y-values have to be specified. If all wavelengths shall be weighted equally, the file contains a constant function. Such a file with 1 as g_i values, `EINS.PRN`, is set as default in WASI.

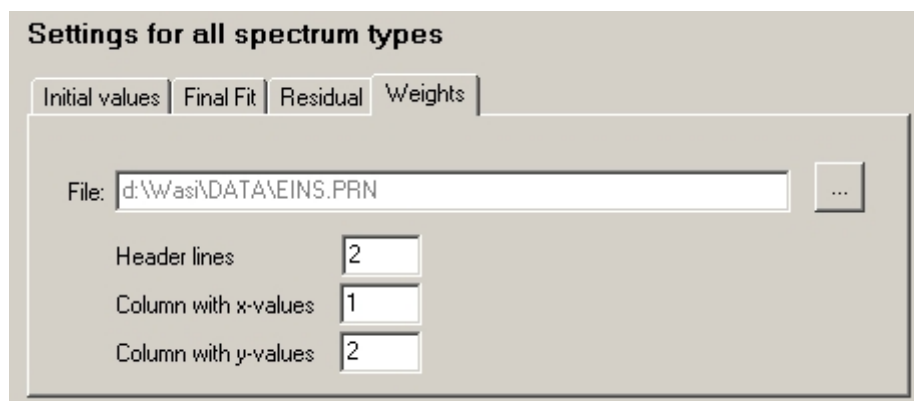


Fig. 4.5: The register card "Weights" of the popup window "Fit tuning".

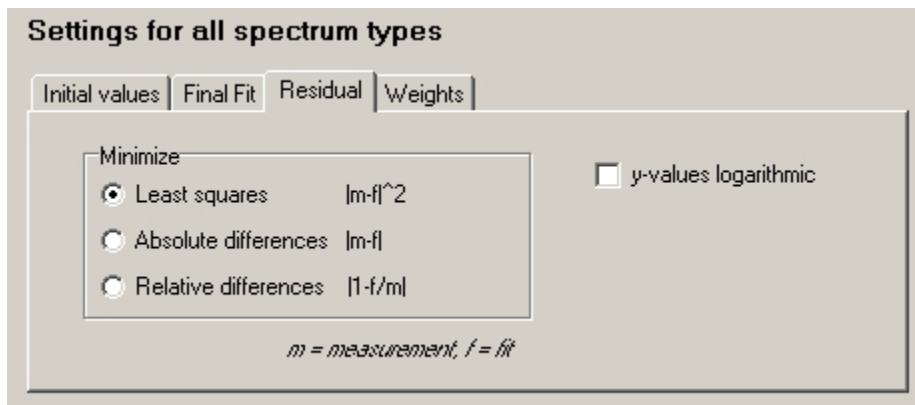


Fig. 4.6: The register card "Residual" of the popup window "Fit tuning".

The equation used to calculate the residuum is selected in the "Residual" register card of the pop-up window "Fit tuning", which is shown in Fig. 4.6.

4.2.4 Definition of fit region and number of iterations

Which part of the spectrum is fitted and which data interval is taken for calculating the residuum is specified in the "Final fit" register card of the "Fit tuning" menu, as shown in Fig. 4.7. The pop-up window is accessed from the menu bar via "Options - Invers calculation - Fit tuning" (see Fig. 8.1). The maximum number of iterations forces the fit routine to stop; the number should be set high enough that a forced stop is exceptional.

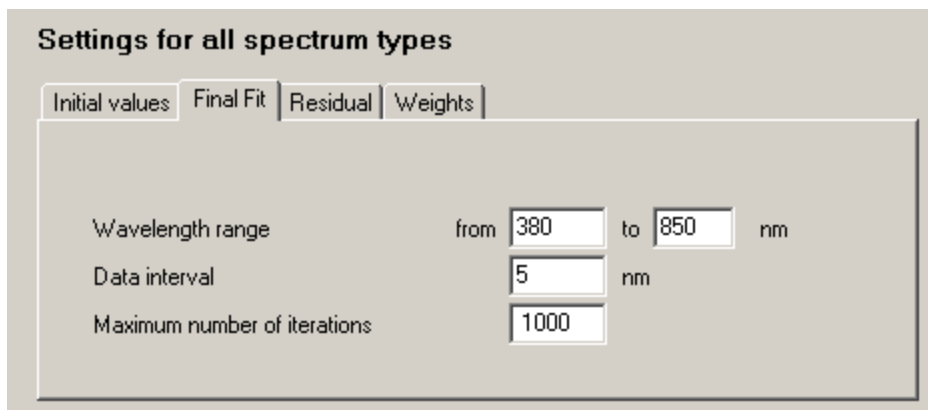


Fig. 4.7: The register card "Final fit" of the popup window "Fit tuning".

4.3 Inversion of a series of spectra

4.3.1 Selection of spectra

A series of spectra is selected for inversion as follows:

- Set the path of the input spectra in the menu "Options - directories", field "Read spectra".
- Set the path for storing the results in the menu "Options - directories", field "Save results", input line "Inversion".
- Activate reading of spectra in the menu "Options - Invers calculation - Data in/out" (Fig. 4.7a), field "Batch processing": mark the box "import series of spectra" with a hook and choose path and files after clicking the "...". Alternately, specify file extension in the input box "Extension".
- Set the properties of the input files in the menu "Options - Invers calculation - Data in/out" (Fig. 4.7a), field "Input file format": number of header lines, column of x-values, column of y-values. If the sun zenith angle is provided in the input file, mark the box "sun zenith angle available" with a hook and specify line, column and format of the angle. The batch mode supports also files which contain several spectra in the format (x, y_1 , y_2 , ... y_N). To read such files, mark the box "multiple columns per file" with a hook and specify the maximum number N of spectra per file by editing the "max. columns" box. "Column with y-values" specifies the column containing the first spectrum y_1 .
- Activate or deactivate saving of each fitted spectrum in the menu "Options - Invers calculation - Data in/out" (Fig. 4.7a), field "Batch processing": select / deselect the box "save calculated spectra" and choose the directory after clicking the "...".

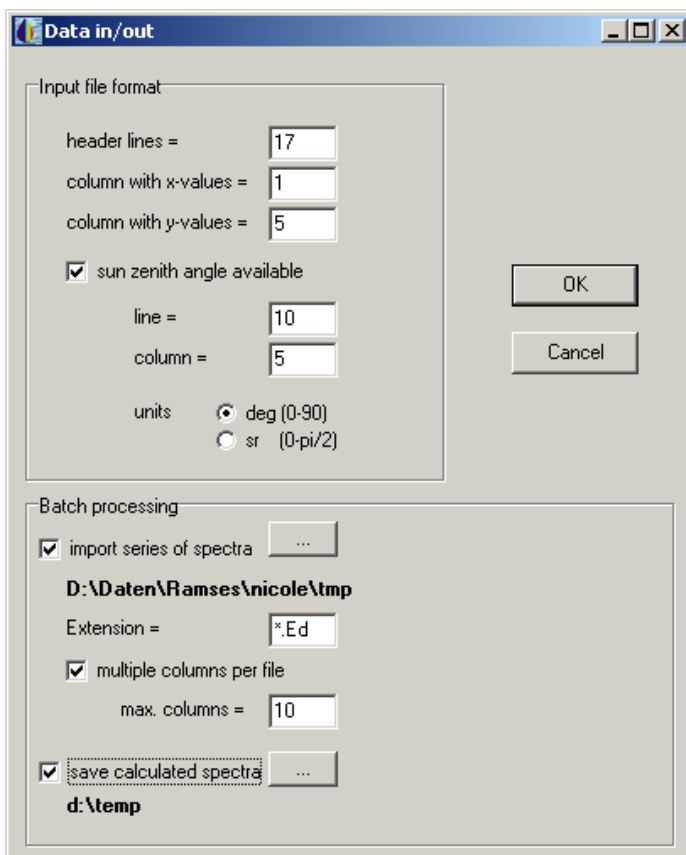


Fig. 4.7a: The pop-up window "Data in/out".

As a result of inversion, the fit results are stored in the table `FITPARS.TXT`. This table is generated at the specified path, irrespective whether saving of spectra is activated or deactivated. If saving of spectra is activated, for each input spectrum a file is generated which lists the spectral values of input and fit curve. The file names are identical to the input file names, but the file extensions are set to `INV`.

4.3.2 Definition of initial values

When a series of spectra shall be inverted, the initial values can either be chosen identically for every spectrum, or they are determined individually. The selection of the method is done in the "Initial values" register card of the pop-up window "Fit tuning" menu, as shown in Fig. 4.8. The pop-up window is accessed from the menu bar via "Options - Invers calculation - Fit tuning".

If the box "identical for all spectra" is marked with a hook, the initial values for every spectrum are taken from the parameter list, as described in section 4.1.3. Otherwise, there are two options: either the results from the previous fit are taken as start values for the subsequent fit, or some start values are determined from the spectrum itself. Which of these options is taken is specified individually for each spectrum type in the register card "Settings for individual spectra types". However, determination of start values from the spectrum itself is not possible for every spectrum type. If there is no register card for a specific spectrum type, or if the register card does not include a box labeled "automatic determination of initial values", the results from the previous fit are taken as start values.

Fig. 4.8 shows as an example the register card for the spectrum type `Irradiance reflectance`. "Automatic determination of initial values" is activated, i.e. the initial values are determined from the spectra themselves. The implemented algorithms for automatic determination and the relevant user interfaces are described in chapter 4.3 "Optimisation of inversion".

Fit tuning

Settings for all spectrum types

Initial values | Final Fit | Residual | Weights

Wavelength range from to nm

Data interval channels

Maximum number of iterations

Settings for individual spectrum types

Irradiance | Irradiance reflectance | Remote sensing reflectance

Analytic estimate of C_L deep water

at +/- nm

Analytic estimate of C[0] and C_Y

at +/- nm and +/- nm

Pre-fit of C_L, C_Y

from to nm steps nm max. Iterations

Pre-fit of C[0], C_Y

from to nm steps nm max. Iterations

Fig. 4.8: The pop-up window "Fit tuning" with the opened register cards "Initial values" and "Irradiance reflectance" of deep water.

4.4 Optimisation of inversion

4.4.1 Irradiance reflectance of deep water

The most important parameters that can be determined from irradiance reflectance spectra of deep water are the concentrations of phytoplankton, Gelbstoff and suspended matter. A study has been performed which investigated their retrieval sensitivity to errors (Gege 2002). It resulted a very small sensitivity for suspended matter, some sensitivity for Gelbstoff, but very high sensitivity for phytoplankton. The study suggested a procedure for initial values determination, which has been optimised by further simulations. Finally the 5-steps-procedure summarised in Table 4.2 was implemented in WASI. The user can fine-tune the procedure in the "Fit tuning" pop-up window, which is shown in Fig. 4.8. It is accessed from the menu bar via "Options - Invers calculation - Fit tuning".

Step	determine	algorithm	Procedure
1	C_X, C_{Mie}	analytical	Determine a first estimate of C_X and C_{Mie} from an analytic equation at a wavelength in the Infrared.
2	Y, C_0	analytical	Determine a first estimate of Y and C_0 from analytic equations at two wavelengths; for C_X and C_{Mie} the values from step 1 are taken.
3	C_X, C_{Mie}, Y	fit	Determine initial values of C_X, C_{Mie} and Y by fit; C_0 is kept constant at the value from step 2, C_X, C_{Mie} and Y are initialized using the values from steps 1 and 2, respectively.
4	C_0, Y, S	fit	Determine initial values of C_0, Y and S by fit; C_X is kept constant at the value from step 3, Y is initialized using the value from step 3, S is initialized by the user-setting from the parameter list.
5	All parameters	fit	All parameters are fitted, starting with initial values for C_X, C_{Mie}, C_0, Y and S from steps 3 and 4.

Table 4.2: Procedure for inversion of irradiance reflectance spectra of deep water.

Fine-tuning of steps 1 to 4 is done in the "Irradiance reflectance" register card of the "Fit tuning" pop-up window. It is shown in Fig. 4.9. Steps 1 and 2 are performed if the check boxes "Analytic estimate of ..." are marked with a hook. Otherwise the initial values from the parameter list or from the previous fit are taken, as described in section 4.2.2. Steps 3 and 4 are tuned in the "Pre-fit" frames. The pre-fits are performed if "max. iterations" is set to a value larger than 1. At step 5 the user can define the wavelength range to be fitted, the intervals between data points, and the maximum number of iterations. The relevant user interface is shown in Fig. 4.7.

Step 1. Suspended matter backscattering B_0 can be calculated analytically from the reflectance at any wavelength, for which phytoplankton and Gelbstoff absorption are either known or can be neglected. The equation of determination is obtained from the irradiance reflectance model described in section 2.5.1. Two models are implemented:

$$R(\lambda) = f \cdot \frac{b_{b,w}(\lambda) + B_0}{a(\lambda) + b_{b,w}(\lambda) + B_0}, \quad (4.1a)$$

$$R(\lambda) = f \cdot \frac{b_{b,w}(\lambda) + B_0}{a(\lambda)}. \quad (4.1b)$$

Settings for individual spectrum types

Irradiance Irradiance reflectance Remote sensing reflectance

Analytic estimate of C_X deep water

at +/- nm

Analytic estimate of C[0] and C_Y

at +/- nm and +/- nm

Pre-fit of C_X, C_Y

from to nm steps nm max. iterations

Pre-fit of C[0], C_Y

from to nm steps nm max. iterations

Fig. 4.9: The register card "Irradiance reflectance" for deep water of the pop-up window "Fit tuning".

Eq. (4.1a) is the Gordon et al. (1975) model, eq. (4.1b) the Prieur (1976) model, see section 2.5.1. If absorption of water and its constituents, a , is known at a certain wavelength λ_{IR} , B_0 is calculated as follows:

$$B_0 = \frac{a(\lambda_{IR}) \cdot R(\lambda_{IR})}{f - R(\lambda_{IR})} - b_{b,W}(\lambda_{IR}), \quad (4.2a)$$

$$B_0 = \frac{a(\lambda_{IR}) \cdot R(\lambda_{IR})}{f} - b_{b,W}(\lambda_{IR}). \quad (4.2b)$$

These equations are obtained by solving eqs. (4.1a) and (4.1b) for B_0 , respectively. Which is used for calculating B_0 depends on the selected R model. $a(\lambda_{IR})$ is calculated according to eq. (2.3) using as inputs the values from the parameter list; typically $a(\lambda_{IR})$ is very close to pure water absorption, $a_W(\lambda_{IR})$, except for high Gelbstoff concentration.

The calculation of f depends on the selected f model, cf. chapter 6.2. If f is parameterised solely as a function of the sun zenith angle (eqs. 6.1, 6.3), the f value resulting from the given sun zenith angle is taken. If f is parameterised additionally as a function of backscattering (eqs. 6.2, 6.4), f is calculated in two steps. First, the values from the parameter list are taken to calculate backscattering at wavelength λ_{IR} using eq. (2.4); with that result a first estimate of f is calculated. In the second step, eq. (4.2a) or (4.2b) is applied to calculate B_0 using the f value from the first step. Then f is calculated again using eq. (6.2) or (6.4).

A special algorithm has been implemented for the f model $f = \text{constant}$. Obviously a constant f value needs no further consideration for applying eq. (4.2a) or (4.2b). However, if that f model is selected, f can be treated as a fit parameter. If fitting of f is activated, an initial value for f can be calculated in addition to B_0 as described in the following.

Special case: Initial values for f and B_0

Calculation is based on reflectance values at two wavelengths $\lambda_{IR,1}$ and $\lambda_{IR,2}$ ($\lambda_{IR,2} > \lambda_{IR,1}$). It requires that $R(\lambda_{IR,1}) \neq R(\lambda_{IR,2})$; if that is not the case, f is kept constant at the value from the parameter list, and B_0 is calculated as described above. Initial values determination makes use of eq. (4.1a); no corresponding algorithm for eq. (4.1b) is implemented.

First the factor f is eliminated by taking the ratio of eq. (4.1a) for two wavelengths $\lambda_{IR,1}$ and $\lambda_{IR,2}$:

$$\frac{R(\lambda_{IR,1}) \cdot (a(\lambda_{IR,1}) + b_{b,W}(\lambda_{IR,1}) + B_0)}{R(\lambda_{IR,2}) \cdot (a(\lambda_{IR,2}) + b_{b,W}(\lambda_{IR,2}) + B_0)} = \frac{b_{b,W}(\lambda_{IR,1}) + B_0}{b_{b,W}(\lambda_{IR,2}) + B_0}. \quad (4.3)$$

Eq. (4.3) assumes that B_0 is the same at $\lambda_{IR,1}$ and $\lambda_{IR,2}$. Multiplication of eq. (4.3) with the product of both denominators leads to a quadratic expression in B_0 of the form

$$\alpha \cdot B_0^2 + \beta \cdot B_0 + \gamma = 0, \quad (4.4)$$

with

$$\alpha = R(\lambda_{IR,1}) - R(\lambda_{IR,2}); \quad (4.5a)$$

$$\beta = R(\lambda_{IR,1}) \cdot (a(\lambda_{IR,1}) + b_{b,W}(\lambda_{IR,1}) + b_{b,W}(\lambda_{IR,2})) - R(\lambda_{IR,2}) \cdot (a(\lambda_{IR,2}) + b_{b,W}(\lambda_{IR,1}) + b_{b,W}(\lambda_{IR,2})); \quad (4.5b)$$

$$\gamma = R(\lambda_{IR,1}) \cdot (a(\lambda_{IR,1}) + b_{b,W}(\lambda_{IR,1})) \cdot b_{b,W}(\lambda_{IR,2}) - R(\lambda_{IR,2}) \cdot (a(\lambda_{IR,2}) + b_{b,W}(\lambda_{IR,2})) \cdot b_{b,W}(\lambda_{IR,1}). \quad (4.5c)$$

It has two solutions:

$$B_0 = \frac{-\beta \pm \sqrt{\beta^2 - 4\alpha\gamma}}{2\alpha}. \quad (4.6)$$

The positive solution gives the correct value of B_0 . This is the algorithm for calculating B_0 . The algorithm for calculating f is obtained directly from eq. (4.1a):

$$f = R(\lambda_{IR,2}) \cdot \frac{a(\lambda_{IR,2}) + b_{b,W}(\lambda_{IR,2}) + B_0}{b_{b,W}(\lambda_{IR,2}) + B_0}. \quad (4.7)$$

It has been investigated how the accuracy of the retrieved C_L values depends on the choice of the wavelengths $\lambda_{IR,1}$ and $\lambda_{IR,2}$ and on the errors of the initial Y and C_L values. The more $\lambda_{IR,1}$ and $\lambda_{IR,2}$ are shifted towards longer wavelengths, the better are the results. For Gelbstoff concentrations below 1 m^{-1} the relative error of C_L is always below 20 % if both wavelengths are above 820 nm. For the MERIS channels $\lambda_{IR,1} = 870 \text{ nm}$ and $\lambda_{IR,2} = 900 \text{ nm}$ the relative errors are always below 5 % for $Y \leq 0.5 \text{ m}^{-1}$ and below 12 % for $Y \leq 1 \text{ m}^{-1}$. Hence, for sensors equipped with two or more channels above 820 nm and for moderate Gelbstoff concentrations the analytical equations are well-suited to determine initial values of C_L and f.

The conversion from optical units B_0 to gravimetric concentrations C_L , C_S is based on eq. (2.4) assuming $b_L(\lambda) = 1$. Accordingly it is $B_0 \equiv b_b(\lambda) - b_{b,W}(\lambda) = C_L \cdot b_{b,L}^* + C_S \cdot b_{b,S}^* \cdot (\lambda/\lambda_S)^n$. If $C_S = 0$, C_L is calculated as

$$C_L = \frac{B_0}{b_{b,L}^*}. \quad (4.8a)$$

Otherwise, i.e. for $C_S \neq 0$, the user-defined ratio $r_{LS} = C_L/C_S$ is retained, hence the initial values of C_L and C_S are calculated as follows:

$$C_L = \frac{B_0}{b_{b,L}^* + \frac{b_{b,S}^*}{r_{LS}} \cdot \left(\frac{\lambda_{IR}}{\lambda_S} \right)^n}; \quad C_S = \frac{C_L}{r_{LS}}. \quad (4.8b)$$

C_L can be determined in that way with an accuracy in the order of 1 % (Gege and Albert 2005).

Step 2. A non-iterative procedure based on two channels was found to be practicable for calculating the initial concentrations of phytoplankton and Gelbstoff at an accuracy in the order of 30 % (Gege and Albert 2005). If suspended matter concentration and the factor f are known with little error, e.g. from step 1, the concentrations C_0 and Y can be determined analytically from two wavelengths λ_1 and λ_2 . The equations of determination are obtained from the irradiance reflectance model described in chapter 2.5.1:

$$R(\lambda) = f \cdot \frac{b_b(\lambda)}{a_w(\lambda) + Y \cdot a_Y^*(\lambda) + C_0 \cdot a_0^*(\lambda) + b_b(\lambda)}. \quad (4.9)$$

Resolving the equation for the sum $Y \cdot a_Y^*(\lambda) + C_0 \cdot a_0^*(\lambda)$, and ratioing that equation for two wavelengths yields the following ratio R_A :

$$R_A := \frac{Y \cdot a_Y^*(\lambda_1) + C_0 \cdot a_0^*(\lambda_1)}{Y \cdot a_Y^*(\lambda_2) + C_0 \cdot a_0^*(\lambda_2)} = \frac{f \cdot \frac{b_b(\lambda_1)}{R(\lambda_1)} - a_w(\lambda_1) - b_b(\lambda_1)}{f \cdot \frac{b_b(\lambda_2)}{R(\lambda_2)} - a_w(\lambda_2) - b_b(\lambda_2)}. \quad (4.10)$$

Since all functions on the right-hand side of this equation are known, R_A can be calculated. Division of nominator and denominator of the center expression by C_0 leads to an equation which has as single unknown parameter the ratio Y/C_0 . Rewriting this equation yields the following expression:

$$\frac{Y}{C_0} = \frac{R_A \cdot a_p^*(\lambda_2) - a_p^*(\lambda_1)}{a_Y^*(\lambda_1) - R_A \cdot a_Y^*(\lambda_2)}. \quad (4.11)$$

The ratio of Gelbstoff to phytoplankton concentration is calculated using this equation. It is a matter of optimisation to determine the best-suited wavelengths λ_1 and λ_2 . By inserting $Y = (Y/C_0) \cdot C_0$ into eq. (4.9) and solving eq. (4.9) for C_0 the following expression is obtained:

$$C_0 = \frac{f \cdot \frac{b_b(\lambda_3)}{R(\lambda_3)} - a_w(\lambda_3) - b_b(\lambda_3)}{a_0^*(\lambda_3) + \frac{Y}{C_0} \cdot a_Y^*(\lambda_3)}. \quad (4.12)$$

Eq. (4.12) is used to calculate the phytoplankton concentration. It is a matter of optimisation to determine the best-suited wavelength λ_3 . Gelbstoff concentration is then calculated using eq. (4.13) with the results from eqs. (4.11) and (4.12):

$$Y = \frac{Y}{C_0} \cdot C_0. \quad (4.13)$$

It has been investigated how the accuracy of the ratio Y/C_0 and of the C_0 and Y values depends on the choice of the wavelengths λ_1 , λ_2 and λ_3 , on the errors of C_L determination from step 1 and on suspended matter concentration. The results of these studies are as follows:

- λ_1 should be chosen below 470 nm;
- λ_2 should be chosen below 500 nm;
- λ_3 should be chosen below 550 nm.

In each case, preference should be given to shorter wavelengths. A good choice is $\lambda_2 = \lambda_0$ since S errors don't affect Gelbstoff absorption at λ_0 . For λ_3 no separate wavelength must be chosen, it can be set $\lambda_3 = \lambda_2$. Consequently, selection of only two wavelengths is implemented in WASI. Their defaults are: $\lambda_1 = 413$ nm, $\lambda_2 = 440$ nm.

Steps 3 and 4. These steps were suggested by Gege (2002). The newly developed steps 1 and 2 make them now unnecessary in most cases, but they are useful under certain conditions, for instance if no suitable infrared channel is available for accurate determination of C_L or C_S , or if S is fit parameter. Steps 3 and 4 improve the estimates for C_0 , C_L , C_S and Y by including additional spectral information, and a start value of S can be determined. Wavelength range, data interval and maximum number of iterations for the fits of steps 3 and 4 are specified in the "Pre-fit" frames of the register card "Irradiance reflectance" of Fig. 4.9. If `max. iterations` is set to 0 or 1, the respective fit is not performed.

Step 5. Wavelength range, data interval and maximum number of iterations for the fit of step 5 are specified in the "Final fit" register card of the "Fit tuning" pop-up window, see Fig. 4.7. The maximum number of iterations forces the fit routine to stop; the number should be set high enough that a forced stop is exceptional.

4.4.2 Irradiance reflectance of shallow water

Inversion of a shallow water irradiance reflectance spectrum determines in addition to the parameters of deep water several parameters related to the bottom: bottom depth z_B and areal fractions f_n of up to 6 bottom albedo spectra. The analytic function $R^{sh}(\lambda)$ used for inversion is given by eq. (2.16). Since it consists of as much as 21 parameters, it is very important to initialise the fit parameters with realistic values. Otherwise the probability is large that the Simplex gets lost in the high dimensional search space (up to 22 dimensions) and hence the fit provides completely wrong results. Albert (2004) developed the well-working methodology of Table 4.3 to increase step by step the number of estimated parameters, and he implemented it in WASI.

Step	determine	algorithm	Procedure
1	z_B	analytical	Determine a first estimate of z_B from an analytic equation at a wavelength interval in the red.
2	C_L, C_S	analytical	Determine a first estimate of C_L and C_S from an analytic equation at a wavelength in the Infrared using the z_B value from step 1.
3	$a_{WC}(\lambda)$	nested intervals	Estimate the total absorption spectrum of all water constituents for a wavelength interval in the visible using nested intervals. The required values of z_B, C_L and C_S are taken from steps 1 and 2.
4	C_0, Y	fit	Determine a first estimate of C_0 and Y by fitting the spectrum $a_{WC}(\lambda)$ of step 3.
5	f_n	$f_n = 1/N$	The areal fractions of all bottom types are set equal; N = number of considered bottom types.
6	C_L, C_S, Y, z_B	fit	Determine a second estimate of C_L, C_S, Y and z_B by fitting a wavelength interval in the infrared.
7	C_0, Y, S, z_B	fit	Determine a first estimate of S , a second of C_0 , and a third of Y and z_B by fitting a wavelength interval in the blue.
8	All parameters	fit	All fit parameters are fitted.

Table 4.3: Procedure for inversion of irradiance reflectance spectra of shallow water.

Fine-tuning of steps 1, 2, 4, 6, and 7 is done in the "Irradiance reflectance" register card of the "Fit tuning" pop-up window. It is shown in Fig. 4.10. Steps 1 and 2 are performed if the check boxes "Analytic estimate of ..." are marked with a hook. Otherwise the initial values from the parameter list or from the previous fit are taken, as described in section 4.2.2. Steps 4, 6 and 7 are tuned in the "Pre-fit" frames. The pre-fits are performed if "max. iterations" is set to a value larger than 1. At step 8 the user can define the wavelength range to be fitted, the intervals between data points, and the maximum number of iterations. The relevant user interface is shown in Fig. 4.7.

Step 1. The equation (2.16), which parameterises irradiance reflectance of shallow water, is simplified by setting $K_{uW}(\lambda) = K_{uB}(\lambda) = K_d(\lambda)$. The resulting equation,

$$R^{sh}(\lambda) = R(\lambda) - A_1 \cdot R(\lambda) \cdot \exp\{-2K_d(\lambda) \cdot z_B\} + A_2 \cdot R^b(\lambda) \cdot \exp\{-2K_d(\lambda) \cdot z_B\}, \quad (4.14)$$

is solved for z_B :

$$z_B = \frac{1}{2K_d(\lambda)} \ln \frac{A_1 \cdot R(\lambda) - A_2 \cdot R^b(\lambda)}{R(\lambda) - R^{sh}(\lambda)}. \quad (4.15)$$

Various simulations were performed to study the accuracy of this equation depending on wavelength and on errors of concentration and bottom type (Albert 2004). The wavelength interval 600–650 nm was found to be best-suited, thus it is used by default in WASI. By averaging the z_B values of that interval, an accuracy of z_B of typically 20–40 % can be expected at moderate suspended matter concentration (< 10 mg/l) and $z_B < 10$ m. Such accuracy is sufficient to initialise z_B .

Settings for individual spectrum types

Irradiance | Irradiance reflectance | Remote sensing reflectance

Analytic estimate of z_B shallow water
at 630 +/- 20 nm

Analytic estimate of C_L
at 760 +/- 2.0 nm

C[0] and C_Y by nested intervals and fit of absorption spectrum
from 400 to 800 nm steps 5 nm max. Iterations 100

Pre-Fit of C_L, C_S and C_Y
from 700 to 800 nm steps 5 nm max. Iterations 100

Pre-Fit of C[0], C_Y and S
from 400 to 500 nm steps 5 nm max. Iterations 100

Fig. 4.10: The register card "Irradiance reflectance" for shallow water of the pop-up window "Fit tuning".

Step 2. Like in the deep water case, an analytic approximation of the reflectance spectrum is solved for suspended matter backscattering $B_0 \equiv b_b(\lambda) - b_{b,w}(\lambda)$ to obtain an analytic equation for B_0 . The analytic approximation of the reflectance spectrum is given by eq. (4.14) in which $R(\lambda)$ is replaced by eq. (4.1a). Solving this equation for B_0 yields:

$$B_0 = \frac{\mathfrak{R}^0(\lambda) \cdot [a(\lambda) + b_{b,w}(\lambda)] - b_{b,w}(\lambda)}{1 - \mathfrak{R}^0(\lambda)}, \quad (4.16)$$

where

$$\mathfrak{R}^0(\lambda) = \frac{1}{f} \cdot \frac{R^{sh}(\lambda) - A_2 \cdot R^b(\lambda) \cdot \exp\{-2K_d(\lambda) \cdot z_B\}}{1 - A_1 \cdot \exp\{-2K_d(\lambda) \cdot z_B\}}. \quad (4.17)$$

The conversion from optical units B_0 to gravimetric units C_L , C_S uses eq. (4.8a) or (4.8b), as for deep water.

Simulations of Albert (2004) showed that for $z_B > 2$ m the accuracy is typically better than 20 % for $C_L + C_S < 5$ mg/l and better than 40 % for $C_L + C_S < 25$ mg/l if 760 nm is taken as reference wavelength, which is used as default in WASI. Such accuracy is sufficient for initialising C_L and C_S .

Step 3. Because eq. (4.14) cannot be solved analytically for C_0 and Y , an intermediate step is required to estimate the total absorption of all water constituents, a_{WC} . This is done iteratively by the method of nested intervals, which is described in the following.

At wavelengths of non-negligible absorption of water constituents the values of R and K_d depend on a_{WC} . When R is calculated using eq. (4.1a) and K_d using eq. (2.5), values for b_b and a

have to be assigned first. b_b is calculated using eq. (2.4); for its critical parameters C_L and C_S the values from step 2 are taken. a is calculated using eq. (2.3); the value of a_{WC} in that equation is treated as unknown and determined iteratively as follows. In the first step R and K_d are calculated using a start value A_0 for a_{WC} in eq. (2.3), and with these R and K_d values R^{sh}_0 is calculated using eq. (4.14). In the next steps A_0 is replaced in a systematic way with different A_i values until one of the following stop criteria is reached: (1) the ratio $\delta = R^{sh}_i / R^{sh} - 1$, which is a measure of the deviation between calculated value R^{sh}_i and measurement R^{sh} , is below a threshold δ_{min} ; (2) the number of iterations exceeds a threshold i_{max} . The rule for calculating A_{i+1} from A_i is as follows:

$$A_{i+1} = \begin{cases} A_i + \frac{\Delta}{i} & \text{if } \delta < 0 \\ A_i - \frac{\Delta}{i} & \text{if } \delta > 0 \end{cases} \quad (4.18)$$

The value of the last iteration, A_{i+1} , is assigned to a_{WC} . These iterations are performed wavelength for wavelength. The wavelength range 400–800 nm and a wavelength interval of 5 nm were found suitable, thus these are used by default in WASI. As a result an estimate of the spectrum $a_{WC}(\lambda)$ is obtained. $A_0 = 5 \text{ m}^{-1}$, $\Delta = 1 \text{ m}^{-1}$, $\delta_{min} = 0.01$ and $i_{max} = 100$ are set as defaults in WASI. Wavelength range, wavelength interval, and i_{max} can be changed in the frame labeled "C[0] and C_Y by nested intervals and fit of absorption spectrum" of Fig. 4.10. A_0 , Δ , and δ_{min} can be changed by editing the WASI.INI file.

Step 4. A first estimate of the two parameters C_0 and Y is determined by fitting the spectrum $a_{WC}(\lambda)$ from step 3 with the Simplex algorithm using eq. (2.1). The parameters $C_1 \dots C_5$ and D of eq. (2.1) are set to zero in this step. For wavelength range, wavelength interval, and i_{max} the same values are taken as in step 3.

Step 5. The areal fractions f_n of all those bottom types are set equal which are marked as fit parameters.

Steps 6 and 7. These steps can be tuned by the parameters in the two "Pre fit ..." frames of Fig. 4.10.

Step 8. Wavelength range, data interval and maximum number of iterations are specified in the "Final fit" register card of the "Fit tuning" pop-up window, see Fig. 4.7. The maximum number of iterations forces the fit routine to stop; the number should be set high enough that a forced stop is exceptional.

4.4.3 Remote sensing reflectance of deep water

The remote sensing reflectance of deep water above the surface, $R_{rs}(\lambda)$, is calculated using eq. (2.20a), (2.20b) or (2.20c); that below the surface, $R_{rs}^-(\lambda)$, according to eq. (2.17a) or (2.17b). $R_{rs}(\lambda)$ has 25 parameters which may be fitted, $R_{rs}^-(\lambda)$ has 15. This high number of fit parameters makes fit tuning necessary. In particular it is important to find suitable start values of the parameters, i.e. to start with initial values which are not too different from the final results. The user interface for controlling fit tuning is shown in Fig. 4.11. It is accessed from the menu bar via "Options - Invers calculation - Fit tuning".

Settings for individual spectrum types

Irradiance | Irradiance reflectance | **Remote sensing reflectance**

use Ed measurement (for wavelength-dependent surface reflections) deep water

File: ...

Header lines X-Column Y-Column

Pre-Fit Ed measurement

from to nm steps nm max. Iterations

Pre-Fit Infrared

from to nm steps nm max. Iterations

Pre-Fit Blue

from to nm steps nm max. Iterations

Fig. 4.11: The register card "Remote sensing reflectance" for deep water of the pop-up window "Fit tuning".

If a downwelling irradiance measurement is available, the number of fit parameters for $R_{rs}(\lambda)$ can be reduced by 4 (α , β , γ , δ). In this case the box "use Ed measurement" should be marked with a hook, and the measured spectrum has to be specified.

Most of the initial values are taken from the parameter list in the main window. However, for some parameters an automatic determination is possible: for α , β , γ , δ if an Ed measurement is available, for C_X and σ_L from a pre-fit in the Infrared, and for C_0 , Y , S and Q from a pre-fit in the Blue. These pre-fits are activated by choosing a value >1 for "max. Iterations". The wavelength intervals, steps and maximum number of iterations have to be specified for each pre-fit. If "max. Iterations" is set to 0 or 1, the corresponding pre-fit is not performed.

4.4.4 Remote sensing reflectance of shallow water

For inversion of remote sensing reflectance spectra also the 8 steps of Table 4.3 are performed. The only difference to the case of irradiance reflectance is that all R spectra are replaced by the corresponding R_{rs} spectra.

4.4.5 Downwelling irradiance

The downwelling irradiance above the water surface, $E_d(\lambda)$, is calculated according to eq. (2.1) as a weighted sum of 4 spectra. Since the curve forms of these spectra are quite different, it is not possible to obtain similar sum curves by using rather different sets of weights. In other words, the solution of the inversion is unequivocal. Consequently, no fine-tuning of the inversion scheme is necessary.

The downwelling irradiance below the water surface, $E_d^-(\lambda)$, is calculated according to eq. (2.4) using the above-water spectrum $E_d(\lambda)$. For $E_d(\lambda)$ either the parameterization of eq. (2.1) can be chosen, or a measured spectrum can be taken. The selection is done in the register card "Irradiance" of the pop-up window "Fit tuning", which is shown in Fig. 4.12. It is accessed from the menu bar via "Options - Invers calculation - Fit tuning".

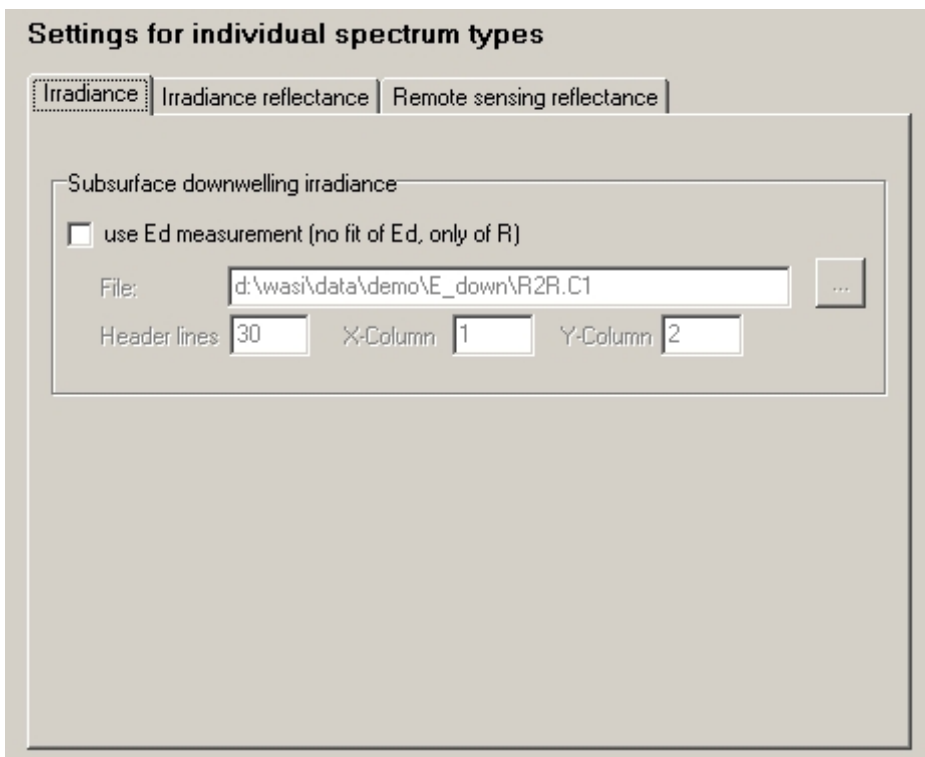


Fig. 4.12: The register card "Irradiance" of the pop-up window "Fit tuning".

Downwelling irradiance spectra below the water surface are not very different from those above the surface, i.e. the curve form of $E_d^-(\lambda)$ depends much more on the parameters of $E_d(\lambda)$ than on those of $R(\lambda)$. Hence small errors of $E_d(\lambda)$ cause large errors of the retrieved parameters of $R(\lambda)$. Thus the option of using $E_d(\lambda)$ measurements for fitting $E_d^-(\lambda)$ must be applied with care; in general it should not be used.⁷

⁷ The option has been included for consistency reasons: $E_d(\lambda)$ measurements are useful for inversion of upwelling radiance and specular reflectance spectra.

5. Reconstruction mode

The reconstruction mode is a combination of forward and inverse mode: A spectrum is calculated in the forward mode, and subsequently this spectrum is fitted in the inverse mode. The model parameters of the forward calculation are stored together with the fit parameters of the inversion in one file; the spectrum may be saved or not. Analogously to the forward mode, up to three parameters can be iterated simultaneously. Parameters of the forward mode and of the inverse mode can be chosen differently. The mode is called reconstruction mode because inversion reconstructs model parameters of the forward mode at altered conditions. It is useful for sensitivity studies.

5.1 Definition of parameter values

Initial values of each fit parameter are read from the WASI.INI file. The user can change them most conveniently in the parameter list at the left side of the main window (or alternatively in the "Fit parameters" pop-up window, see Fig. 4.4). An example is shown in Fig. 5.1.

The figure displays two screenshots of a software interface for parameter configuration. Both screenshots show a dropdown menu set to "Downwelling irradiance" and a "Start" button.

Top Screenshot (Forward Modeling):

Parameter	Value
alpha	0.200
beta	0.100
gamma	0.100
delta	0
nue	1

Additional options: invert spectra, above water.

Bottom Screenshot (Start Values of Inversion):

Parameter	Fit?	Value
alpha	<input checked="" type="checkbox"/>	0.200
beta	<input checked="" type="checkbox"/>	0.0500
gamma	<input checked="" type="checkbox"/>	0.200
delta	<input type="checkbox"/>	0
nue	<input type="checkbox"/>	0

Additional options: invert spectra, batch mode, read from file, above water.

Fig. 5.1: Example of a parameter list. Top: values of forward modeling; bottom: start values of inversion.

By clicking the "invert spectra" check box, the user can quickly switch between the forward and inverse values. Fig. 5.1 shows as an example the parameter list of the downwelling irradiance model above the water surface. On top the forward values are shown, on bottom the start values of the inverse mode. The forward and inverse values are chosen identical for two parameters (alpha, delta), and differently for three other parameters (beta, gamma, nue).

Fig. 5.1 is an example how to study propagation of model errors. A different value of the parameter nue is chosen for forward and inverse calculation, and nue is not fitted. This is an efficient way to introduce a well-defined model error: the error of the inverse model is attributed to the parameter nue, and the error is given quantitatively as $nue^{wrong} - nue^{correct} = 0 -$

1. Due to the wrong nue value, the fit cannot find the correct values of the fit parameters alpha, beta, gamma. The errors of these parameters depend only on the nue error. In this way, the sensitivity of alpha, beta, gamma on nue errors can be studied. Systematic investigations of such error propagation are the basis of sensitivity studies.

Error propagation can be investigated systematically by iterating the erroneous model parameter during forward calculation. The way to do this is explained in section 3.3.2. Fig. 5.2 shows as example how to study systematically the errors caused by wrong values of the parameter nue: nue is iterated from -1 to 1 in 11 steps. Thus, 11 spectra are calculated in the forward mode with nue values of -1, -0.8, ..., 1, and these spectra are subsequently fitted. If nue is fixed during inversion like in Fig. 5.1, a series of inversion results is obtained for a systematically changing error of the parameter nue.

Parameter	from	to	steps	log
nue	-1.00	1	11	<input type="checkbox"/>
none	1	20.0	20	<input type="checkbox"/>
none	0.01000	10.0	19	<input checked="" type="checkbox"/>

Fig. 5.2: Iteration of the parameter nue.

5.2 Definition of output information

The results of fitting a series of spectra are stored in a single file, FITPARS.TXT. Fig. 5.3 shows as an example a listening of this file for the settings of Figs. 5.1 and 5.2. The first lines explain the file content and summarize relevant information.

The first column of the data block of the file FITPARS.TXT, headed "File", lists the file names of the calculated spectra. Whether the spectra are saved or not, decides the user. As sensitivity

```

This file was generated by the program WASI
Version 2.4 - Latest update: 6 July 2004

List of fitted parameters which may differ from one spectrum to the next
Common parameter set of all spectra in file: WASI.INI
Errors are given in %: error = 100*(inv/fwd-1)

```

File	fwd nue	Inversion Iterations	Residuum	inv alpha	inv beta	inv gamma	error alpha	error beta	error gamma
B01	-1.000	105	0.166	0.186	0.0741	0.146	-7.00	-25.9	46.0
B02	-0.8000	111	0.129	0.189	0.0794	0.136	-5.50	-20.6	36.0
B03	-0.6000	112	0.0957	0.192	0.0845	0.126	-4.00	-15.5	26.0
B04	-0.4000	114	0.0654	0.195	0.0895	0.117	-2.50	-10.5	17.0
B05	-0.2000	118	0.0383	0.197	0.0945	0.108	-1.50	-5.50	8.00
B06	-5.551E-17	103	0.0147	0.199	0.0993	0.0998	-0.500	-0.700	-0.200
B07	0.2000	99	0.0103	0.201	0.104	0.0919	0.500	4.00	-8.10
B08	0.4000	110	0.0281	0.203	0.109	0.0844	1.50	9.00	-15.6
B09	0.6000	111	0.0444	0.204	0.113	0.0773	2.00	13.0	-22.7
B10	0.8000	142	0.0585	0.206	0.118	0.0705	3.00	18.0	-29.5
B11	1	96	0.0703	0.207	0.123	0.0641	3.50	23.0	-35.9
mean=	-6.056E-17	111	0.06557	0.1981	0.09894	0.1019	2.86	13.2	22.3
max=	-1.000	142	0.1663	0.2070	0.1230	0.1460	-7.00	-25.9	46.0

Fig. 5.3: Example of the output file FITPARS.TXT.

studies are generally based on a large number of spectra, usually not all spectra are saved, but only a few for illustration purposes. Thus, a study may be performed in two steps: in the first step, the parameters of interest are iterated over the interesting ranges with few steps, and the resulting spectra are saved; in the second step, the calculations of step 1 are repeated, but with much more steps, and without saving the spectra. How to save forward calculated spectra is described in sections 3.2.4 and 3.3.3, the corresponding pop-up window is shown in Fig. 3.2. How to save fit spectra is described in section 4.3.1. How the directories are selected is described in section 8.1, the corresponding pop-up window is shown in Fig. 8.2.

The second column of the data block lists the values of the parameter which is iterated during forward calculation. The abbreviation "fwd" in the heading of this column means "value of forward calculation", the heading's second line specifies the parameter name. If more than one parameter is iterated, similar columns are added. In the example of Fig. 5.3, 11 values of the parameter ν (-1.000, -0.800, ..., 1) were taken for forward calculation. Since the other model parameters were hold constant for the series of forward calculations, these are not included in this file; their values are documented in the WASI.INI file, as indicated in the header information.

All subsequent columns summarize the results which were obtained by fitting the forward calculated spectra. The column headed "Inversion Iterations" shows the required number of iterations of the fit routine (see 4.2.4). The next column, "Residuum", lists the residuals, which are a measure for the correspondence between the forward calculated spectrum and the fit curve (see 4.2.3.1). The next columns tabulate the resulting values of the fit parameters. The abbreviation "inv" in their heading means "value of inverse calculation", the heading's second line specifies the parameter name. Each parameter, for which in the parameter list the corresponding check box "Fit?" is marked with a hook, is represented by such a column. In the example of Fig. 5.3 these are the parameters alpha, beta, gamma.

The specific results of the reconstruction mode are tabulated in the last columns. These columns, labeled "error" and headed by parameter names, list the relative errors of user-selected parameters. The selection which parameters to tabulate, is done in the pop-up window "Reconstruction mode settings", which is shown in Fig. 5.4. This window is accessed from the menu bar via "Options – Reconstruction mode", see Fig. 8.1. The relative errors are calculated as $100 * (\text{inv}/\text{fwd} - 1)$, where "inv" is the fit result of inverse modeling and "fwd" is the parameter value used during forward calculation. Hence, the relative errors are the fit parameter's deviations from the "true" values in percent.

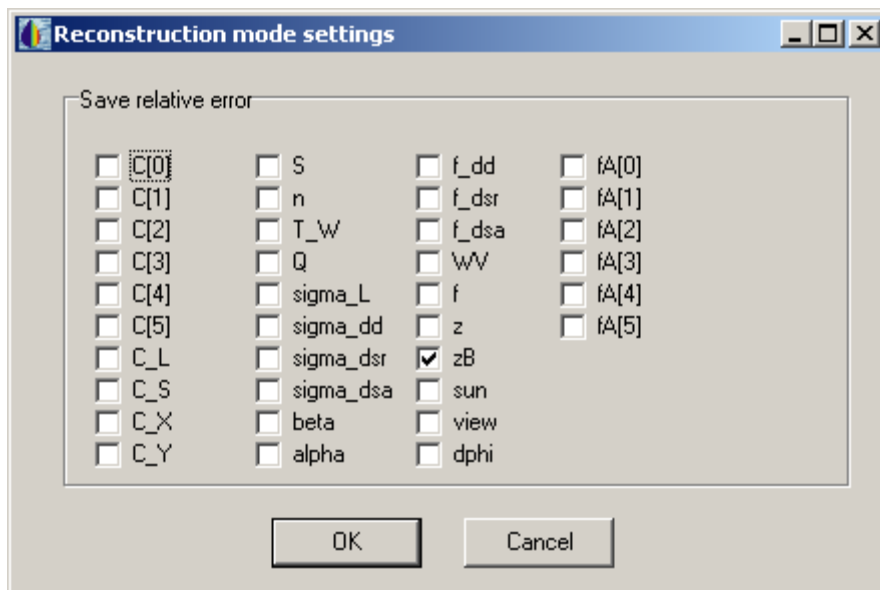


Fig. 5.4: The pop-up window "Reconstruction mode settings".

6. 2D mode

The 2D mode allows to visualize and invert hyperspectral and multispectral image data using the models described in chapter 2. It is intended primarily to process atmospherically corrected images from airborne sensors and satellite instruments in units of upwelling radiance or remote sensing reflectance. Please refer to Gege (2014) for a detailed description.

7. Model options

7.1 Downwelling irradiance

The spectrum type "Downwelling irradiance" is activated by selecting in the main window "Downwelling irradiance" from the drop-down list above the "Start" button, see Fig. 6.1 right. After the spectrum type is selected, the check box "above water" appears on the screen, and the relevant parameters are activated in the parameter list (Fig. 7.1 left). The example of Fig. 7.1 shows the parameters of the irradiance model below the water surface (equation 2.29).

Parameter	Value	Parameter	Value
C[0]	2.000	sun	30.00
C[1]	0	view	0
C[2]	0	f_dd	1
C[3]	0	f_ds	1
C[4]	0	H_oz	0.3000
C[5]	0	alpha	1.317
fluo	0.01000	beta	0.2606
C_L	1	WV	2.500
C_S	0	sigma_dd	1
C_D	0	rho_dd	0.0211
C_Y	0.3000	rho_ds	0.0679
S	0.01400	fa[0]	0
n	0	fa[1]	0
T_W	20.00	fa[2]	0
f	0.4000	fa[3]	0
Q	5.000	fa[4]	0
z	0.5000	fa[5]	0
zB	100.0		

Downwelling irradiance

Start

above water

Fig. 7.1: Parameter settings of the spectrum type "Downwelling irradiance". Left: Parameter list for in-water calculation. Right: Drop-down list with "Downwelling irradiance" selected as spectrum type and "above water" check box.

A number of options are available for calculating downwelling irradiance. These are set in the register card shown in Fig. 7.2. It is accessed from the menu bar via "Options – Models - Irradiance".

The first panel "Reflection factors for downwelling irradiance" is used to specify how reflection of downwelling irradiance at the water surface is calculated. The reflection factor for the direct component, ρ_{dd} , is calculated by default using the Fresnel equation (the check box "Calculate rho_dd using sun zenith angle and Fresnel equation" is marked with a hook). Alternately, a user-defined value can be used (by de-selecting that check box and entering the

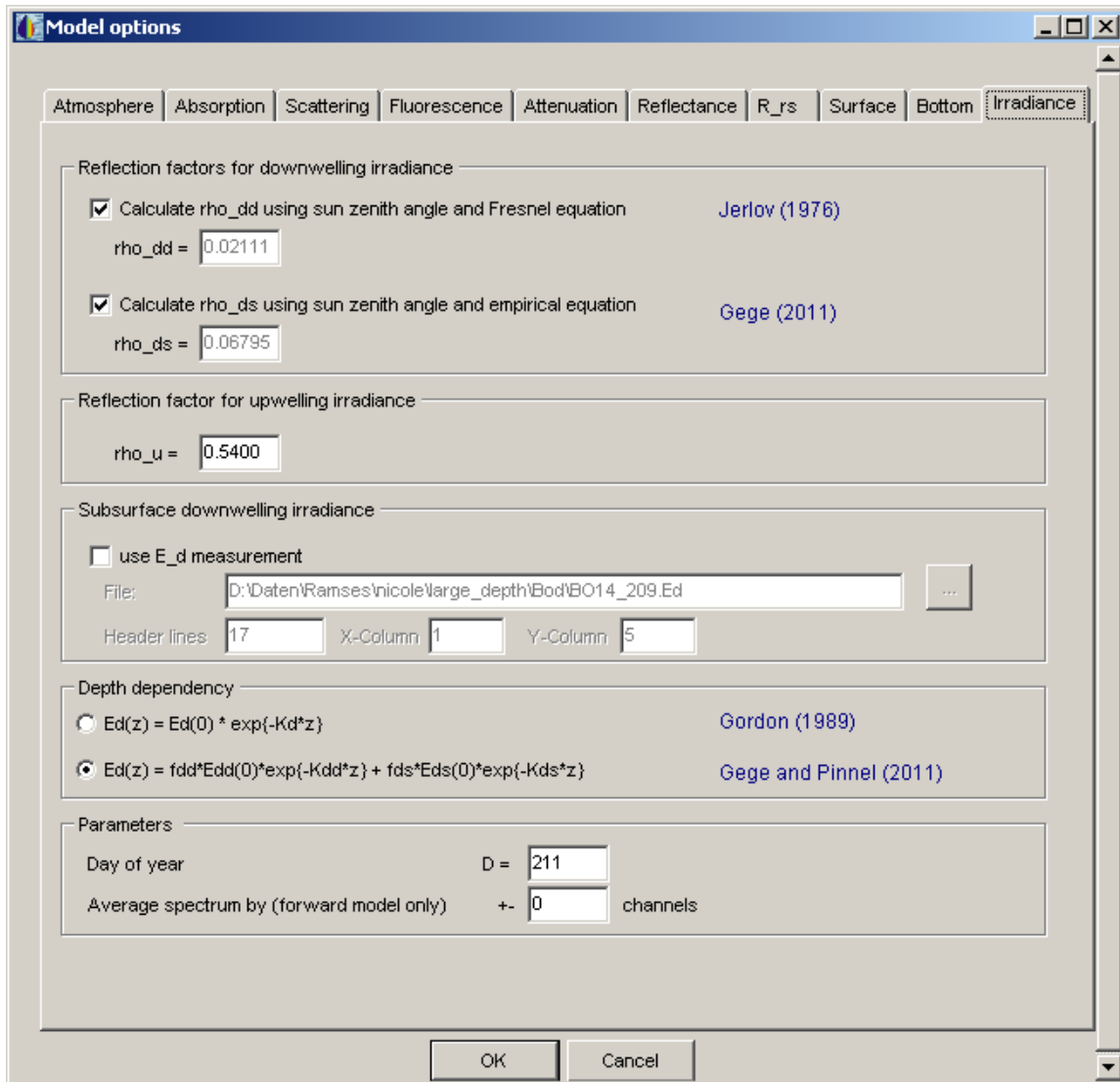


Fig. 7.2: The register card "Irradiance" of the pop-up window "Options – Model".

desired value in the "rho_dd" box). Similarly, the reflection factor for the diffuse component, ρ_{ds} , can either be calculated using equation (2.24) by activating the check box "Calculate rho_ds using sun zenith angle and empirical equation", or the value of ρ_{ds} can be specified by the user in the "rho_ds" edit box. The second panel "Reflection factor for upwelling irradiance" is used to specify the value of ρ_u .

7.2 Irradiance reflectance

The spectrum type "Irradiance reflectance" is activated by selecting this type in the main window from the drop-down list above the "Start" button, see Fig. 7.2 left. After the spectrum type is selected, one of the two parameter lists shown in Fig. 7.2 is displayed: if the check box "shallow water" below the "Start button" is not marked, the short list is displayed (Fig. 7.2 center), otherwise the long list is displayed (Fig. 7.2 right). Only 25 of the 36 parameters of the shallow water model can be displayed simultaneously; for displaying the hidden param-

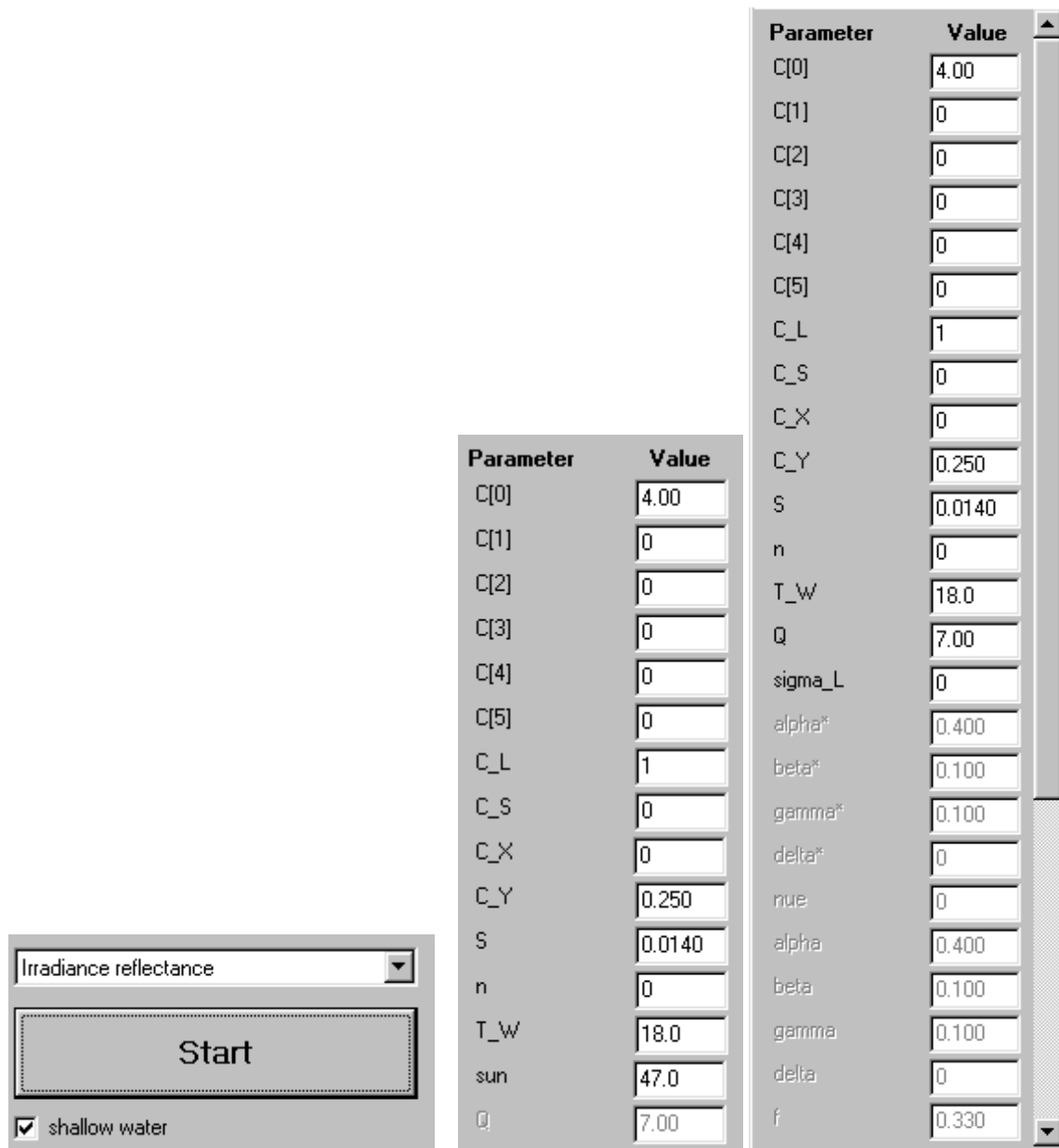


Fig. 6.2: Settings of the spectrum type "Irradiance reflectance" in the main window. Left: Drop-down list with "Irradiance reflectance" selected as spectrum type. Center: Parameter list of the deep-water model. Right: Parameter list of the shallow-water model.

ters, the scroll bar to the right of the "Value" fields has to be moved up- or downwards.

Irradiance reflectance spectra $R(\lambda)$ are calculated using the Gordon algorithm, see eq. (2.14a), or the Priour algorithm, see eq. (2.14b). Both algorithms parameterize $R(\lambda)$ as a function of

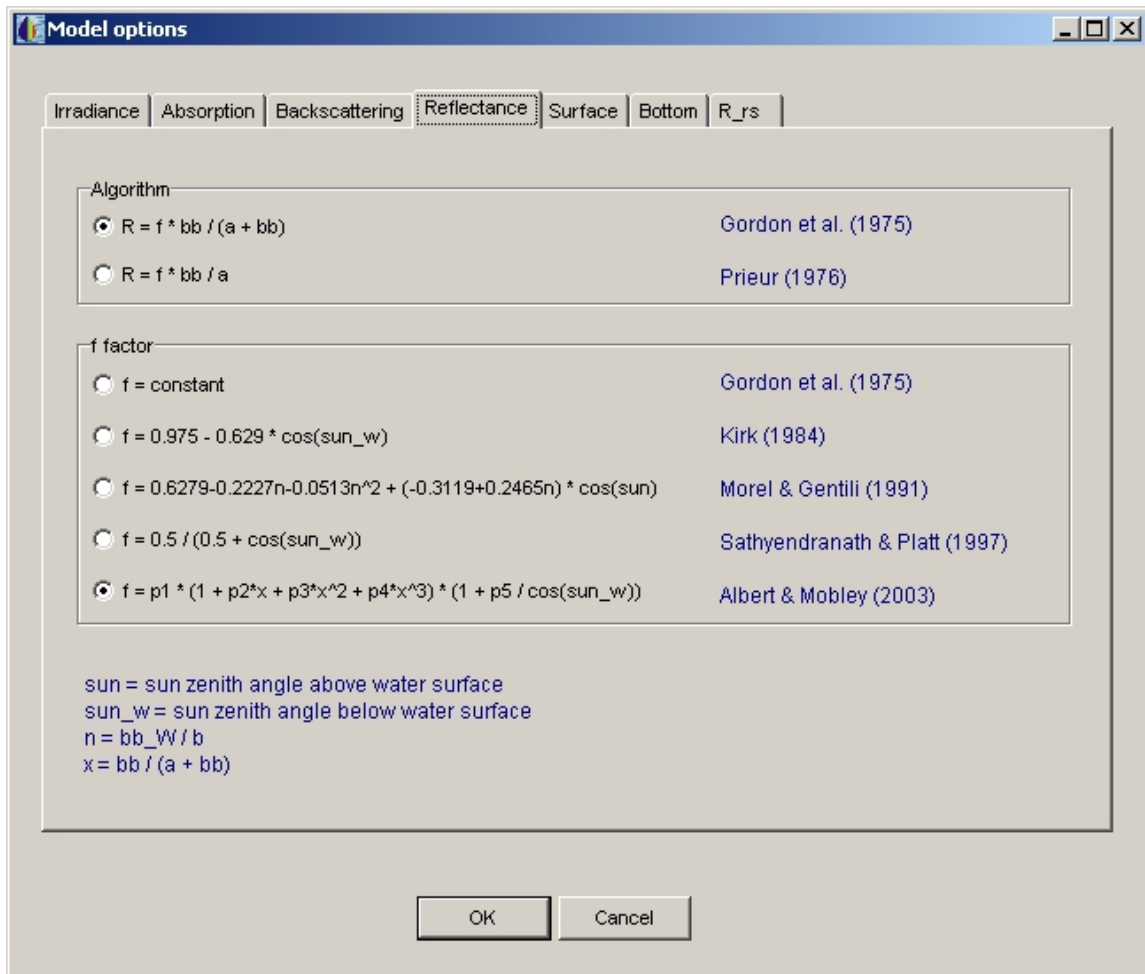


Fig. 6.3: The register card "Reflectance" of the pop-up window "Model options".

absorption and backscattering and thus require as parameters the concentrations of the different phytoplankton classes ($C_i = C[i]$, $i = 0, 1, \dots, 5$), of large ($C_L = C_L$) and small ($C_S = C_S$) suspended particles, of detritus ($D = C_D$) and of Gelbstoff ($Y = C_Y$), and the Angström exponent (n), water temperature ($T = T_W$), proportionality factor (f), and eventually Gelbstoff exponent (S). f can either be treated as a parameter, or it can be calculated as a function of absorption, backscattering and the sun zenith angle.

R algorithm and f calculation method are selected in the "Reflectance" register card of the "Model options" pop-up window, which is shown in Fig. 6.3. The pop-up window is accessed from the menu bar via "Options – Models".

The factor of proportionality, f , depends on the scattering properties of the water and on the illumination geometry. In WASI, f can either be treated as a parameter, or it can be calculated using one of the following algorithms:

$$f = 0.975 - 0.629 \cdot \cos \theta'_{\text{sun}} \quad (6.1)$$

$$f = 0.6279 - 0.2227 \cdot \eta_b - 0.0513 \cdot \eta_b^2 + (-0.3119 + 0.2465 \cdot \eta_b) \cdot \cos \theta_{\text{sun}} \quad (6.2)$$

$$f = \frac{0.5}{0.5 + \cos \theta_{\text{sun}}} \quad (6.3)$$

Fig. 6.4: The register card "Backscattering" of the pop-up window "Model options". The settings are not the default settings of WASI; they correspond to the model of Sathyendranath et al. (1989).

$$f = 0.1034 \cdot (1 + 3.3586 \cdot x - 6.5358 \cdot x^2 + 4.6638 \cdot x^3) \cdot \left(1 + \frac{2.4121}{\cos \theta'_{\text{sun}}}\right). \quad (6.4)$$

Equation (6.1) is taken from Kirk (1984), (6.2) from Morel and Gentili (1991), (6.3) from Sathyendranath and Platt (1997), and (6.4) from Albert and Mobley (2003). θ_{sun} is the sun zenith angle above the water surface, θ'_{sun} below the surface. The factor η_b in eq. (6.2) is the ratio $b_{b,w}/b_b$. The factor x in eq. (6.4) is $b_b/(a+b_b)$ for the Gordon algorithm and b_b/a for the Prieur algorithm.

The options for calculating absorption are described in section 6.3. Those for calculating backscattering are set in the register card "Backscattering" of the pop-up window "Model options", see Fig. 6.4.

Backscattering by large particles

In Fig. 6.4 the box "correlate with phytoplankton" determines whether C_L of eq. (2.15) is treated as an independent parameter (no hook), or if $C_L = C_0$ is set, with $C_0 = C[0]$ denoting phytoplankton concentration (hook). In case-1 water types suspended matter is highly corre-

lated with phytoplankton, hence it is suggested to mark the box for case-1 waters, but not for case-2 waters.

The boxes "scattering function from file" and "scattering function calculated from phytoplankton absorption" are exclusive, i.e. exact one of both is marked with a hook. They determine how the function $b_L(\lambda)$ of eq. (2.15) is selected: it is either read from file ("scattering function from file" is marked) or it is calculated from the specific absorption spectrum of phytoplankton (the other box is marked). Calculation is useful when suspended matter and phytoplankton are highly correlated, i.e. for case-1 waters, otherwise a spectrum independent from phytoplankton should be taken. If no information about the spectral dependency of backscattering by large particles is available, it is a good idea to use a constant function $b_L(\lambda) = 1$. This provides good results for instance in Lake Constance (Heege 2000). By default, $b_L(\lambda) = 1$ is read from the file `eins.prn`. For reading another file, the WASI.INI file must be changed accordingly.

The box "nonlinear with concentration" determines whether the specific backscattering coefficient $b_{b,L}^*$ of eq. (2.15) is treated as constant (no hook), or if it is calculated as $A \cdot C_L^B$ (hook). B is the value in the input field "Power of C_L", which is visible only in the nonlinear case. The value in the input field "Specific backscattering coefficient" corresponds to $b_{b,L}^*$ in the linear case, and to A in the nonlinear case. The "at ... nm" input field of Fig. 6.4 specifies the wavelength where the specific backscattering coefficient is valid. After a scattering function is read from file or calculated from phytoplankton absorption, it is normalized at that wavelength.

Backscattering by small particles

The value in the input field "Specific backscattering coefficient" of the "Small particles" section of Fig. 6.4 corresponds to $b_{b,S}^*$ of eq. (2.15). The "at ... nm" input field specifies the wavelength λ_S of eq. (2.15).

7.3 Absorption

The spectrum type "Absorption" is activated by selecting in the main window "Absorption" from the drop-down list above the "Start" button, see Fig. 6.5 left. After the spectrum type is set to "Absorption", the check box "include pure water" (Fig. 6.5 left) and the parameter list shown in Fig. 6.5 right are displayed.

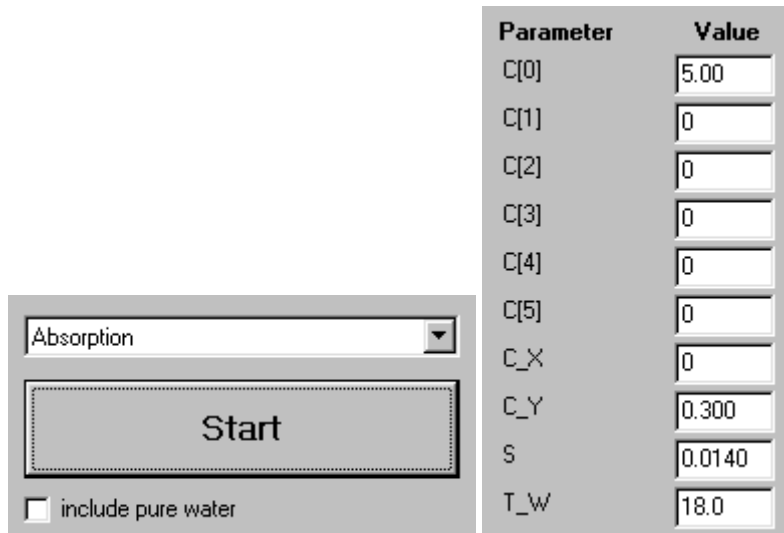


Fig. 6.5: Settings of the spectrum type "Absorption" in the main window. Left: Drop-down list with "Absorption" selected as spectrum type and "include pure water" check box. Right: Parameter list.

The spectrum type "Absorption" supports two options: include or exclude pure water absorption. If pure water absorption is included (check box is marked with a hook), the absorption spectrum of the water body is calculated using eq. (2.3). Otherwise (no hook) absorption of the water constituents alone is calculated using eq. (2.1).⁸

Parameters of the absorption model are the concentrations of the 6 phytoplankton classes ($C_i = C[i]$, $i = 0, 1, \dots, 5$), the concentration of detritus ($D = C_D$), Gelbstoff concentration ($Y = C_Y$), and eventually Gelbstoff exponent (S) and water temperature ($T = T_W$). T is model parameter if pure water absorption is included; it is not required for calculating absorption of the water constituents.

Whether S is model parameter or not depends on the choice of the specific Gelbstoff absorption spectrum $a_Y^*(\lambda)$. It can either be read from file, or it can be calculated during runtime using eq. (2.2). The selection is done in the "Absorption" register card of the pop-up window "Model options", which is shown in Fig. 6.6. The corresponding boxes "exponential function" and "specific absorption from file" are exclusive, i.e. exact one of both is marked with a hook. The input field "Normalize absorption spectrum at ... nm" specifies the wavelength λ_0 where $a_Y^*(\lambda)$ is normalised.

⁸ Most spectrum types included in WASI depend on the absorption of the water body. For all types which use absorption implicitly, the absorption spectrum includes pure water, i.e. absorption is calculated according to eq. (2.3).

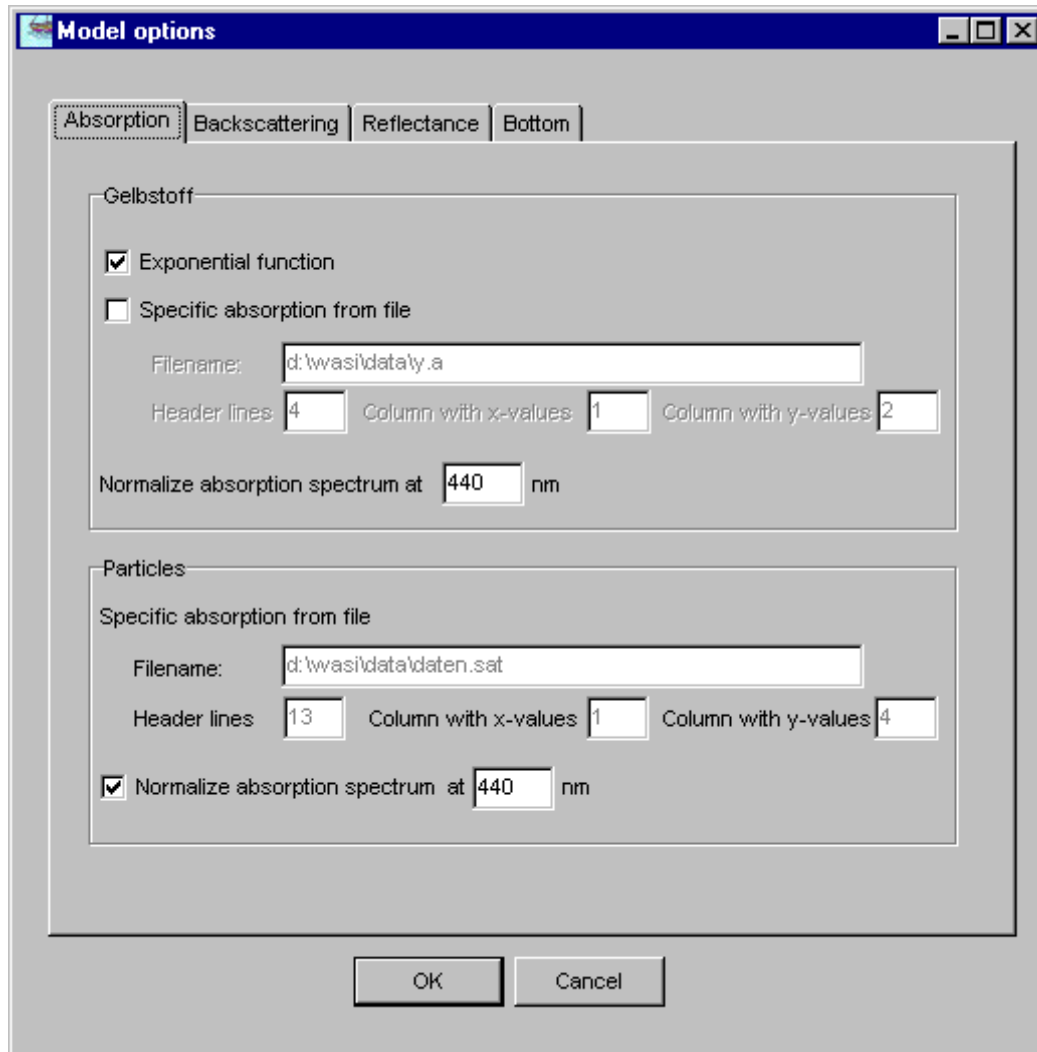


Fig. 6.6: The register card "Absorption" of the pop-up window "Model options".

The input spectrum $a_X^*(\lambda)$ may be normalized after it is read from file, or not. The selection is done in the check box "Normalize absorption spectrum" of the "Particles" section of Fig. 6.6. If normalization is selected, the corresponding wavelength λ_0 must be specified in the "at ... nm" input field. When $a_X^*(\lambda)$ is normalized, the concentration of large suspended particles is given in units of absorption at the reference wavelength λ_0 , otherwise it is given in units related to the units of the input file. By default $a_X^*(\lambda)$ is normalized.

The 10 input spectra $a_W(\lambda)$, $da_W/dT(\lambda)$, $a_Y^*(\lambda)$, $a_X^*(\lambda)$, $a_i^*(\lambda)$ with $i=0..5$, are read from files which are specified in the initialisation file WASI.INI. If these spectra should be replaced by other spectra, the WASI.INI file must be changed accordingly.

7.4 Bottom reflectance

The spectrum type "Bottom reflectance" is activated by selecting this type in the main window from the drop-down list above the "Start" button, see Fig. 6.7 left. After the spectrum type is set to "Bottom reflectance", the check box "radiance sensor" (Fig. 6.7 left) and the parameter list shown in Fig. 6.7 right are displayed.

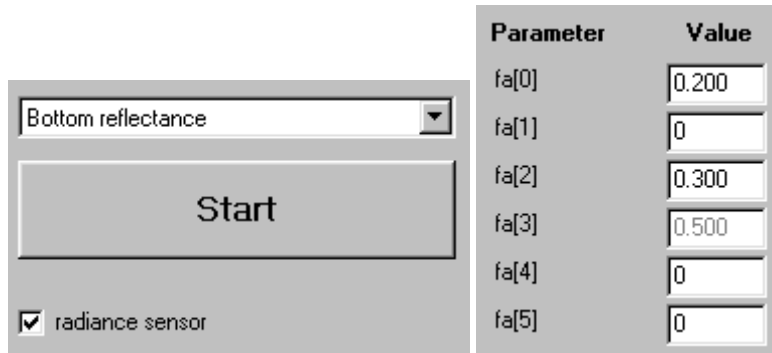


Fig. 6.7: Settings of the spectrum type "Bottom reflectance" in the main window. Left: Drop-down list with "Bottom reflectance" selected as spectrum type. Right: Parameter list of the forward mode.

If the check box "radiance sensor" is marked with a hook (like in Fig. 6.7 left), the bottom reflectance is calculated for a radiance sensor using eq. (2.22). Otherwise, it is calculated for an irradiance sensor using eq. (2.21).

Bottom albedo (irradiance reflectance) is calculated as a weighted sum of 6 albedo spectra. The weights $f_n = fa[n]$, $n = 0..5$, are the relative areas of the 6 bottom types within the sensor's field of view. Consequently, it is $\sum f_n = 1$, thus only 5 of the f_n are independent parameters, while one is calculated using $\sum f_n = 1$. Which of the weights is adjusted in this manner is defined in the register card "Bottom" of the pop-up window "Model options", see Fig. 6.8. It is accessed from the menu bar via "Options – Models" (see Fig. 8.1). The selection is done in the box "Adjust bottom albedo". If "none" is selected, the weights are not automatically adjusted. In the example of Fig. 6.8 the weight for surface no. 3 is automatically adjusted. This is visible in the main window by an inactive input box for $fa[3]$ in the parameter list, i.e. the calculated value is displayed in gray instead of black, see Fig. 6.7 right.

For a radiance sensor the bottom reflectance spectra are weighted additionally to f_n with reflection factors B_n , which are the ratio of radiance reflected in the direction of the sensor relative to the downwelling irradiance. For an isotropic (Lambertian) reflecting surface it is $B_n = 1/\pi = 0.318 \text{ sr}^{-1}$, thus 0.318 sr^{-1} are the default values for all B_n 's. The reflection factors can be set for each surface type individually in the register card "Bottom" of the pop-up window "Model options", see Fig. 6.8.

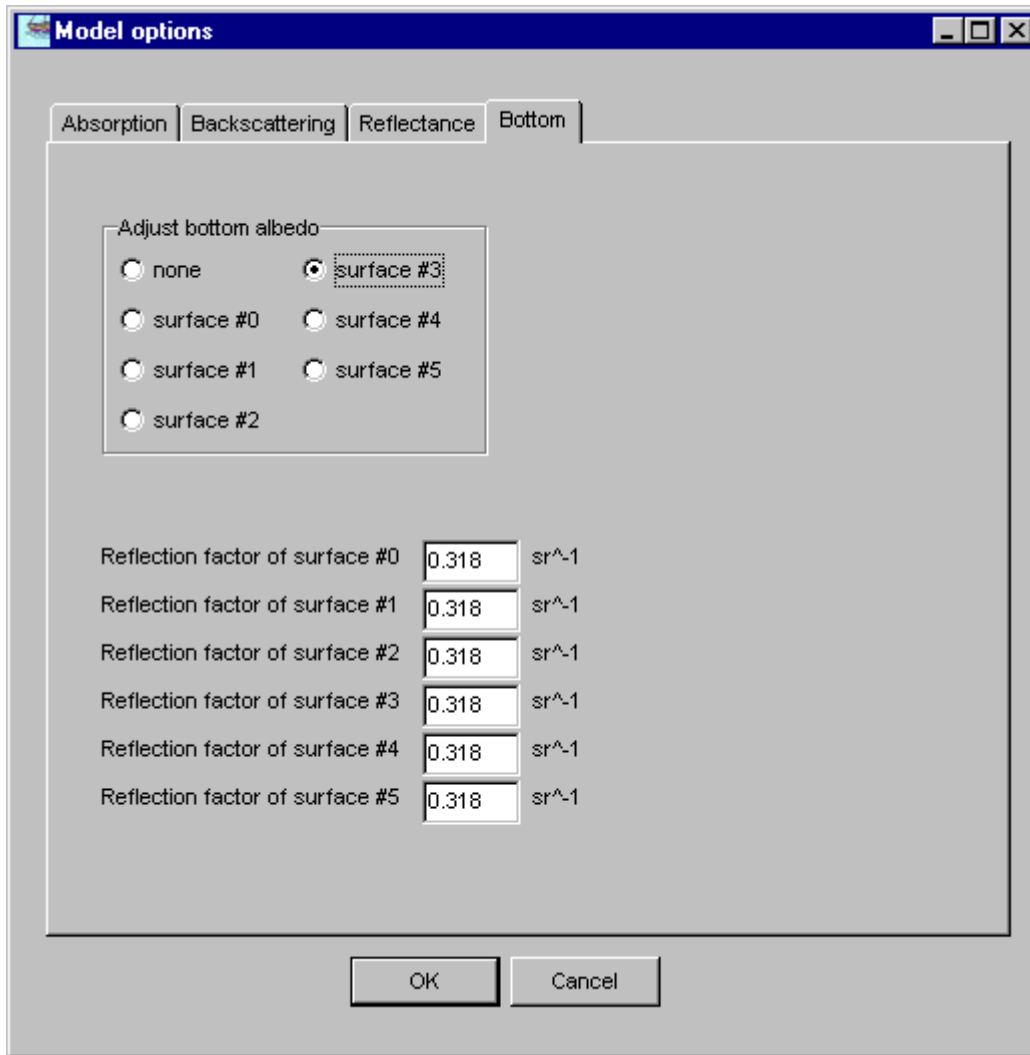


Fig. 6.8: The register card "Bottom" of the pop-up window "Model options".

8. Implicite spectra

All calculations of WASI make use of spectral data which are either imported from file or calculated during run-time. In particular some calculated spectra can be of interest, for instance to estimate spectral details of the radiation or bulk optical properties of the atmosphere or the water body, or for comparison with independent measurements. All implicite spectra can be visualised using the "Display" item of the menu bar as shown in Fig. 8. 1.

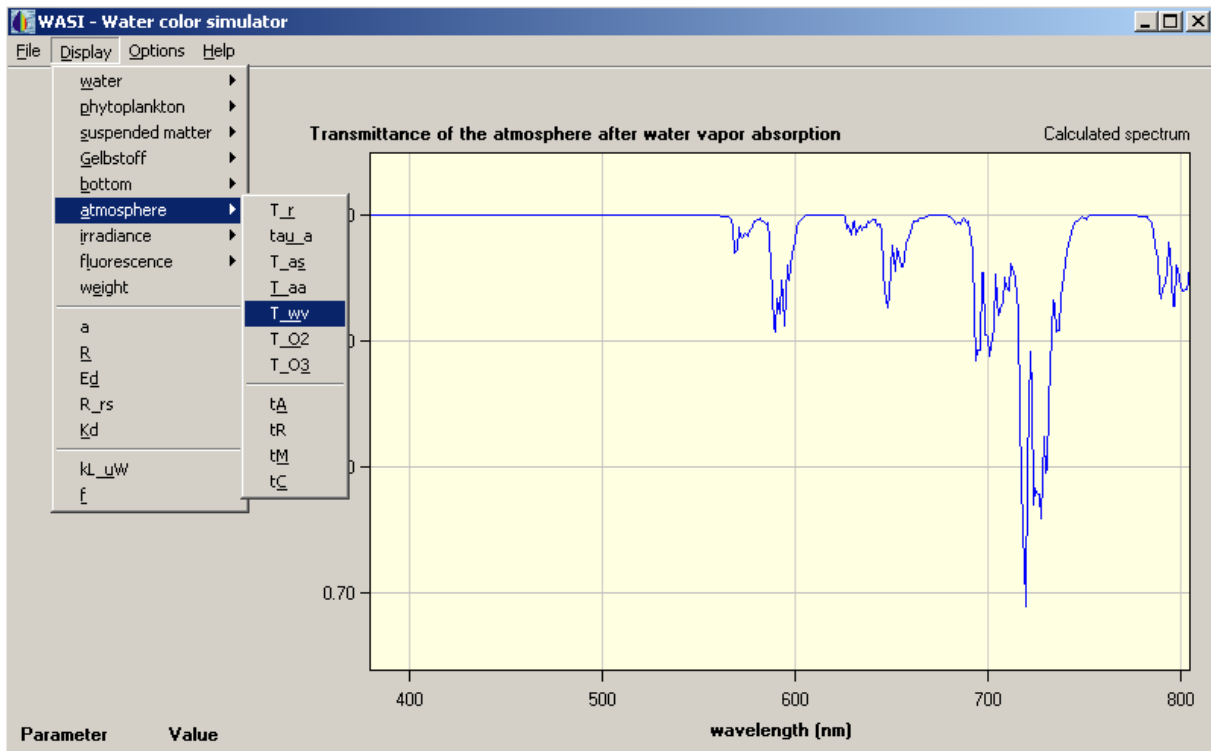


Fig. 8. 1: Visualising of an implicite spectrum using the "Display" menu.

The example of Fig. 8. 1 shows how to visualise an implicite spectrum of atmosphere modelling, here the atmospheric transmittance after water vapor absorption, $T_{wv}(\lambda)$, which is calculated using eq. (2.32). A visualised spectrum can be exported to file using a dialog window which pops up after selecting "File – Save" as shown in Fig. 8. 2.

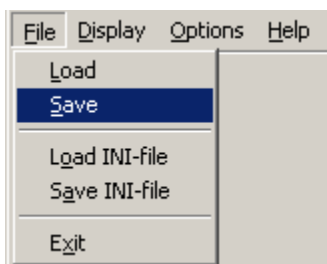


Fig. 8. 2: Saving an implicite spectrum.

The file format of exported spectra is ASCII. An example is shown in Fig. 8. 3.

Transmittance of the atmosphere after water vapor absorption

This file was generated by the program WASI
Version 4 - Latest update: 29 July 2010
Parameter values in files: WASI4.INI, CHANGES.TXT

```
350.00      1
351.00      1
352.00      1
353.00      1
354.00      1
355.00      1
356.00      1
357.00      1
358.00      1
359.00      1
360.00      1
```

Fig. 8. 3: First lines of an exported spectrum.

The interesting spectra are calculated during run-time. When these are exported, also the parameter values used for calculation should be documented. This can be done by updating the file WASI.INI as shown in Fig. 8. 4 and archiving a copy of this file.

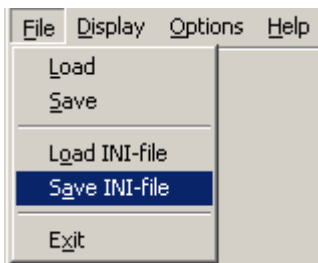


Fig. 8. 4: Documenting the parameter settings.

A summary of all implicate spectra of WASI is given in Appendix 5 (input spectra) and Appendix 6 (internal spectra).

9. Program options

The "Options" item of the menu bar on top of the WASI window is the entry point to all program settings. Fig. 8.1 shows the main menu bar of WASI and the structure of the "Options" item. The various program settings are grouped in 8 thematic areas; one of these ("Invers calculation") is further divided into 2 themes. When one of the themes is selected, a pop-up window shows up which allows to inspect and modify the settings.

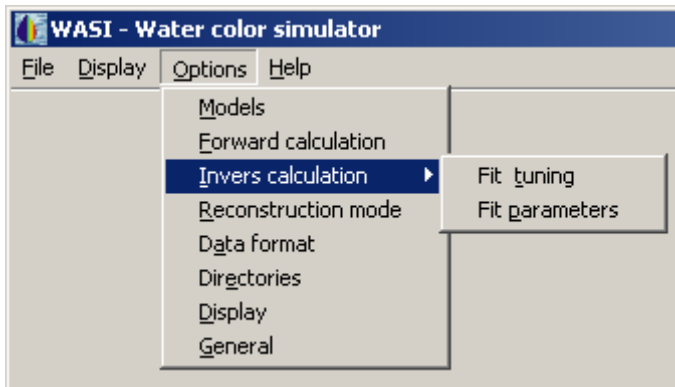


Fig. 9.1: The structure of the "Options" menu.

The pop-up menus of the first four thematic areas are described in the previous chapters: "Models" in chapter 6 (Figs. 6.3, 6.4, 6.6, 6.8), "Forward calculation" in chapter 3 (Fig. 3.2), "Invers calculation" in chapter 4 (Figs. 4.4 to 4.12), and "Reconstruction mode" in chapter 5 (Fig. 5.3). The pop-up menus of the four remaining themes are described in the following.

9.1 Data format

The pop-up window for specifying parameters related to data formats is shown in Fig. 8.2. The window consists of three sections.

Wavelengths of calculated spectra. The wavelength range and the data interval of the calculated spectra can be selected in two ways:

- If the spectra shall be calculated at equidistant wavelengths, the check box "x-values from file" has to be deselected. The first wavelength is specified in the "xmin" field, the last wavelength in the "xmax" field, and the intervals in the "dx" field.
- For non-equidistant intervals, e.g. if calculations should be performed for channels of a specific sensor, the wavelengths are read from an ASCII table.⁹ In this case the box "x-values from file" must be marked with a hook, and the corresponding file must be selected. The pre-selected file can be changed by pressing the button , which causes the opening of a file-selection window. The number of lines in the ASCII file that are skipped are specified in the "header lines" input field; the column with the wavelengths is specified in the "column with x-values" field.

If calculated spectra should be saved to file at reduced data interval, the "Interval for saving data" can be set to a value > 1 .

⁹ Spectral weighting using sensor-specific response functions is not supported.

Fig. 9.2: The pop-up window "Data format".

File format of measurements. This section specifies the data format of input spectra. Any ASCII table can be used as input. Basic settings which need to be specified are the number of header lines, column of x-values, and column of y-values. The columns can be separated either by TAB or by an arbitrary number of blanks. However, for large multi-column tables which have lines longer than 256 bytes, only TABs are supported as column separators.

If the sun zenith angle is provided in the input file, mark the box "sun zenith angle available" with a hook and specify line, column and units. If the day of year is provided in the input file, mark the box "day of year available" with a hook and specify line and column; otherwise, specify it in the "day of year" box.

Batch processing. The batch mode can be used to process automatically a series of files, i.e. to import one file after the other in WASI, analyze each file by inverse modeling, and store the resulting fit parameters to file. This mode is activated by marking the box "import series of spectra" with a hook. The user has to choose path and files after clicking the "..." button.

Alternately, if the path is already set, the file extension can be changed in the input box "Extension".

The batch mode supports files which contain several spectra in the format $(x, y_1, y_2, \dots, y_N)$. To read such tables, mark the box "multiple columns per file" with a hook and specify the maximum number of spectra per file, N , by editing the "max. columns" box. The first spectrum y_1 is specified via "Column with y-values" in the section "File format of measurements".

While the fit parameters are always saved automatically in the batch mode, the user can choose if he wants to save also each calculated spectrum. This selection is done by activating or deactivating the box "save calculated spectra". The directory in which the calculated spectra are stored, is chosen by clicking the corresponding "..." button.

9.2 Directories

The directories for saving calculated spectra and for reading import spectra are selected in the "Directories" pop-up window. It is accessed from the menu bar via "Options – Directories" (see Fig. 8.1) and shown in Fig. 8.3. The pre-selected directories can be changed by entering a new directory name or by pressing the button and selecting a directory from the displayed directory tree (not shown).

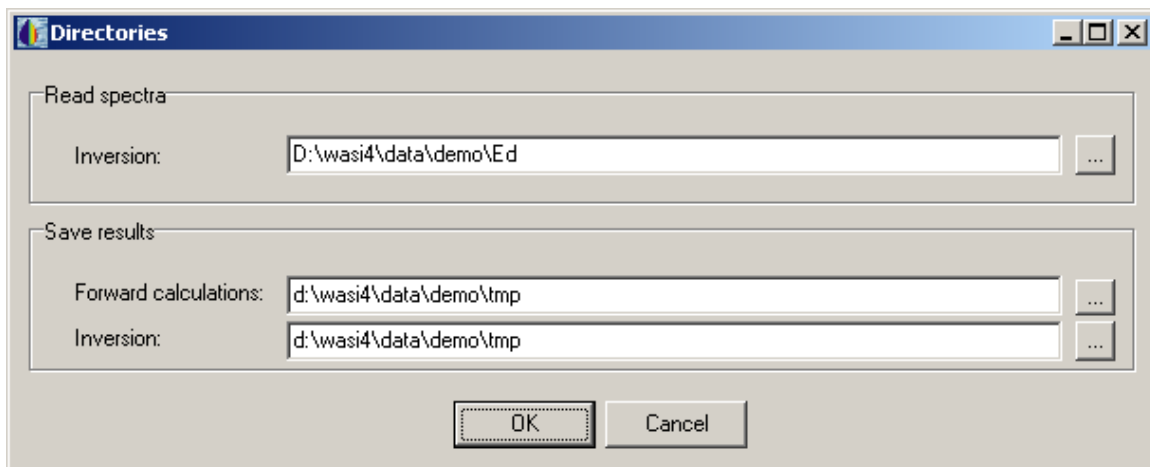


Fig. 9.3: The pop-up window "Directories".

9.3 Display options

The pop-up window for settings concerning visualisation is shown in Fig. 8.4. It appears when the thematic area "Display" is selected in the "Options" menu (see Fig. 8.1).

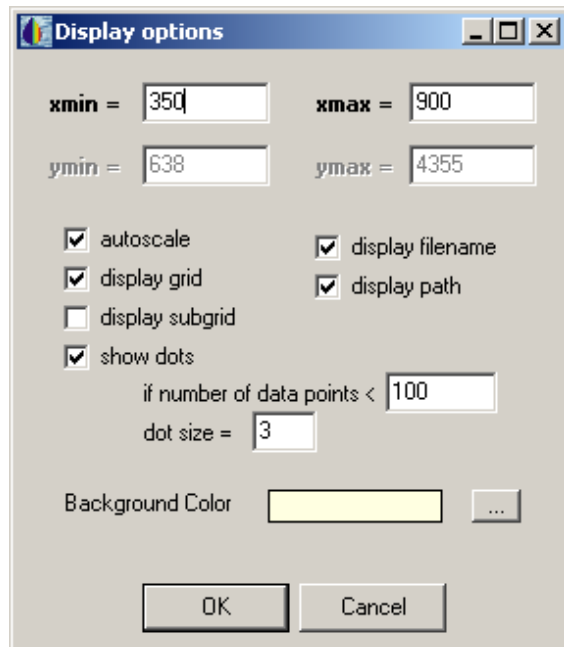


Fig. 9.4: The popup-window "Display options".

Range of x and y values. The range of the displayed x-values is defined by the values in the fields "xmin =" and "xmax =". The range of the displayed y-values is either defined by the values in the fields "ymin =" and "ymax =", or adjusted automatically to the actual spectrum if the check box "autoscale" is marked with a hook. In the latter case the input fields for ymin and ymax are deactivated. By default the autoscale option is activated.

Spectrum information. On top right of the plot window the file name of the actual spectrum can be displayed, either excluding or including the path. The selection is made using the check boxes "display filename" and "display path".

Layout. The spectra can be plotted either on a blank background, or on a coarse or fine grid. The selection is made using the check boxes "display grid" and "display subgrid". The background colour can be changed by pressing the button and selecting the desired colour in the upcoming popup-window (not shown).

9.4 General options

The pop-up window for some general settings is shown in Fig. 8.5. It appears when the thematic area "General" is selected in the "Options" menu (see Fig. 8.1).

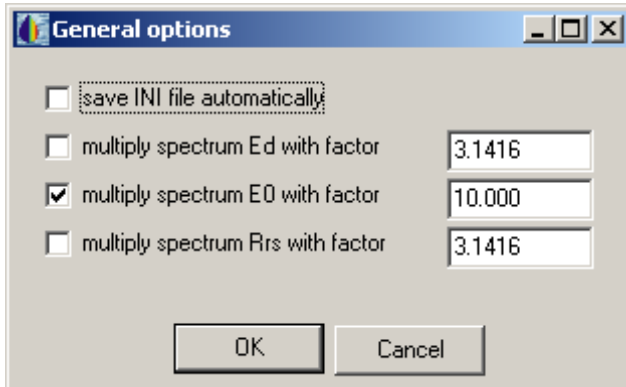


Fig. 9.5: The pop-up window "General options".

Four yes-no-decisions can be made:

- The check box "save INI file automatically" selects whether or not the file WASI.INI is updated automatically at program termination.
- The check box "multiply spectrum E_d with factor" allows to multiply automatically each downwelling irradiance spectrum $E_d(\lambda)$, which is read from file, with a factor whose value is set in the adjacent input field. This is useful if $E_d(\lambda)$ was measured as radiance upwelling from a horizontally oriented diffuse reflecting panel, $L_{up}(\lambda)$. In this case it is $E_d(\lambda) = \pi \cdot \rho \cdot L_{up}(\lambda)$, where ρ is the panel's reflectance. The conversion factor is set to $\pi = 3.1416$ by default, which corresponds to $\rho = 1$.
- The check box "multiply spectrum E_0 with factor" allows to multiply automatically the spectrum of the extraterrestrial solar irradiance, $E_0(\lambda)$, with a conversion factor. This is useful if the spectrum $E_0(\lambda)$ is given in units which are different from the units of the other irradiance spectra. For example, the spectrum $E_0(\lambda)$ provided with WASI is given in units of $\mu\text{W cm}^{-2} \text{sr}^{-1}$, while the common units in WASI are $\text{mW m}^{-2} \text{sr}^{-1}$. This leads to a conversion factor of 0.1.
- The check box "multiply spectrum R_{rs} with factor" allows to multiply automatically all remote sensing reflectance spectra $R_{rs}(\lambda)$ (those read from file as well as those forward calculated) with a factor whose value is set in the adjacent input field. This provides a fast way to convert $R_{rs}(\lambda)$ to irradiance reflectance $R(\lambda)$ using the model of Eq. (2.13a), $R_{rs}(\lambda) = R(\lambda)/Q$. The conversion factor is set to $Q = \pi = 3.1416$ by default, which represents the idealized case of isotropic reflection.

10. References

- E. Aas (1987): Two-stream irradiance model for deep waters. *Applied Optics* 26(11), 2095-2101.
- M. R. Abbott and R. M. Letelier (1999): Algorithm theoretical basis document chlorophyll fluorescence (MODIS product number 20). NASA.
- Y. H. Ahn, A. Bricaud, A. Morel (1992): Light backscattering efficiency and related properties of some phytoplankton. *Deep-Sea Res.* 39, 1835-1855.
- A. Albert, C. D. Mobley (2003): An analytical model for subsurface irradiance and remote sensing reflectance in deep and shallow case-2 waters. *Optics Express* 11, 2873-2890. <http://www.opticsexpress.org/abstract.cfm?URI=OPEX-11-22-2873>.
- A. Albert (2004): Inversion technique for optical remote sensing in shallow water. *Ph.D. thesis, University of Hamburg*. <http://www.sub.uni-hamburg.de/opus/volltexte/2005/2325/>
- A. Albert, P. Gege (2005): Inversion of irradiance and remote sensing reflectance in shallow water between 400 and 800 nm for calculations of water and bottom properties. *Applied Optics* 45(10), 2331-2343.
- D. Antoine, D. A. Siegel, T. Kostadinov, S. Maritorena, N. B. Nelson, B. Gentili, V. Vellucci, and N. Guillocheau (2011): Variability in optical particle backscattering in contrasting bio-optical oceanic regimes. *Limnol. Oceanogr.* 56: 955–973.
- M. Babin, A. Morel, and B. Gentili (1996): Remote sensing of sea surface Sun-induced chlorophyll fluorescence: consequences of natural variations in the optical characteristics of phytoplankton and the quantum yield of chlorophyll a fluorescence. *Int. J. Remote Sens.* 17, 2417–2448.
- M. Babin, A. Morel, V. Fournier-Sicre, F. Fell, and D. Stramski (2003): Light scattering properties of marine particles in coastal and open ocean waters as related to the particle mass concentration. *Limnol. Oceanogr.* 48: 843–859.
- R. E. Bird, C. Riordan (1986): Simple solar spectral model for direct and diffuse irradiance on horizontal and tilted planes at the Earth's surface for cloudless atmospheres. *Journal of Climate and Applied Meteorology* 25, 87–97.
- A. Bricaud, A. Morel, L. Prieur (1981): Absorption by dissolved organic matter of the sea (yellow substance) in the UV and visible domains. *Limnol. Oceanogr.* 26, 43-53 .
- H. Buiteveld, J. H. M. Hakvoort, M. Donze (1994): The optical properties of pure water. *SPIE Vol. 2258, Ocean Optics XII*, 174-183.
- M. S. Caceci, W. P. Cacheris (1984): Fitting Curves to Data. *Byte May 1984*: 340-362.
- K. L. Carder, G. R. Harvey, P. B. Ortner (1989): Marine humic and fulvic acids: their effects on remote sensing of ocean chlorophyll. *Limnol. Oceanogr.* 34: 68-81.

- M. Chami, E. B. Shybanov, T. Y. Churilova, G. A. Khomenko, M. E.-G. Lee, O. V. Martynov, G. A. Berseneva, and G. K. Korotaev (2005): Optical properties of the particles in the Crimea coastal waters (Black Sea). *J. Geophys. Res.* 110: C11020. doi:10.1029/2005JC003008.
- C. Cox, W. Munk (1954): Statistics of the sea surface derived from sun glitter. *J. Marine Res.*, 13, 198-227.
- C. Cox, W. Munk (1956): Slopes of the sea surface deduced from photographs of sun glitter. *Bulletin Scripps Inst. Oceanogr. Univ. Calif.*, 6, 401-488.
- J. Dera, D. Stramski (1993): Focusing of sunlight by sea surface waves: new results from the Black Sea. *Oceanologia* 34, 13-25.
- R. Doerffer and H. Schiller (2007): The MERIS Case 2 water algorithm. *Int. J. of Remote Sensing* 28, 517–535.
- P. Gege (1994): Gewässeranalyse mit passiver Fernerkundung: Ein Modell zur Interpretation optischer Spektralmessungen. *PhD thesis. DLR-Forschungsbericht 94-15*, 171 p.
- P. Gege (1995): Water analysis by remote sensing: A model for the interpretation of optical spectral measurements. *Technical Translation ESA-TT-1324*, 231 pp., July 1995.
- P. Gege (1998a): Correction of specular reflections at the water surface. *Ocean Optics XIV, November, 10-13, 1998, Kailua-Kona, Hawaii, USA. Conference Papers, Vol. 2.*
- P. Gege (1998b): Characterization of the phytoplankton in Lake Constance for classification by remote sensing. *Arch. Hydrobiol. Spec. Issues Advanc. Limnol.* 53, p. 179-193, Dezember 1998: *Lake Constance, Characterization of an ecosystem in transition.*
- P. Gege (2000): Gaussian model for yellow substance absorption spectra. *Proc. Ocean Optics XV conference, October 16-20, 2000, Monaco.*
- P. Gege (2002). Error propagation at inversion of irradiance reflectance spectra in case-2 waters. *Ocean Optics XVI Conference, November 18-22, 2002, Santa Fe, USA.*
- P. Gege (2004): The water color simulator WASI: an integrating software tool for analysis and simulation of optical in situ spectra. *Computers & Geosciences*, 30, 523-532.
- P. Gege (2005): The Water Colour Simulator WASI. User manual for version 3. *DLR Internal Report IB 564-01/05*, 83 pp.
- P. Gege, A. Albert (2006): A tool for inverse modeling of spectral measurements in deep and shallow waters. In: L.L. Richardson and E.F. LeDrew (Eds): *"Remote Sensing of Aquatic Coastal Ecosystem Processes: Science and Management Applications"*, *Kluwer book series: Remote Sensing and Digital Image Processing*, Springer, ISBN 1-4020-3967-0, pp. 81-109.
- P. Gege, N. Pinnel (2011): Sources of variance of downwelling irradiance in water. *Applied Optics* 50, 2192-2203.

- P. Gege (2012): Analytic model for the direct and diffuse components of downwelling spectral irradiance in water. *Applied Optics* 51, 1407-1419.
- P. Gege (2014): WASI-2D: A software tool for regionally optimized analysis of imaging spectrometer data from deep and shallow waters. *Computers & Geosciences* 62, 208-215. <http://dx.doi.org/10.1016/j.cageo.2013.07.022>.
- A. Gilerson, J. Zhou, S. Hlaing, I. Ioannou, J. Schalles, B. Gross, F. Moshary, S. Ahmed (2007). Fluorescence component in the reflectance spectra from coastal waters. Dependence on water composition. *Optics Express* 15, 15702-15721.
- A. A. Gitelson, G. Dall'Olmo, W. Moses, D. C. Rundquist, T. Barrow, T. R. Fisher, D. Gurlin, J. Holz (2008). A simple semi-analytical model for remote estimation of chlorophyll-a in turbid waters: Validation. *Remote Sensing of Environment* 112, 3582–3593.
- H. R. Gordon, O. B. Brown, M. M. Jacobs (1975): Computed Relationships between the Inherent and Apparent Optical Properties of a Flat Homogeneous Ocean. *Applied Optics* 14, 417-427.
- H. R. Gordon (1979): Diffuse reflectance of the ocean: the theory of its augmentation by chlorophyll a fluorescence. *Applied Optics* 21, 2489-2492.
- H. R. Gordon (1989): Can the Lambert-Beer law be applied to the diffuse attenuation coefficient of ocean water? *Limnol. Oceanogr.* 34(8), 1389-1409.
- W. W. Gregg, K. L. Carder (1990): A simple spectral solar irradiance model for cloudless maritime atmospheres. *Limnol. Oceanogr.* 35(8), 1657–1675.
- T. Heege (2000): Flugzeuggestützte Fernerkundung von Wasserinhaltsstoffen am Bodensee. *PhD thesis. DLR-Forschungsbericht 2000-40, 134 p.*
- Y. Huot, C. A. Brown, and J. J. Cullen (2005): New algorithms for MODIS sun-induced chlorophyll fluorescence and a comparison with present data products. *Limnol. Oceanogr. Methods* 3, 108–130.
- N. G. Jerlov (1976): *Marine Optics. Elsevier Scientific Publ. Company.*
- J. H. Jerome, R. P. Bukata, J. E. Bruton (1990): Determination of available subsurface light for photochemical and photobiological activity. *J. Great Lakes Res.* 16(3), 436-443.
- F. Kasten, A. T. Young (1989): Revised optical air mass tables and approximation formula. *Applied Optics* 28, 4735–4738.
- J. T. O. Kirk (1984): Dependence of relationship between inherent and apparent optical properties of water on solar altitude. *Limnol. Oceanogr.* 29, 350-356.
- J. T. O. Kirk (1991): Volumen scattering function, average cosines, and underwater lightfield. *Limnol. Oceanogr.* 36, 455-467
- Z. P. Lee, K. L. Carder, C. D. Mobley, R. G. Steward, J. S. Patch (1998): Hyperspectral remote sensing for shallow waters. I. A semianalytical model. *Appl. Optics* 37, 6329-6338.

- Z. P. Lee, A. Weidemann, J. Kindle, R. Arnone, K. L. Carder, and C. Davis (2007): Euphotic zone depth: Its derivation and implication to ocean-color remote sensing. *J. Geophysical Research* 112, C03009.
- S. Maritorena, A. Morel, and B. Gentili (2000): Determination of the fluorescence quantum yield by oceanic phytoplankton in their natural habitat. *Applied Optics* 39, 6725–6737.
- C. D. Mobley, B. Gentili, H. R. Gordon, Z. Jin, G. W. Kattawar, A. Morel, P. Reinersman, K. Stamnes, R. H. Stavn (1993): Comparison of numerical models for computing underwater light fields. *Appl. Optics* 32, 7484-7504.
- C. D. Mobley (1994): *Light and Water*. Academic Press, 592 pp.
- C. D. Mobley (1999): Estimation of the remote-sensing reflectance from above-surface measurements. *Appl. Optics* 38, 7442-7455.
- A. Morel (1974): Optical Properties of Pure Water and Pure Sea Water. In: Jerlov, N. G., Steemann Nielsen, E. (Eds.): *Optical Aspects of Oceanography*. Academic Press London, 1-24.
- A. Morel (1980): In water and remote measurements of ocean colour. *Boundary-Layer Meteorology* 18, 177-201.
- A. Morel (1988): Optical modeling of the upper ocean in relation to its biogenous content (case I waters). *J. Geophys. Res.* 93: 10,749–10,768.
- A. Morel, B. Gentili (1991): Diffuse reflectance of oceanic waters: its dependence on Sun angle as influenced by the molecular scattering contribution. *Appl. Optics* 30, 4427-4438.
- A. Morel, S. Maritorena (2001): Bio-optical properties of oceanic waters: A reappraisal. *J. Geophys. Res.* 106: 7163–7180.
- J. L. Mueller, R. W. Austin (1995): Volume 25 of Ocean Optics Protocols for SeaWiFS Validation, Revision 1. S. B. Hooker, E. R. Firestone, and J. G. Acker, eds., NASA Tech. Memo. 104566. NASA Goddard Space Flight Center, Greenbelt, Md.
- J. A. Nelder, R. Mead (1965): A simplex method for function minimization. *Computer J.* 7, 308-313.
- G. Nyquist (1979): Investigation of some optical properties of seawater with special reference to lignin sulfonates and humic substances. *PhD Thesis, Göteborgs Universitet*, 200 p.
- T. G. Owens (1991): Energy transformation and fluorescence in photosynthesis. In: *Particle Analysis in Oceanography*, S. Demers, ed. Springer-Verlag, Berlin, pp. 101–137.
- K. F. Palmer, D. Williams (1974): Optical properties of water in the near infrared. *J. Optical Soc. of America* 64, 1107-1110.
- N. Pinnel (2007): A method for mapping submerged macrophytes in lakes using hyperspectral remote sensing. *PhD thesis. Technical University Munich*, 165 p.

- R. W. Preisendorfer, C. D. Mobley (1985): Unpolarized irradiance reflectances and glitter patterns of random capillary waves on lakes and seas, by Monte Carlo simulation. *NOAA Tech. Memo. ERL PMEL-63, Pacific Mar. Environ. Lab., Seattle, WA, 141 pp.*
- R. W. Preisendorfer, C. D. Mobley (1986): Albedos and glitter patterns of a wind-roughened sea surface. *J. Phys. Ocean., 16, 1293-1316.*
- L. Prieur (1976): Transfers radiatifs dans les eaux de mer. *Thesis, Doctorat d'Etat, Univ. Pierre et Marie Curie, Paris, 243 pp.*
- L. Prieur, S. Sathyendranath (1981): An optical classification of coastal and oceanic waters based on the specific spectral absorption curves of phytoplankton pigments, dissolved organic matter, and other particulate materials. *Limnol. Oceanogr. 26, 671-689.*
- T. Pyhälähti, P. Gege (2001): Retrieval of water quality parameters using different channel configurations. *Proc. ISPRS symposium "Physical measurements & signatures in remote sensing", Jan. 8-12, 2001, Aussous, France.*
- T. I. Quickenden, J.A. Irvin (1980): The ultraviolet absorption spectrum of liquid water. *J. Chem. Phys. 72(8), 4416-4428.*
- S. Sathyendranath, T. Platt (1988): Oceanic Primary Production: Estimation by Remote Sensing at Local and Regional Scales. *Science, 241, 1613-1620.*
- S. Sathyendranath, L. Prieur, A. Morel (1989): A three-component model of ocean colour and its application to remote sensing of phytoplankton pigments in coastal waters. *Int. J. Remote Sensing 10, 1373-1394.*
- S. Sathyendranath, T. Platt (1997): Analytic model of ocean color. *Applied Optics 36, 2620-2629.*
- J. N. Schwarz, P. Kowalczyk, S. Kaczmarek, G. Cota, B. G. Mitchell, M. Kahru, F. Chavez, A. Cunningham, D. McKee, P. Gege, M. Kishino, D. Phinney, R. Raine (2002): Two models for absorption by coloured dissolved organic matter (CDOM). *Oceanologia 44(2), 209-241.*
- M. M. Tilzer, N. Stambler, C. Lovengreen (1995): The role of phytoplankton in determining the underwater light climate in Lake Constance. *Hydrobiologia 316, 161-171.*
- D. A. Toole, D. A. Siegel, D. W. Menzies, M. J. Neumann, R. C. Smith (2000): Remote-sensing reflectance determinations in the coastal ocean environment: impact of instrumental characteristics and environmental variability. *Applied Optics 39, 456-469.*
- J. R. V. Zanefeld, E. Boss, A. Barnard (2001): Influence of surface waves on measured and modeled irradiance profiles. *Applied Optics 40, 1442-1449.*

Appendix 1: Installation

WASI has no custom setup routine like most WINDOWS programs. However, installation is very easy.

Method 1:

The simplest method is to install WASI in the directory D:\WASI4. The steps are:

- Create the directory D:\WASI4
- Copy WASI.ZIP into D:\WASI4
- Unzip WASI4.ZIP

Method 2:

If you prefer to install WASI in another directory than D:\WASI4, then installation needs a little bit more effort. The steps are:

- Create the desired directory
- Copy WASI4.ZIP into that directory
- Unzip WASI4.ZIP
- Edit WASI4.INI: Replace with a text editor all occurrences of "D:\WASI4\" with your directory

To start WASI, execute the file WASI4.EXE.

Appendix 2: WASI4.INI

WASI4.INI is the initialization file of WASI. It is read automatically during program start. All program settings are stored in this file. To facilitate the usage of WASI, it is convenient to save the current program settings in that file. The default file WASI4.INI is shown in the following. A copy of that file is stored in the directory d:\wasi4\data\additional.

Initialization file for the program WASI - water colour simulator

 WASI4.INI version 14 January 2014
 WASI4.EXE Version 4 - Latest update: 17 January 2014

```
[ Spectrum of x-values ]
d:\wasi4\data\ch_meris.txt
6   = Header lines
1   = Column with x-values
2   = Column with FWHM-values

[ noise = Spectrum of measurement noise ]
d:\wasi4\data\noise.txt
10  = Header lines
1   = Column with x-values
3   = Column with y-values

[ offset = Spectrum of measurement offset ]
d:\wasi4\data\offset.txt
2   = Header lines
1   = Column with x-values
2   = Column with y-values

[ E0 = Extraterrestrial solar irradiance ]
d:\wasi4\data\E0_sun.txt
11  = Header lines
1   = Column with x-values
2   = Column with y-values

[ a02 = Absorption coefficient of oxygene ]
d:\wasi4\data\O2.a
4   = Header lines
1   = Column with x-values
2   = Column with y-values

[ a03 = Absorption coefficient of ozone ]
d:\wasi4\data\O3.a
4   = Header lines
1   = Column with x-values
2   = Column with y-values

[ aWV = Absorption coefficient of water vapor ]
d:\wasi4\data\WV.a
4   = Header lines
1   = Column with x-values
2   = Column with y-values

[ aW = Absorption coefficient of pure water ]
d:\wasi4\data\water.a
11  = Header lines
1   = Column with x-values
2   = Column with y-values

[ dadT = Temperature gradient of pure water absorption ]
d:\wasi4\data\daWdT.txt
10  = Header lines
1   = Column with x-values
2   = Column with y-values

[ aP[0] = Specific absorption of phytoplankton class no. 0 ]
d:\wasi4\data\phyto.a
12  = Header lines
1   = Column with x-values
2   = Column with y-values

[ aP[1] = Specific absorption of phytoplankton class no. 1 ]
d:\wasi4\data\cry-lo.a
10  = Header lines
1   = Column with x-values
2   = Column with y-values

[ aP[2] = Specific absorption of phytoplankton class no. 2 ]
d:\wasi4\data\cry-hi.a
11  = Header lines
1   = Column with x-values
```

```

2      = Column with y-values

[ aP[3] = Specific absorpion of phytoplankton class no. 3 ]
d:\wasi4\data\dia.a
10     = Header lines
1      = Column with x-values
2      = Column with y-values

[ aP[4] = Specific absorpion of phytoplankton class no. 4 ]
d:\wasi4\data\dinoflagellates.a
11     = Header lines
1      = Column with x-values
2      = Column with y-values

[ aP[5] = Specific absorpion of phytoplankton class no. 5 ]
d:\wasi4\data\green_algae.a
11     = Header lines
1      = Column with x-values
2      = Column with y-values

[ aD = Normalized absorpion coefficient of detritus ]
d:\wasi4\data\detritus.a
258    = Header lines
1      = Column with x-values
2      = Column with y-values

[ aY = Normalized absorpion coefficient of Gelbstoff ]
d:\wasi4\data\Y.a
262    = Header lines
1      = Column with x-values
2      = Column with y-values

[ bX = (Normalized) scattering coeff. of suspended particles Type I ]
d:\wasi4\data\X.B
2      = Header lines
1      = Column with x-values
2      = Column with y-values

[ albedo[0] = Albedo of bottom type #0 = const ]
d:\wasi4\data\const.R
9      = Header lines
1      = Column with x-values
2      = Column with y-values

[ albedo[1] = Albedo of bottom type #1 = sand ]
d:\wasi4\data\sand.r
21     = Header lines
1      = Column with x-values
2      = Column with y-values

[ albedo[2] = Albedo of bottom type #2 = silt ]
d:\wasi4\data\silt.r
9      = Header lines
1      = Column with x-values
2      = Column with y-values

[ albedo[3] = Albedo of bottom type #3 = green makrophyte "Chara contraria" ]
d:\wasi4\data\chara.r
26     = Header lines
1      = Column with x-values
2      = Column with y-values

[ albedo[4] = Albedo of bottom type #4 = green makrophyte "Potamogeton perfoliatus" ]
d:\wasi4\data\perfol.r
9      = Header lines
1      = Column with x-values
2      = Column with y-values

[ albedo[5] = Albedo of bottom type #5 = green makrophyte "Potamogeton pectinatus" ]
d:\wasi4\data\pectin.r
9      = Header lines
1      = Column with x-values
2      = Column with y-values

[ Measurement ]
D:\WASI4\DATA\demo\R_rs\STA11_09.Rrs
17     = Header lines
1      = Column with x-values
5      = Column with y-values
10     = Line with sun zenith angle
5      = Column with sun zenith angle
7      = Line with day of year
4      = Column with day of year

[ Measurement: Irradiance reflectance, R ]
D:\WASI4\DATA\demo\R\FWD.R
8      = header lines
1      = column with x-values
2      = column with y-values

```

```

[ Measurement: Downwelling irradiance, Ed ]
D:\WASI4\DATA\demo\Ed\BO9_109.Ed
17   = header lines
1    = column with x-values
2    = column with y-values

[ Measurement: Sky radiance reflected at surface, Ls ]
d:\wasi4\data\demo\L_sky\Ls.fwd
8    = header lines
1    = column with x-values
2    = column with y-values

[ Measurement: Attenuation for downwelling irradiance, Kd ]
d:\wasi4\data\demo\Kd\K.prn
5    = Header lines
1    = Column with x-values
3    = Column with y-values

[ Weight function for inversion ]
D:\WASI4\data\eins.txt
2    Header lines
1    = Column with x-values
2    = Column with y-values

[ HSI_img = Hyperspectral image ]
D:\WASI4\DATA\demo\2D\Stasee_05_rad_atm_geo_100a

[ file_LUT = Look-up table ]
d:\wasi4\data\LUT\rainbow3.lut

[ Spectra inverted in batch mode ]
D:\WASI4\DATA\demo\R_rs\*.Rrs

[ Directories: save FWD, save INV ]
d:\wasi4\data\demo\tmp
d:\wasi4\data\demo\tmp

[ General settings and parameters ]
300  = MinX           = lowest x-value allowed for data import and calculation
1000 = MaxX           = highest x-value allowed for data import and calculation
0.10 = MinDX         = lowest dx-value allowed for calculation
-100 = MinY           = lowest y-value allowed for display
1.0E+5 = MaxY         = highest y-value allowed for display
400  = xu            = lowest x-coordinate displayed
800  = xo            = highest x-coordinate displayed
-9.4E-5 = yu         = lowest y-coordinate displayed
0.0072 = yo          = highest y-coordinate displayed
350  = xub           = lowest x-coordinate calculated
1000 = xob           = highest x-coordinate calculated
1    = dxb           = wavelength interval for calculation
0    = dsmpl         = resampling distance (channels); 0 = no resampling
1    = dxs           = interval for saving data (channels)
10.0 = FWHM0         = spectral resolution (nm)
1    = FWHM0_min     = lowest allowed spectral resolution (nm)
50.0 = FWHM0_max     = highest allowed spectral resolution (nm)
3    = dotsize       = size of plotted dots
100  = dotMaxN       = max. number of data points to plot dots
600  = PopupDirW     = width of popup window 'directories'
3.1416 = Ed_factor   = multiplier of spectrum E_down
1    = E0_factor     = multiplier of spectrum E0
3.1416 = Rrs_factor  = multiplier of spectrum R_rs
2    = spec_type     = type of spectrum: 0=E_d, 1=L_up, 2=R_rs, 3=R, 4=R_surf, 5=a, 6=K_d, 7=R_bottom,
8=Ed_Gege, 9=Test
1    = Model_Ed      = Ed model: 0 = simple, 1 = separation between direct and diffuse component
0    = Model_R       = R model: 0=f*bb/(a+bb), 1=f*bb/a
0    = Model_R_rsA   = R_rs above surface is a function of 0=R_rs(0-), 1=R, 2=both
0    = Model_R_rsB   = R_rs model below surface: 0=f_rs*bb/(a+bb), 1=f_rs*bb/a, 2=R/Q
4    = Model_f       = f model: 0=const, 1=Kirk, 2=Morel+Gentili, 3=Sath.+Platt, 4=Albert+Mobley
0    = Model_f_rs    = f_rs model: 0=Albert, 1=f/Q
0    = Model_Kdd     = Kdd model: 0=Gege, 1=Grötsch
-1   = bottom_fill   = bottom surface type adjusted to yield sum of weights = 1
$00E1FFFF = clPlotBk = color of plot background
$002E5A5A = clMask   = color of image mask

[ Flags: 0 = FALSE, 1 = TRUE ]
0    = flag_SubGrid  = draw subgrid
1    = flag_Grid     = draw grid
1    = flag_Dots     = draw dots
1    = flag_Autoscale = autoscale plot
1    = flag_ShowFile = display filename
1    = flag_ShowPath = display path
0    = flag_INI      = save INI file automatically
1    = flag_sv_table = save forward-spectra as table
0    = flag_save_t   = save calculation time
0    = flag_mult_Ed  = multiply spectrum Ed with factor
0    = flag_mult_E0  = multiply spectrum E0 with factor
0    = flag_mult_Rrs = multiply spectrum R_rs with factor
0    = flag_x_file   = read x-values from file
0    = flag_fwhm     = use sensor resolution
1    = flag_read_day = read day of year from file

```

```

1   = flag_read_sun   = read sun zenith angle from file
1   = flag_sun_unit   = sun zenith angle in deg
0   = Par1_log        = Logarithmic steps of Parameter 1
0   = Par2_log        = Logarithmic steps of Parameter 2
0   = Par3_log        = Logarithmic steps of Parameter 3
1   = flag_batch     = batch mode (including forward mode)
1   = flag_b_SaveFwd  = save all spectra of forward mode
0   = flag_b_SaveInv  = save all spectra of invers mode
1   = flag_b_LoadAll  = load spectra from files
1   = flag_b_Reset    = reset start values
0   = flag_b_Invert   = invert spectra
0   = flag_avg_err    = reconstruction mode: save average errors?
0   = flag_multi     = multiple columns per file
0   = flag_Res_log    = weight residuals logarithmically
1   = flag_Y_exp      = exponential Gelbstoff absorption
1   = flag_surf_inv   = wavelength dependent surface reflections (inversion)
1   = flag_surf_fw    = wavelength dependent surface reflections (forward mode)
0   = flag_fluo       = include fluorescence of chl-a
0   = flag_use_Ed     = make use of Ed measurement
0   = flag_use_Ls     = make use of Ls measurement
0   = flag_use_R      = make use of R measurement
0   = flag_radiom     = reduce radiometric resolution
0   = flag_offset     = add measurement offset
0   = flag_offset_c   = offset is constant
0   = flag_noise      = add measurement noise
0   = flag_noise_c    = noise is constant
0   = flag_Tab        = only TAB separates columns
1   = flag_aW         = include water absorption in bulk absorption
0   = flag_above      = above water
0   = flag_shallow    = shallow water
1   = flag_L          = bottom signal from radiance sensor
1   = flag_anX_R      = analytic determination X start value for R spectra in deep waters
1   = flag_anX_Rsh    = analytic determination X start value for R spectra in shallow waters
1   = flag_anCY_R     = analytic determination C, Y start values for R spectra
1   = flag_anzB       = analytic determination of zB start value in shallow waters
1   = flag_Fresnel_view = calculate Fresnel reflectance from viewing angle
1   = flag_bX_file    = scattering coefficient of particles Type I from file
1   = flag_bX_linear   = scattering coefficient of particles Type I linear with C_X
0   = flag_CXisC0     = set C_X = C[0]
0   = flag_norm_D     = normalize detritus absorption spectrum from file at Lambda_0
1   = flag_norm_Y     = normalize Gelbstoff spectrum from file at Lambda_0

[ Settings for batch mode ]
0   = iter_type       = parameter that is iterated
2.0 = rangeMin        = first value of successive calculation
4.0 = rangeMax        = last value of successive calculation
1   = rangeDelta      = interval of successive calculation
0   = Par1_Type       = Parameter 1
0   = Par2_Type       = Parameter 2
0   = Par3_Type       = Parameter 3
0   = Par1_Min        = Minimum of Parameter 1
0   = Par2_Min        = Minimum of Parameter 2
1   = Par3_Min        = Minimum of Parameter 3
1   = Par1_Max        = Maximum of Parameter 1
0.400 = Par2_Max      = Maximum of Parameter 2
5.00 = Par3_Max      = Maximum of Parameter 3
5     = Par1_N         = Steps of Parameter 1
5     = Par2_N         = Steps of Parameter 2
5     = Par3_N         = Steps of Parameter 3
80    = ycol_max      = Max. number of y-columns

[ Settings for inverse mode ]
[ from to step MaxIter ]
400 800 2 800 = fit settings of pre-fit 1
600 800 5 0   = fit settings of pre-fit 2 (IR region)
380 450 5 0   = fit settings of pre-fit 3 (UV region)
400 800 5 1000 = fit settings of final fit
400 800 5 0   = fit of a (shallow water)
700 800 5 0   = fit of R and Rrs in IR region (shallow water)
400 500 5 0   = fit of R and Rrs in UV region (shallow water)
400 800 1 2000 = fit of R and Rrs (shallow water)
870 900       = LambdaLf = wavelengths for C_X and f initialisation
5 0           = dLambdaLf = wavelength intervals of LambdaLf
760          = LambdaLsh = wavelengths for C_X initialisation (shallow water)
2           = dLambdaLsh = wavelength interval of LambdaLsh (shallow water)
413 440 440   = LambdaCY = wavelengths for C[0] and C_Y initialisation
5 5 870       = dLambdaCY = wavelength intervals of LambdaCY
625         = LambdazB = wavelength for zB initialisation (shallow water)
25          = dLambdazB = wavelength interval of LambdazB (shallow water)
0.10        = zB_inimin = zB minimum during initial value determination (shallow water)
0.10        = CL_inimin = C_X minimum during initial value determination (shallow water)
0.10        = CO_inimin = C[0] minimum during initial value determination (shallow water)
0.010       = CY_inimin = C_Y minimum during initial value determination (shallow water)
5.0         = a_ini     = start value of absorption for nested intervals (shallow water)
1.0         = da_ini    = initial absorption interval for a_ini (shallow water)
0.010       = delta_min = threshold of spectrum change for nested intervals (shallow water)
0.50        = SFA_min   = minimum sum of fA[i] (shallow water)
2.0         = SFA_max   = maximum sum of fA[i] (shallow water)
1.0E-4      = res_max   = maximum allowed residuum
0           = res_mode  = type of residuum (0=|m-f|^2 = least squares, 1=|m-f|, 2=|1-f/m|)

```

```

[ Model constants ]
189 = day = Day of year
20.0 = T_W0 = Temperature of water absorption spectrum (°C)
1.33000 = nW = Refractive index of water
550 = Lambda_a = Reference wavelength for aerosol optical thickness (nm)
440 = Lambda_0 = Reference wavelength for Gelbstoff absorption (nm)
550 = Lambda_L = Reference wavelength for scattering of particles Type I (nm)
500 = Lambda_S = Reference wavelength for scattering of particles Type II (nm)
685.0 = Lambda_f0 = Center wavelength of chl-a fluorescence (nm)
10.62 = Sigma_f0 = Standard deviation of chl-a fluorescence (nm)
400 = PAR_min = PAR range: lower boundary (nm)
700 = PAR_max = PAR range: upper boundary (nm)
400 = Lmin = Spectrum average: lower boundary (nm)
700 = Lmax = Spectrum average: upper boundary (nm)
0.00111 = bbW500 = Backscattering coefficient of pure water (1/m)
0.00060 = bbX_A = Factor A in backscattering to concentration relationship (m^2/g)
-0.3700 = bbX_B = Factor B in backscattering to concentration relationship
0.00860 = bbX = Specific backscattering coeff. of particles Type I (m^2/g)
0.00420 = bbMie = Specific backscattering coeff. of particles Type II (m^2/g)
0.45000 = b_X = Specific scattering coeff. of particles Type I (m^2/g)
0.30000 = b_Mie = Specific scattering coeff. of particles Type II (m^2/g)
0.06087 = rho0 = rho_ds polynomial: 0th order value
0.03751 = rho1 = rho_ds polynomial: 1st order value
0.11430 = rho2 = rho_ds polynomial: 2nd order value
0.54000 = rho_Eu = Reflection factor for upwelling irradiance
0.06600 = rho_Ed = Reflection factor for downwelling irradiance
0.02000 = rho_Lu = Reflection factor for upwelling radiance
0.00500 = dynamics = Radiometric resolution
0.03000 = offset_c = Measurement offset (constant)
0.00020 = noise_std = Noise level (standard deviation)
1.00000 = ldd = Path length of direct irradiance: 0th order value
1.01700 = ldda = Path length of direct irradiance: 1st order value
1.95000 = lddb = Path length of direct irradiance: 2nd order value
1.11600 = lds0 = Path length of diffuse irradiance: 0th order value
0.55040 = lds1 = Path length of diffuse irradiance: 1st order value
0.00000 = ldsb = Path length of diffuse irradiance: 2nd order value
1.05460 = ld = Path length factor of total irradiance, Ed
0.31800 = BRDF[0] = BRDF of bottom type #0
0.31800 = BRDF[1] = BRDF of bottom type #1
0.31800 = BRDF[2] = BRDF of bottom type #2
0.31800 = BRDF[3] = BRDF of bottom type #3
0.31800 = BRDF[4] = BRDF of bottom type #4
0.31800 = BRDF[5] = BRDF of bottom type #5

[ Parameters of 2D module ]
1 = flag_2D = 2D version of WASI (1=TRUE)
1 = flag_JoinBands = Identical scaling for 3 preview bands
1 = flag_3Bands = Preview 3 bands / 1 band
1 = flag_LUT = Use lookup table
1 = flag_ENVI = Read ENVI header file
100 = Width_in = Input image width
100 = Height_in = Input image height
160 = Channels_in = Input image channels
7 = Channels_out = Output image channels
0 = HSI_header = Input image header bytes
55 = band_R = Preview band red
41 = band_G = Preview band green
12 = band_B = Preview band blue
0 = interleave_in = Input image interleave (0=BIL, 1=BSQ)
1 = interleave_out = Output image interleave (0=BIL, 1=BSQ)
12 = Datentyp = Input image data type
1000 = x_scale = Scale factor of x-axis (1=nm, 1000=um)
31416.0 = y_scale = Scale factor of y-axis
103 = band_mask = Preview band of mask
0.0000 = thresh_below = Mask threshold min
0.0040 = thresh_above = Mask threshold max
10 = Plot2D_delta = Interval to plot spectrum
0.25 = contrast = Preview image contrast
26 = Par0_Type = Preview parameter during inversion
5.00 = Par0_Min = Preview parameter min
0 = Par0_Max = Preview parameter max
15 = N_avg = Averaged pixels for parameter initialization

[ Model parameters ]
[ forward default start min max fit sv
1 1 3.00 0 100 1 0 C[0] = Concentration of phytoplankton class #0
0 0 0 0 60.0 0 0 C[1] = Concentration of phytoplankton class #1
0 0 0 0 60.0 0 0 C[2] = Concentration of phytoplankton class #2
0 0 0 0 60.0 0 0 C[3] = Concentration of phytoplankton class #3
0 0 0 0 60.0 0 0 C[4] = Concentration of phytoplankton class #4
0 0 0 0 60.0 0 0 C[5] = Concentration of phytoplankton class #5
1 0.500 2.00 0.100 10.0 1 0 C_X = Concentration of suspended particles Type I
0 0 0 0 125 0 0 C_Mie = Concentration of suspended particles Type
II
0 0 0 0 100 0 0 C_D = Concentration of detritus
0.300 0.500 1 0 50.0 1 1 C_Y = Gelbstoff absorption
0.0140 0.0140 0.0140 0.00400 0.0250 0 0 S = Gelbstoff exponent
-1.00 -1.00 -1.00 -2.00 2.00 0 0 n = Angström exponent of particle scattering
20.0 18.0 20.0 0 35.0 0 0 T_W = Water temperature (°C)

```

5.00	5.00	5.00	0.500	10.0	0 0	Q	= Anisotropy factor of Lu (1/sr)
0.0242	1.05	0.0222	0	5.00	0 0	rho_dd	= reflection factor of Edd
0.0201	0.0200	0.0201	0	0.500	0 0	rho_L	= Reflection factor of downwelling radiance
0.0660	0.0660	0.0671	0	50.0	0 0	rho_ds	= Reflectance factor of diffuse downwelling
irradiance							
0.2606	0.2606	0.2610	0	20.00	0 0	beta	= Turbidity coefficient
1.317	1.317	1.320	-3.000	3.000	0 0	alpha	= Angström exponent of aerosols
1	1	1	0	20.0	0 0	f_dd	= Fraction of direct downwelling irradiance
1	1	1	0	20.0	0 0	f_ds	= Fraction of diffuse downwelling irradiance
0.300	0.300	0.300	0	5.00	0 0	H_oz	= Ozone scale height (cm)
2.50	1.50	2.50	0	20.0	0 0	WV	= Precipitable water (cm)
0.330	0.330	0.400	0.100	0.900	0 0	f	= f-factor of R
1	0	0.500	0	100	0 0	z	= Sensor depth (m)
4.00	100	1	0	1000	1 1	zB	= Bottom depth (m)
40.0	30.0	40.0	0	89.9	0 0	sun	= Sun zenith angle (°)
0	0	0	0	89.9	0 0	view	= Viewing angle (°)
0	0	20.0	0	180	0 0	dphi	= azimuth difference sun - observer (°)
0	0	0	0	10.0	0 0	fA[0]	= fraction of bottom type #0
0	0	0	0	10.0	0 0	fA[1]	= fraction of bottom type #1
1	0	1	0	10.0	0 0	fA[2]	= fraction of bottom type #2
0	0	0	0	10.0	0 0	fA[3]	= fraction of bottom type #3
0	0	0	0	10.0	0 0	fA[4]	= fraction of bottom type #4
0	0	0	0	10.0	0 0	fA[5]	= fraction of bottom type #5
0.0100	0.0100	0.0100	0	1	0 0	fluo	= chl-a fluorescence quantum yield
0.0500	0.0500	0.0500	0	10.0	0 1	g_dd	= Fraction of sky radiance due to direct
solar radiation							
0	0.500	0	0	10.0	0 0	g_dsr	= Fraction of sky radiance due to Rayleigh
scattering							
0	0.100	0	0	10.0	0 0	g_dsa	= Fraction of sky radiance due to aerosol
scattering							
0	0	0	-5.00	50.0	0 0	dummy	= NOT USED

Appendix 3: Parameters

The following table summarizes the 39 model parameters of all 8 spectrum types. The No.'s are used program-internally as parameter indices. $\Delta\phi$ is included for future developments and so far not used.

No.	WASI	Symbol	Units	Description
1-6	C[i]	C_i	$\mu\text{g/l}$	Concentration of phytoplankton class number i , $i = 0..5$
7	X	C_L	mg/l	Concentration of suspended particles type I
8	C_Mie	C_S	mg/l	Concentration of suspended particles type II
9	C_Y	Y	m^{-1}	Concentration of Gelbstoff (absorption at λ_0)
10	S	S	nm^{-1}	Exponent of Gelbstoff absorption
11	n	n	-	Exponent of backscattering by small particles
12	T_W	T_W	$^{\circ}\text{C}$	Water temperature
13	Q	Q	sr	Anisotropy factor of upwelling radiation ("Q-factor")
14	fluo	η_{chl}	-	Quantum yield of chl-a fluorescence
15	rho_L	ρ_L	-	Reflection factor of downwelling radiance
16	rho_dd	ρ_{dd}	-	Reflection factor of direct downwelling irradiance
17	rho_ds	ρ_{ds}	-	Reflection factor of diffuse downwelling irradiance
18	beta	β	-	Turbidity coefficient
19	alpha	α	-	Angström exponent of aerosol scattering
20	f_dd	f_{dd}	-	Fraction of direct downwelling irradiance
21	f_ds	f_{ds}	-	Fraction of diffuse downwelling irradiance
22	H_oz	H_{oz}	cm	Ozone scale height
23	WV	WV	cm	Precipitable water
24	f	f	-	Proportionality factor of irradiance reflectance ("f-factor")
25	z	z	m	Sensor depth
26	zB	z_B	m	Bottom depth
27	sun	θ_{sun}	$^{\circ}$	Sun zenith angle
28	view	θ_v	$^{\circ}$	Viewing angle (0 = nadir)
29	dphi	$\Delta\phi$	$^{\circ}$	Azimuth difference between sun and viewing direction
30-35	fA[n]	f_n	-	Areal fraction of bottom surface type number n , $n = 0..5$
36	C_D	D	m^{-1}	Concentration of detritus (absorption at λ_0)
37	g_dd	g_{dd}	sr^{-1}	Fraction of sky radiance due to direct solar radiation
38	g_dsr	g_{dsr}	sr^{-1}	Fraction of sky radiance due to molecule scattering
39	g_dsa	g_{dsa}	sr^{-1}	Fraction of sky radiance due to aerosol scattering

Forward mode. Each parameter can be set by the user. When a series of spectra is calculated, iteration can be performed over each of the parameters.

Invers mode. The user defines for each parameter if it should be treated as a constant or as variable to be fitted during inversion.

Appendix 4: Constants

The following table summarizes the model constants of all 8 spectrum types. They can be changed using the GUI or by editing the WASI4.INI file.

WASI4.INI	Symbol	Units	Default value	Description
Day	d	–	94	Day of year
T_W0	T_0	°C	20	Reference temperature of spectrum $a_w(\lambda)$
nW	n_w	–	1.33	Refractive index of water
Lambda_a	λ_a	nm	550	Reference wavelength for aerosol optical thickness
Lambda_0	λ_0	nm	440	Reference wavelength for Gelbstoff absorption
Lambda_L	λ_L	nm	550	Reference wavelength for scattering of large particles
Lambda_S	λ_S	nm	500	Reference wavelength for scattering of small particles
Lambda_f0	λ_F	nm	685	Centre wavelength of chl-a fluorescence
Sigma_f0	σ_F	nm	10.62	Standard deviation of chl-a fluorescence
PAR_min	–	nm	400	PAR range: lower boundary
PAR_max	–	nm	700	PAR range: upper boundary
Lmin	–	nm	400	Spectrum average: lower boundary
Lmax	–	nm	700	Spectrum average: upper boundary
bbW500	b_1	m^{-1}	0.00111	Backscattering coefficient of pure water at 500 nm
bbX_A	A	$m^2 g^{-1}$	0.006	Factor A in backscattering to conc. relationship
bbX_B	B	–	-0.37	Factor B in backscattering to conc. relationship
bb_X	$b_{b,X}^*$	$m^2 g^{-1}$	0.0086	Specific backscattering coefficient of particles Type I
bb_Mie	$b_{b,Mie}^*$	$m^2 g^{-1}$	0.0042	Specific backscattering coefficient of particles Type II
b_X	b_X^*	$m^2 g^{-1}$	0.45	Specific scattering coefficient of particles Type I
b_Mie	b_{Mie}^*	$m^2 g^{-1}$	0.30	Specific scattering coefficient of particles Type II
rho0	–	–	0.06087	rho_ds polynomial: 0th order value
rho1	–	–	0.03751	rho_ds polynomial: 1st order value
rho2	–	–	0.1143	rho_ds polynomial: 2nd order value
rho_Eu	ρ_u	–	0.54	Reflection factor of upwelling irradiance
sigma_Ed	σ	–	0.03	Reflection factor of downwelling irradiance
sigma_Lu	σ_L^-	–	0.02	Reflection factor of upwelling radiance
dynamics	–	–	0.005	Radiometric resolution
noise	–	–	0.0004	Noise level
ldd	–	–	1	Path length of direct irradiance: 0th order value
ldda	–	–	1.017	Path length of direct irradiance: 1st order value
lddb	–	–	1.95	Path length of direct irradiance: 2n order value
lds0	–	–	1.1156	Path length of diffuse irradiance: 0th order value
lds1	–	–	0.5504	Path length of diffuse irradiance: 1st order value
ldsb	–	–	0	Path length of diffuse irradiance: 2n order value
ld	κ_0	–	1.0546	Path length factor of total irradiance, Ed
BRDF[n]	B_n	sr^{-1}	0.318	BRDF of bottom surface no. n, n=0..5

Appendix 5: Input spectra

The following table summarizes the 30 spectra which are imported from files. For each, a default spectrum is provided in the WASI software package, and stored in the directory /WASI4/DATA. The user can replace the default spectra by changing the corresponding file description in the WASI4.INI file.

No.	WASI GUI	Symbol	Units	Description
1	x, FWHM	λ	nm	Wavelengths, Spectral resolution
2	noise	–	<i>variable</i>	Noise
3	offset	–	<i>variable</i>	Offset
4	E0	$E_0(\lambda)$	$\text{mW m}^{-2} \text{nm}^{-1}$	Extraterrestrial solar irradiance
5	a_O2	$a_o(\lambda)$	cm^{-1}	Absorption coefficient of oxygene
6	a_O3	$a_{oz}(\lambda)$	cm^{-1}	Absorption coefficient of ozone
7	a_wv	$a_{wv}(\lambda)$	cm^{-1}	Absorption coefficient of water vapor
8	aW	$a_w(\lambda)$	m^{-1}	Absorption coefficient of pure water
9	daW/dT	$da_w(\lambda)/dT$	$\text{m}^{-1} \text{ }^\circ\text{C}^{-1}$	Temperature gradient of pure water absorption
10	aP[0]	$a_0^*(\lambda)$	$\text{m}^2 \text{mg}^{-1}$	Specific absorption coeff. of phytoplankton class no. 0 Default: Mixture of species typical for Lake Constance
11	aP[1]	$a_1^*(\lambda)$	$\text{m}^2 \text{mg}^{-1}$	Specific absorption coeff. of phytoplankton class no. 1 Default: Cryptophyta type "L"
12	aP[2]	$a_2^*(\lambda)$	$\text{m}^2 \text{mg}^{-1}$	Specific absorption coeff. of phytoplankton class no. 2 Default: Cryptophyta type "H"
13	aP[3]	$a_3^*(\lambda)$	$\text{m}^2 \text{mg}^{-1}$	Specific absorption coeff. of phytoplankton class no. 3 Default: Diatoms
14	aP[4]	$a_4^*(\lambda)$	$\text{m}^2 \text{mg}^{-1}$	Specific absorption coeff. of phytoplankton class no. 4 Default: Dinoflagellates
15	aP[5]	$a_5^*(\lambda)$	$\text{m}^2 \text{mg}^{-1}$	Specific absorption coeff. of phytoplankton class no. 5 Default: Green algae
16	aD*	$a_d^*(\lambda)$	–	Normalized absorption coefficient of detritus
17	aY*	$a_y^*(\lambda)$	–	Normalized absorption coefficient of Gelbstoff
18	bX	$b_x(\lambda)$	–	(Normalized) scattering coeff. of suspended particles Type I
19	albedo[0]	$a_0(\lambda)$	–	Albedo of bottom type no. 0. Default: Constant
20	albedo[1]	$a_1(\lambda)$	–	Albedo of bottom type no. 1. Default: Sand
21	albedo[2]	$a_2(\lambda)$	–	Albedo of bottom type no. 2. Default: Silt
22	albedo[3]	$a_3(\lambda)$	–	Albedo of bottom type no. 3. Default: Chara <i>aspera</i>
23	albedo[4]	$a_4(\lambda)$	–	Albedo of bottom type no. 4. Default: <i>P. perfoliatus</i>
24	albedo[5]	$a_5(\lambda)$	–	Albedo of bottom type no. 5. Default: <i>P. pectinatus</i>
25	–	<i>variable</i>	<i>variable</i>	Measurement: Current input for inverse modeling
26	R	$R(\lambda)$	–	Measurement: Irradiance reflectance
27	Ed	$E_d(\lambda)$	$\text{mW m}^{-2} \text{nm}^{-1}$	Measurement: Downwelling irradiance
28	Ls	$L_s(\lambda)$	$\text{mW m}^{-2} \text{nm}^{-1} \text{sr}^{-1}$	Measurement: Sky radiance
29	Kd	$K_d(\lambda)$	m^{-1}	Measurement: Attenuation for downwelling irradiance
30	weight	$g(\lambda)$	–	Weight function for inversion

Appendix 6: Calculated spectra

During run-time different spectra are calculated as intermediate results, depending on the actual spectrum type and calculation options. Some calculations can replace input spectra ($b_X(\lambda)$, $a_Y^*(\lambda)$, $E_d(\lambda)$, $L_s(\lambda)$, $K_d(\lambda)$, $R(\lambda)$). Each spectrum can be displayed and exported to file.

WASI GUI	Symbol	Units	Description
bbW	$b_{b,W}(\lambda)$	m^{-1}	Backscattering coefficient of pure water
bX	$b_X(\lambda)$	$- / m^{-1}$	(Normalized) scattering coefficient of suspended particles Type I
b_Mie	$b_{Mie}^* \cdot (\lambda/\lambda_s)^n$	$m^2 mg^{-1}$	Scattering coefficient of suspended particles Type II
bb_Mie	$b_{b,Mie}^* \cdot (\lambda/\lambda_s)^n$	$m^2 mg^{-1}$	Backscattering coefficient of suspended particles Type II
aY*	$a_Y^*(\lambda)$	–	Normalized absorption coefficient of Gelbstoff
T_O2	$T_o(\lambda)$	–	Transmittance of the atmosphere after oxygen absorption
T_O3	$T_{oz}(\lambda)$	–	Transmittance of the atmosphere after ozone absorption
T_wv	$T_{wv}(\lambda)$	–	Transmittance of the atmosphere after water vapor absorption
tau_a	$\tau_a(\lambda)$	–	Aerosol optical thickness
T_r	$T_r(\lambda)$	–	Transmittance of the atmosphere after Rayleigh scattering
T_as	$T_{as}(\lambda)$	–	Transmittance of the atmosphere after aerosol scattering
T_aa	$T_{aa}(\lambda)$	–	Transmittance of the atmosphere after aerosol absorption
Ed0	$E_d(\lambda, 0-)$	$mW m^{-2} nm^{-1}$	Downwelling irradiance just beneath water surface
Ed	$E_d(\lambda)$	$mW m^{-2} nm^{-1}$	Downwelling irradiance
fdd*Edd	$f_{dd} \cdot E_{dd}(\lambda)$	$mW m^{-2} nm^{-1}$	Direct component of downwelling irradiance
fds*Eds	$f_{ds} \cdot E_{ds}(\lambda)$	$mW m^{-2} nm^{-1}$	Diffuse component of downwelling irradiance
E_dsr	$E_{dsr}(\lambda)$	$mW m^{-2} nm^{-1}$	Diffuse component of downwelling irradiance caused by Rayleigh scattering
E_dsa	$E_{dsa}(\lambda)$	$mW m^{-2} nm^{-1}$	Diffuse component of downwelling irradiance caused by aerosol scattering
r_d	$r_d(\lambda)$	–	Ratio of direct to diffuse downwelling irradiance
Lu	$L_u(\lambda)$	$mW m^{-2} nm^{-1} sr^{-1}$	Upwelling radiance
Lr	$\rho_L \cdot L_s(\lambda)$	$mW m^{-2} nm^{-1} sr^{-1}$	Radiance reflected at the water surface
Ls	$L_s(\lambda)$	$mW m^{-2} nm^{-1} sr^{-1}$	Sky radiance
Lf	$L_F(\lambda)$	$mW m^{-2} nm^{-1} sr^{-1}$	Chl-a fluorescence component of upwelling radiance
Kd	$K_d(\lambda)$	m^{-1}	Diffuse attenuation coefficient for downwelling irradiance
Kdd	$K_{dd}(\lambda)$	m^{-1}	Attenuation coefficient of direct irradiance
Kds	$K_{ds}(\lambda)$	m^{-1}	Attenuation coefficient of diffuse irradiance
K_uW	$K_{uW}(\lambda)$	m^{-1}	Attenuation of upwelling irradiance backscattered in water
K_uB	$K_{uB}(\lambda)$	m^{-1}	Attenuation of upwelling irradiance reflected from the bottom
k_uW	$k_{uW}(\lambda)$	m^{-1}	Attenuation of upwelling radiance backscattered in water
k_uB	$k_{uB}(\lambda)$	m^{-1}	Attenuation of upwelling radiance reflected from the bottom
R	$R(\lambda)$	–	Irradiance reflectance
Rrs	$R_{rs}(\lambda)$	sr^{-1}	Remote sensing reflectance

Rrs_surf	$R_{rs}^{surf}(\lambda)$	sr^{-1}	Surface reflectance
Rrs_f	$R_{rs,F}(\lambda)$	sr^{-1}	Chl-a fluorescence component of remote sensing reflectance
f	f	–	f factor
frs	f_{rs}	–	f_rs factor
bottom	$R^b(\lambda)$	–	Bottom albedo
bottom	$R_{rs}^b(\lambda)$	sr^{-1}	Bottom remote sensing reflectance
a	$a(\lambda)$	m^{-1}	Absorption coefficient
b	$b(\lambda)$	m^{-1}	Scattering coefficient
bb	$b_b(\lambda)$	m^{-1}	Backscattering coefficient
a_calc	–	m^{-1}	Absorption of water constituents + evtl. water (inverse mode)
aPh_calc	$\sum C_i \cdot a_i^*(\lambda)$	m^{-1}	Phytoplankton absorption (inverse mode)
b_calc	$b(\lambda)$	m^{-1}	Scattering of water + constituents (inverse mode)
bb_calc	$b_b(\lambda)$	m^{-1}	Backscattering of water + constituents (inverse mode)
omega_b	$\omega_b(\lambda)$	–	Ratio backscattering over absorption plus backscattering
z_Ed	–	m	Depth at which p_{Ed} % of surface irradiance remains